**Title:**

**Gauging substituent effect of organic counter-anion in hybrid MOFs derived from γ-cyclodextrin: silver nanoparticle formation as test reaction**

Gangothri M. Venkataswamy[1,2], Nanishankar V.Harohallly[1,2]

1. Plantation Products, Spices and Flavour Technology
CSIR-CFTRI
KRS Road,
Karnataka
India
phone: +91 821 2512352
Fax: +91 821 2517233
email:nani.shankar@gmail.com
nani@cftri.res.in
2. Academy of Scientific and Innovative Research(ACSIR)
Ghaziabad,
India

**Email:** nani.shankar@gmail.com

**ORCID**

Nanishankar V. Harohally: 0000-0003-2306-5897

Table of Contents

**Experimental Section**
**Characterization**:

The $^{1}H$ and $^{13}C$ inverse gated $^{1}H$ decoupled spectra were recorded utilizing Bruker AV I instrument operating at frequently 500 and 125 MHz. For and $^{13}C$ inverse gated $^{1}H$ decoupled spectral recording, the relaxation time of 4 seconds (Bruker parameter d1= 4 s) was employed. FT-IR was recorded in ATR mode utilizing Bruker tensor II model. Scanning electron microscopy (SEM) was employed to study surface morphological changes and it was recorded in LEO435VP of LEO electron microscopy LTD. TEM was recorded employing model Talos F200S of Thermoscientific.While X-ray diffraction (XRD) patterns provided insights into structural features and it was recorded in Bruker XRD instrument, and differential scanning calorimetry (DSC) were utilized to assess thermal characteristics, DSC data was recorded in the model DSC 1800 of Perkin Elmer in temperature range consisting of 35°C to 240°C with a heating rate 5°C per minute. Fluorescence photographs were taken in olympus B51 model (U24ND6).

**Synthesis of cinnamate containing hybrid CDMOF (CIN@HDMOF(1:8)).**

Initially γ-CD (0.324 g, 0.25 mM) was dissolved in 5 mL of $H_2O$ in a 50 mL beaker. To this, potassium cinnamate ( 0.373 g, 2mM) was added and the mixture was stirred for 1 hr. Subsequently, the reaction mixture was filtered through 0.5 µM syringe filer to a 20 mL glass vial. Further, the glass vial was kept in a 100 mL reagent bottle filled with ethanol which facilitated the slow diffusion of ethanol to the vial for a period of 7 days to cause the crystal growth. The resultant cubic crystals were washed with ethanol thrice and subsequently dried at 50 ℃in vacuum oven.The other cinnamate MOFs CIN@HDMOF(1:16), and CIN@HDMOF(1:32) were prepared by utilizing γ-CD (0.324 g, 0.25 mM) and potassium cinnamate ( 0.746 g, 4 mM), potassium cinnamate ( 1.492 g, 8 mM) respectively. The isolation and work up was similar to CIN@HDMOF(1:8).

**Synthesis of cinnamate containing hybrid CDMOF (CIN@HDMOF(1:8)) utilizing methanol solvent**

The cinnamate containing hybrid CDMOFs, CIN@HDMOF(1:8), CIN@HDMOF(1:16), and CIN@HDMOF(1:32) were also accomplished employing methanol as crystallization solvent instead of ethanol following the same protocol which was optimized for ethanol.

**Synthesis of coumarate containing hybrid CDMOF (COU@HDMOF(1:8)**

The synthesis of COU@HDMOF was accomplished utilising γ-CD (0.324 g, 0.25 mM) and potassium coumarate (0.404 g, 2 mM) adopting similar procedure that of

CIN@HDMOF(1:8). The other coumarate MOFs COU@HDMOFs were prepared by utilizing γ-CD (0.324 g, 0.25 mM) and potassium coumarate (0.808 g, 4 mM), potassium coumarate (1.616 g, 8 mM) respectively in separate experiments.

**Synthesis of coumarate containing hybrid CDMOF (COU@HDMOF(1:8)) utilizing methanol solvent**

The coumarate containing hybrid CDMOFs, COU@HDMOF(1:8), COU@HDMOF(1:16), and COU@HDMOF(1:32) were also accomplished employing methanol as crystallization solvent instead of ethanol following the same protocol which was optimized for ethanol.

**Synthesis of ferulate containing hybrid CDMOF(FA@HDMOF(1:8)**

The synthesis of FA@HDMOF was accomplished utilising γ-CD (0.324 g, 0.25 mM) and potassium ferulate (0.464 g, 2mM) adopting similar procedure as that of CIN@HDMOF(1:8). The other coumarate MOFs γ-CD FA@HDMOFs were prepared by utilizing γ-CD (0.324 g, 0.25 mM) and potassium ferulate ( 0.928 g, 4mM), potassium ferulate (1.856 g, 8 mM) respectively in separate experiments.

**Synthesis of ferulate containing hybrid CDMOF (FA@HDMOF(1:8)) utilizing methanol solvent**

The ferulate containing hybrid CDMOFs, FA@HDMOF(1:8), FA@HDMOF(1:16), and FA@HDMOF(1:32) were also accomplished employing methanol as crystallization solvent instead of ethanol following the same protocol which was optimized for ethanol.

**Synthesis of AgNp^COU@HDMOF**

The coumarate containing **γ-CD HD MOF**s, COU@HDMOF(1:8), COU@HDMOF(1:16), and COU@HDMOF(1:32) were employed for the synthesis of silver nano particles stabilized hybrid MOFs. In a typical procedure, 50-60 mm-sized MOF crystals were immersed in acetonitrile solution of AgNO3 (2.5 mM) for 48h, Subsequently, the MOF crystals were removed from the reaction medium and washed with acetonitrile several times over the period of 24 h to completely remove the remaining silver salts. The accomplished various ratios of AgNp^COU@HDMOF crystals were dried in vacuum at 40 ◦C for 6 h.

**Synthesis of AgNp^FA@HDMOF**

The ferulate MOFs FA@HDMOF(1:8), FA@HDMOF(1:16), and FA@HDMOF(1:32) were employed for the synthesis of silver nano particles stabilized hybrid ferulate MOFs. The procedure adopted for AgNp^FA@HDMOF is very similar to that of AgNp^COU@HDMOF.

Figure S1: DSC data; blue- FA@HDMOF (1:8), Green- FA@HDMOF (1:16), Red- FA@HDMOF (1:32), Pink- γ-CDMOF

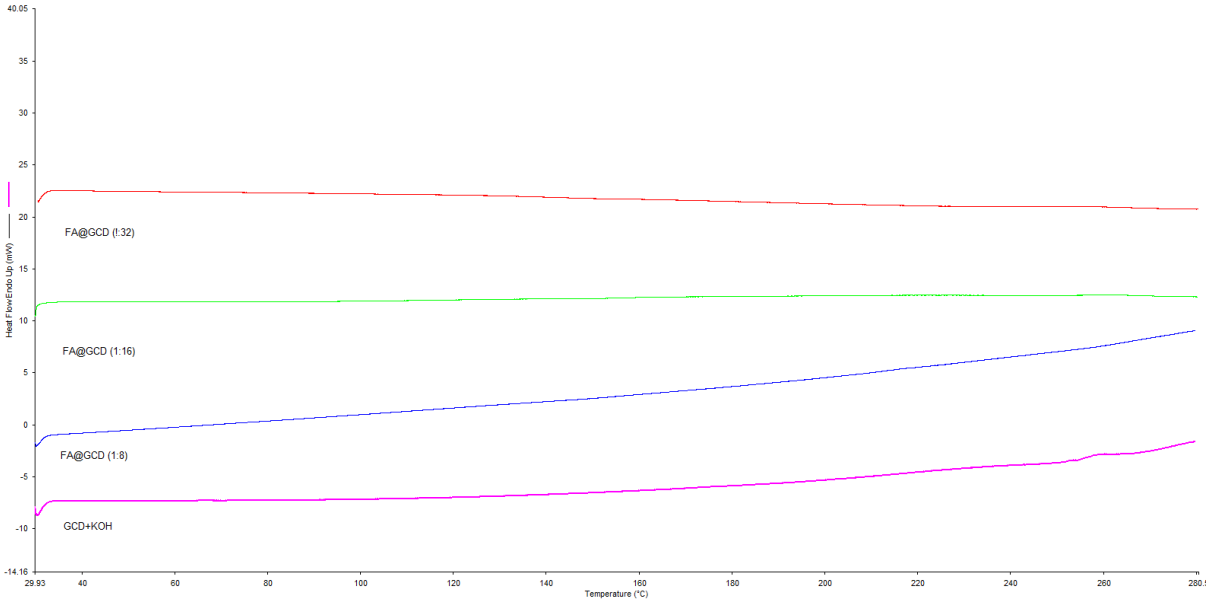

Figure S2: DSC data; Blue-COU@HDMOF( 1:8), Green-COU@HDMOF( 1:16), red-COU@HDMOF( 1:32), Pink- γ-CDMOF

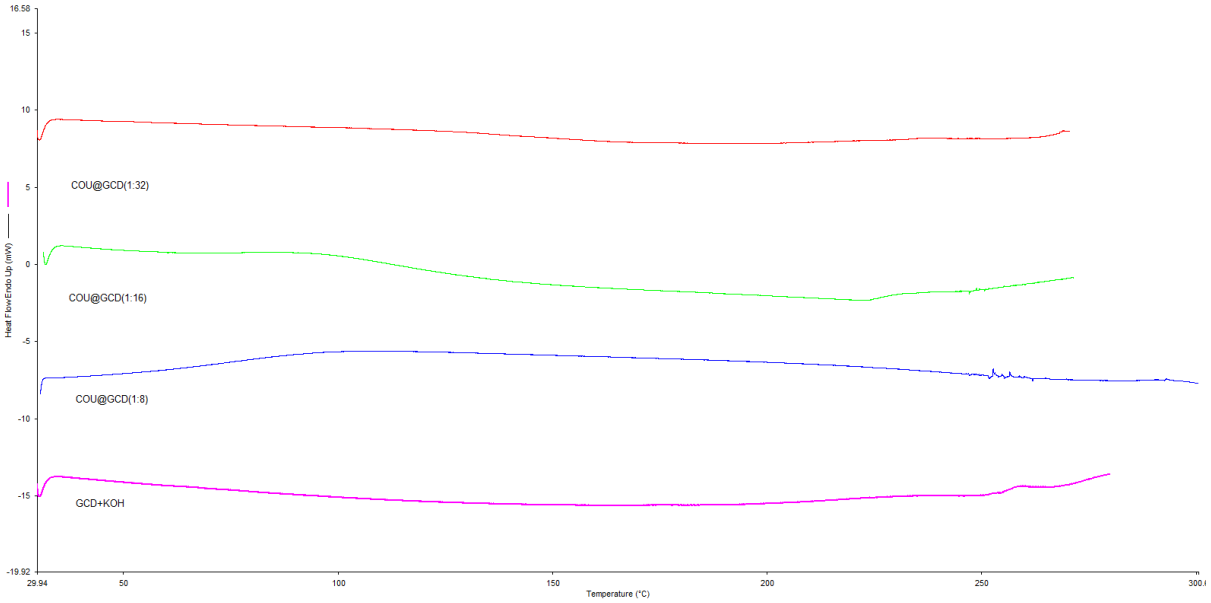

Figure S3: DSC data; Blue-CIN@HDMOF (1:8), Green-CIN@HDMOF (1:16), red-CIN@HDMOF (1:32), Pink- γ-CDMOF

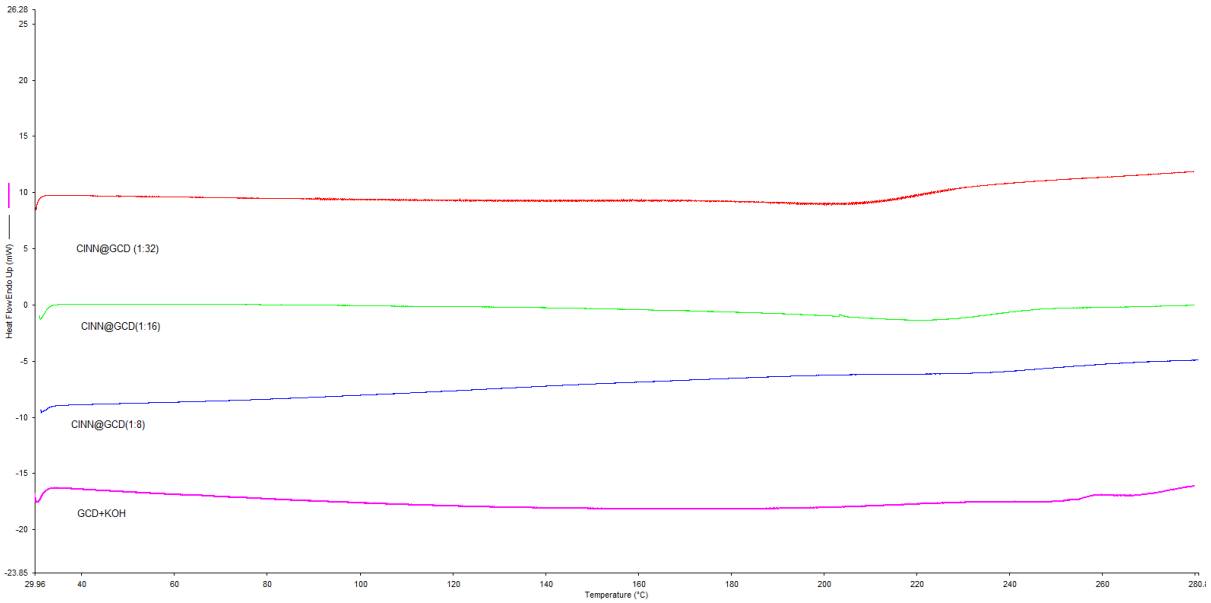

Figure S4: The FT-IR spectra of γ-CD

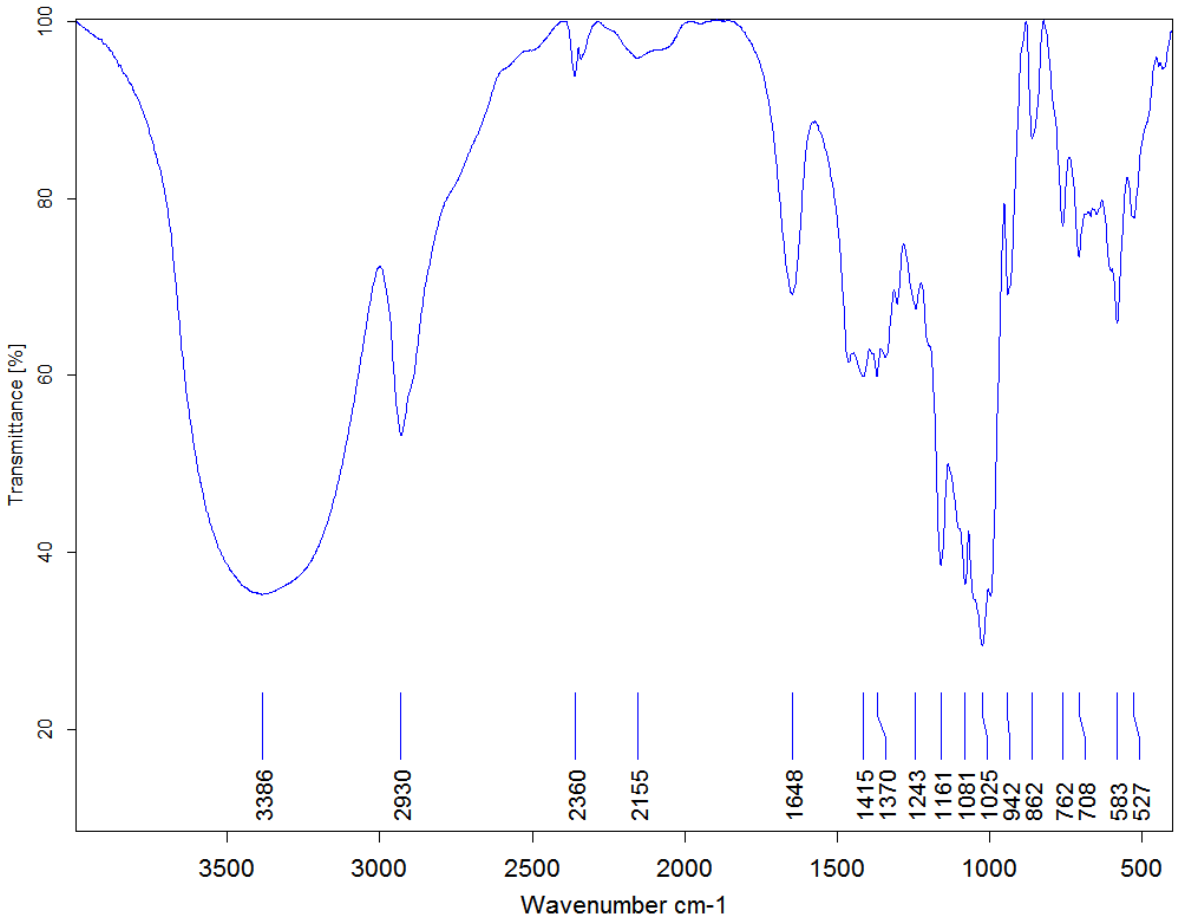

Figure S4: The FT-IR spectra of cinnamic acid

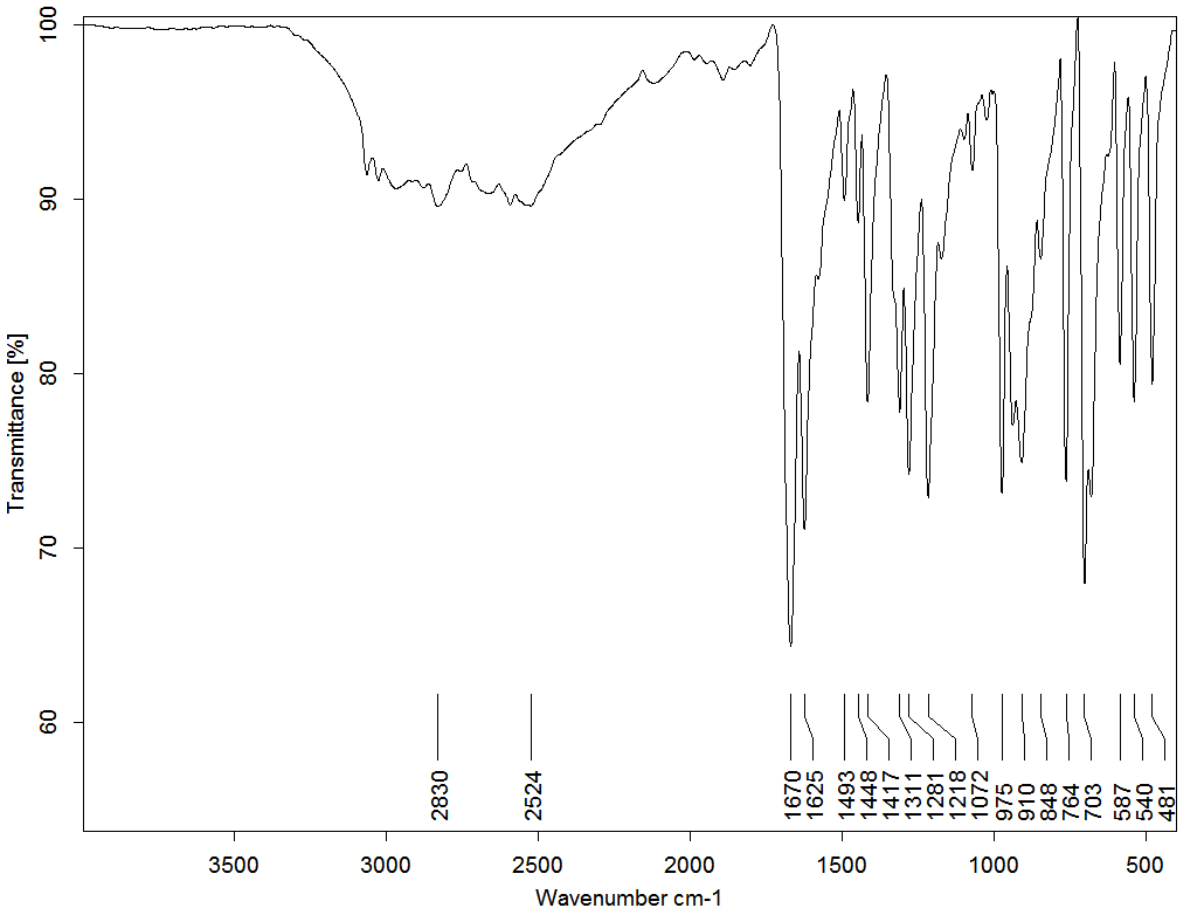

Figure S5: The FT-IR spectra of p-coumaric acid

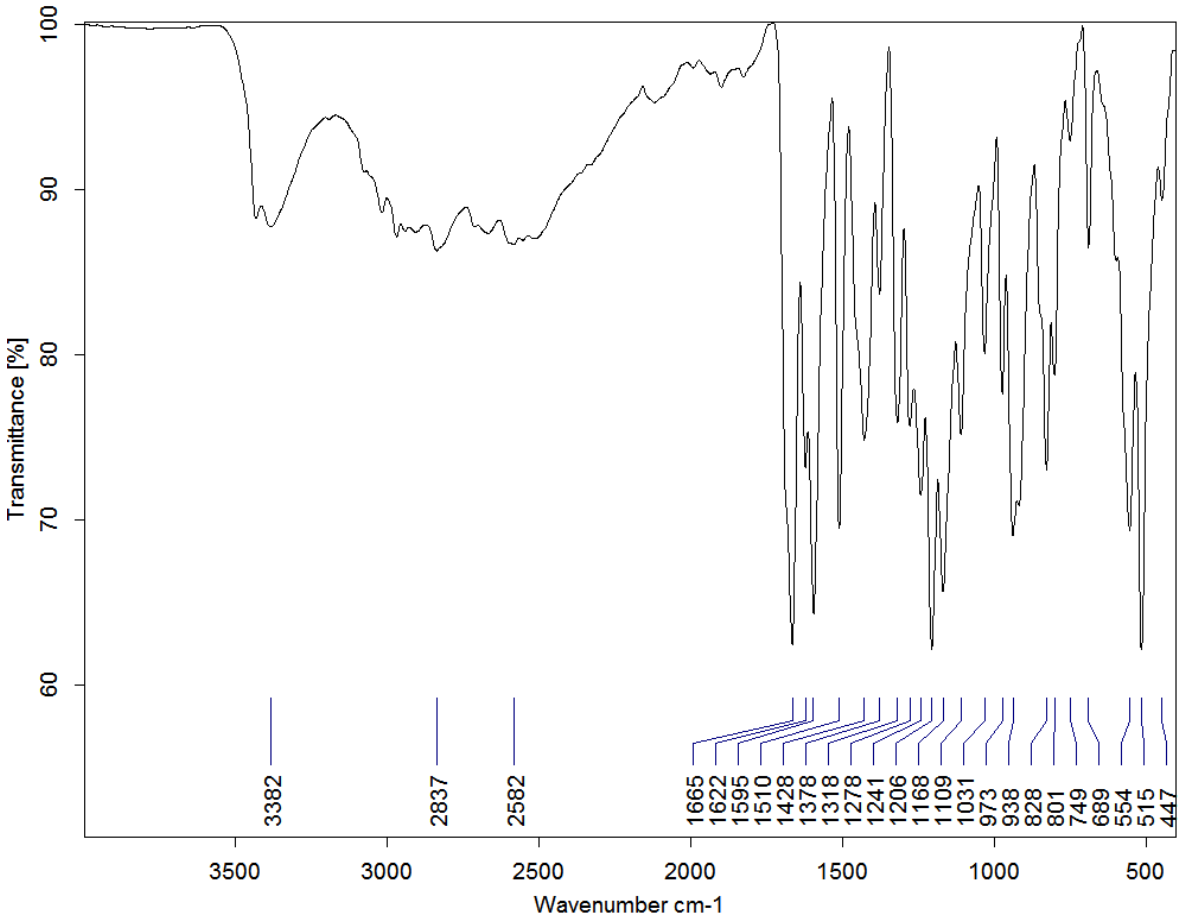

Figure S6: The FT-IR spectra of Ferulic  acid

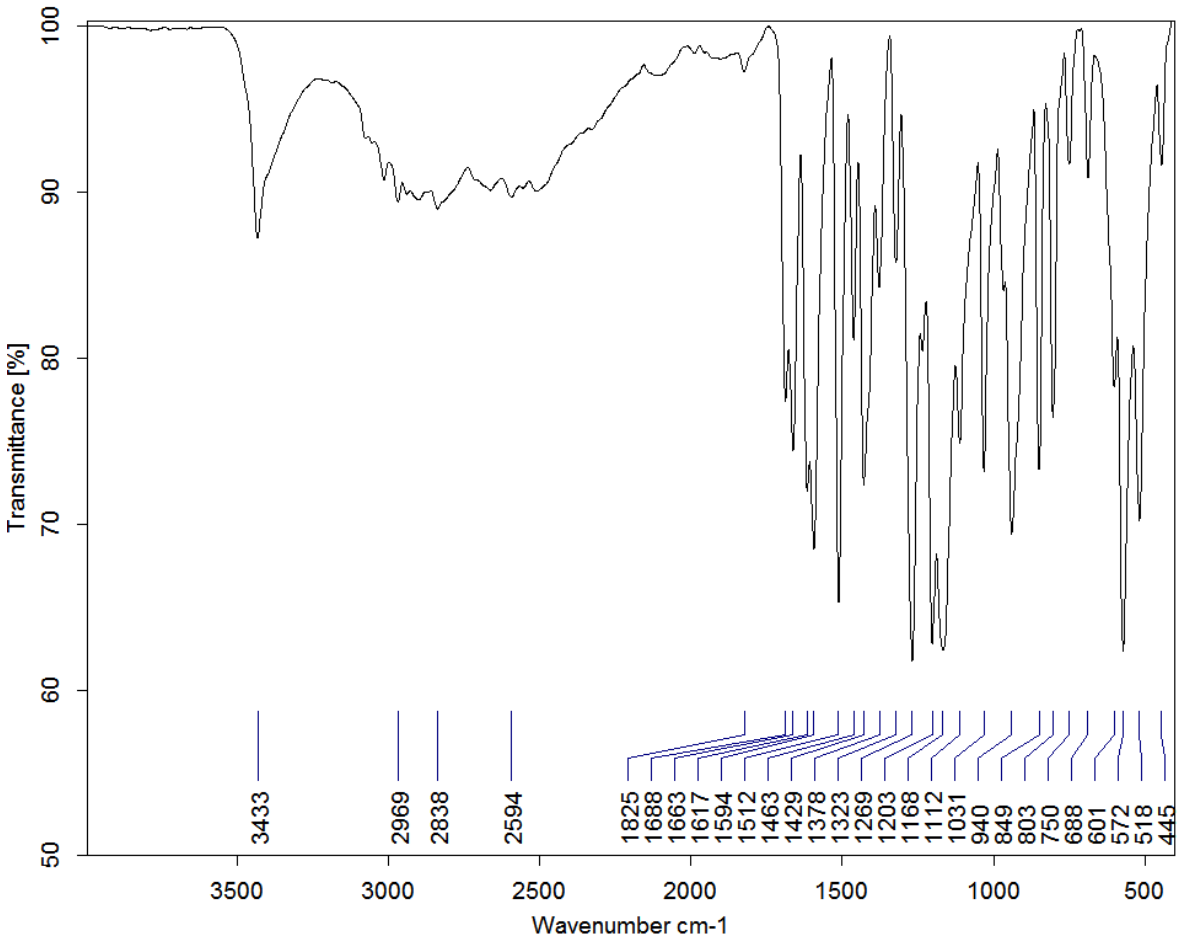

Figure S7: The FT-IR spectra of potassium cinnamate

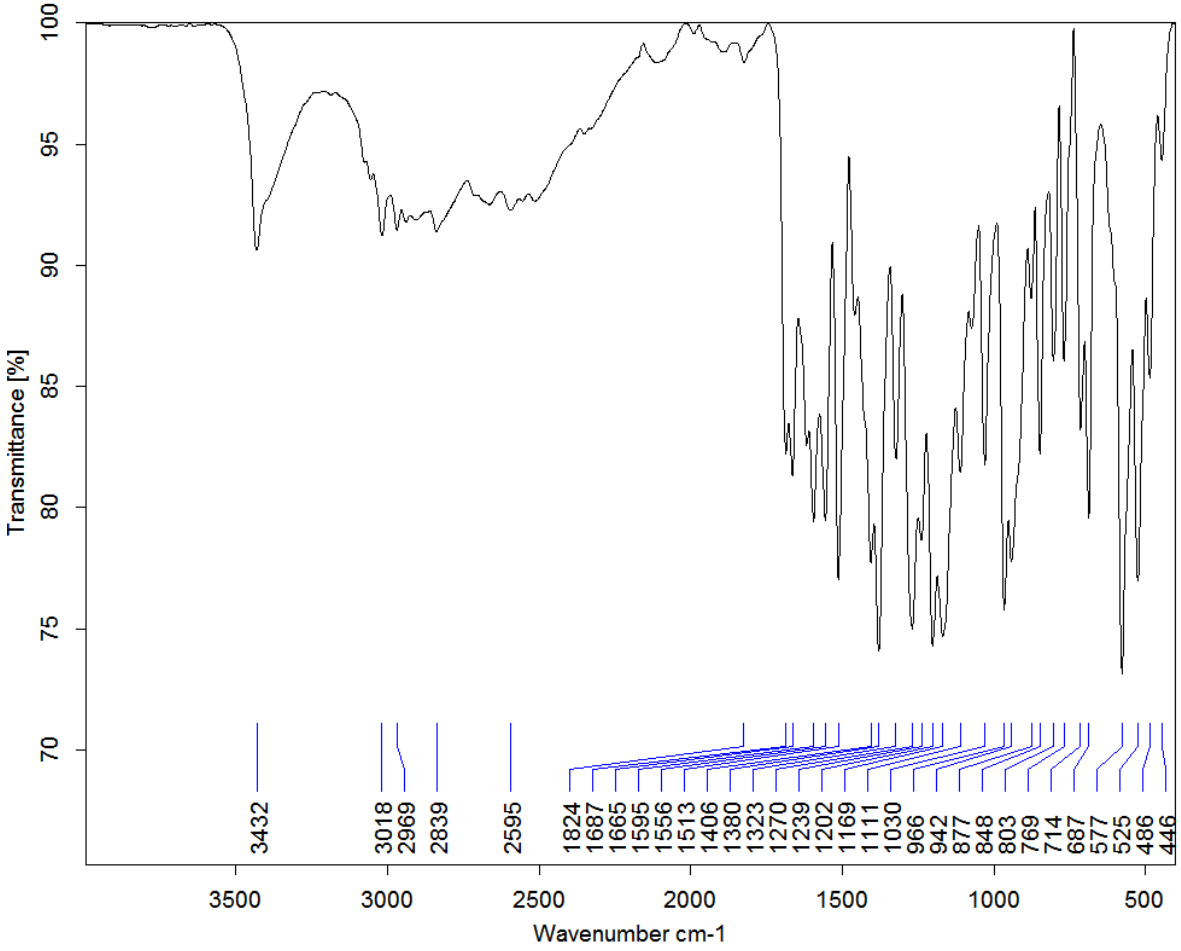

Figure S8: The FT-IR spectra of potassium coumarate

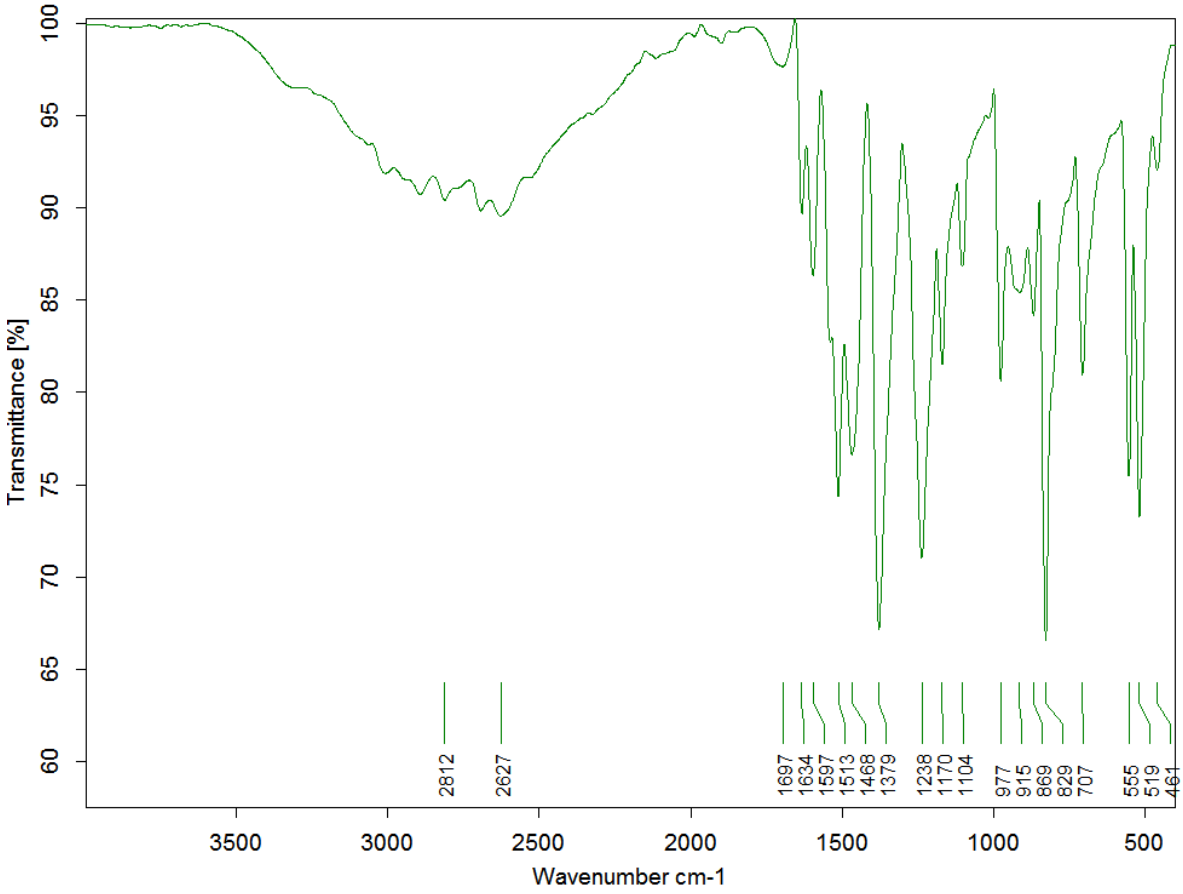

Figure S9: The FT-IR spectra of potassium ferulate

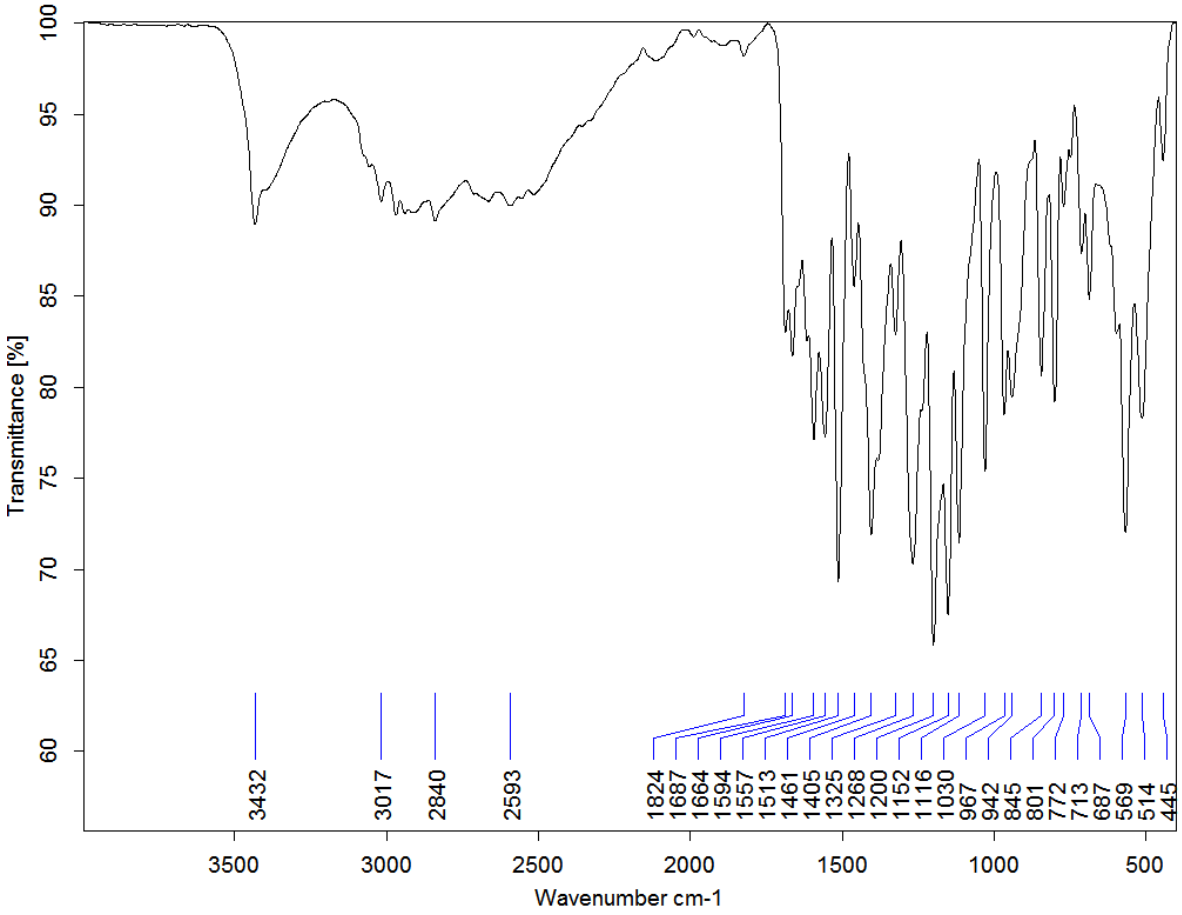

Figure S10: The FT-IR spectra of FA@HDMOF:Red-(1:8), Pink- FA@HDMOF (1:16), Green FA@HDMOF(1:32)

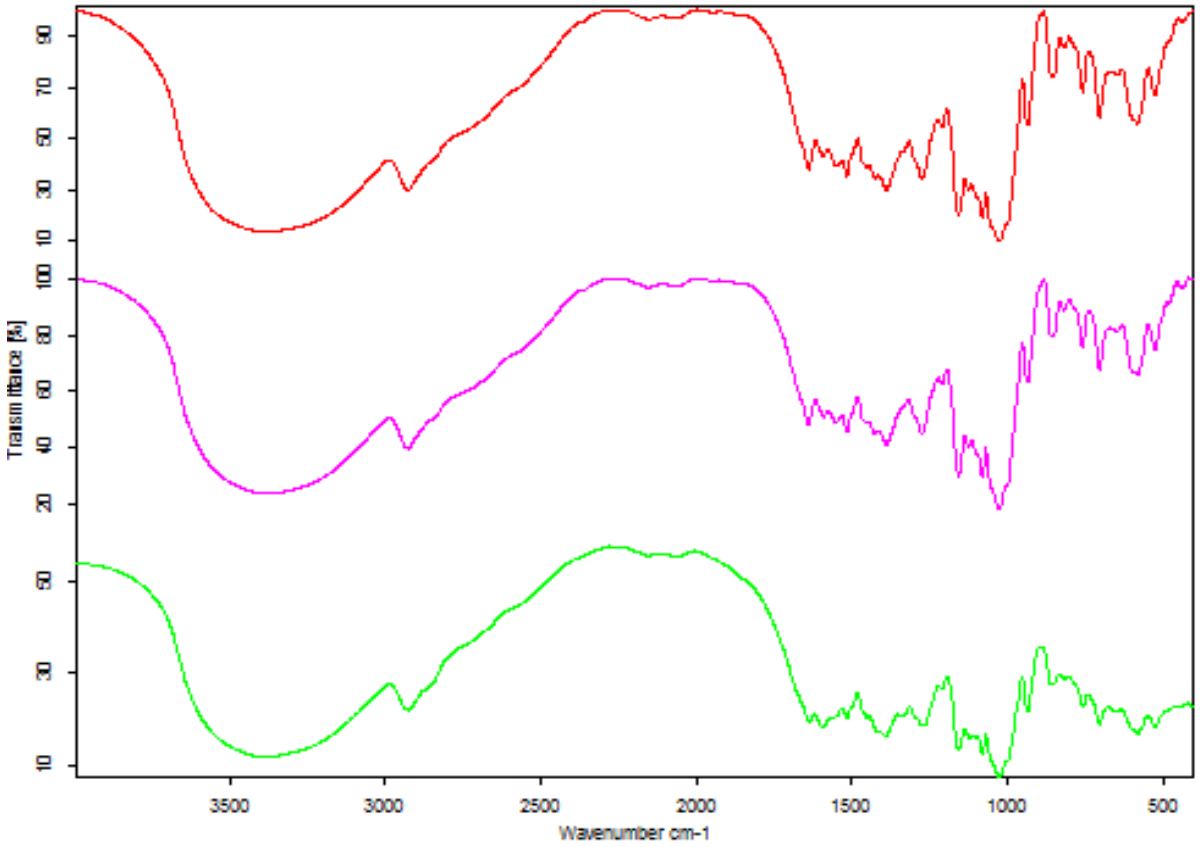

Figure S11: IR Spectra: Blue-COU@HDMOF(1:8), Green-COU@HDMOF(1:16), Red-COU@HDMOF(1:32)

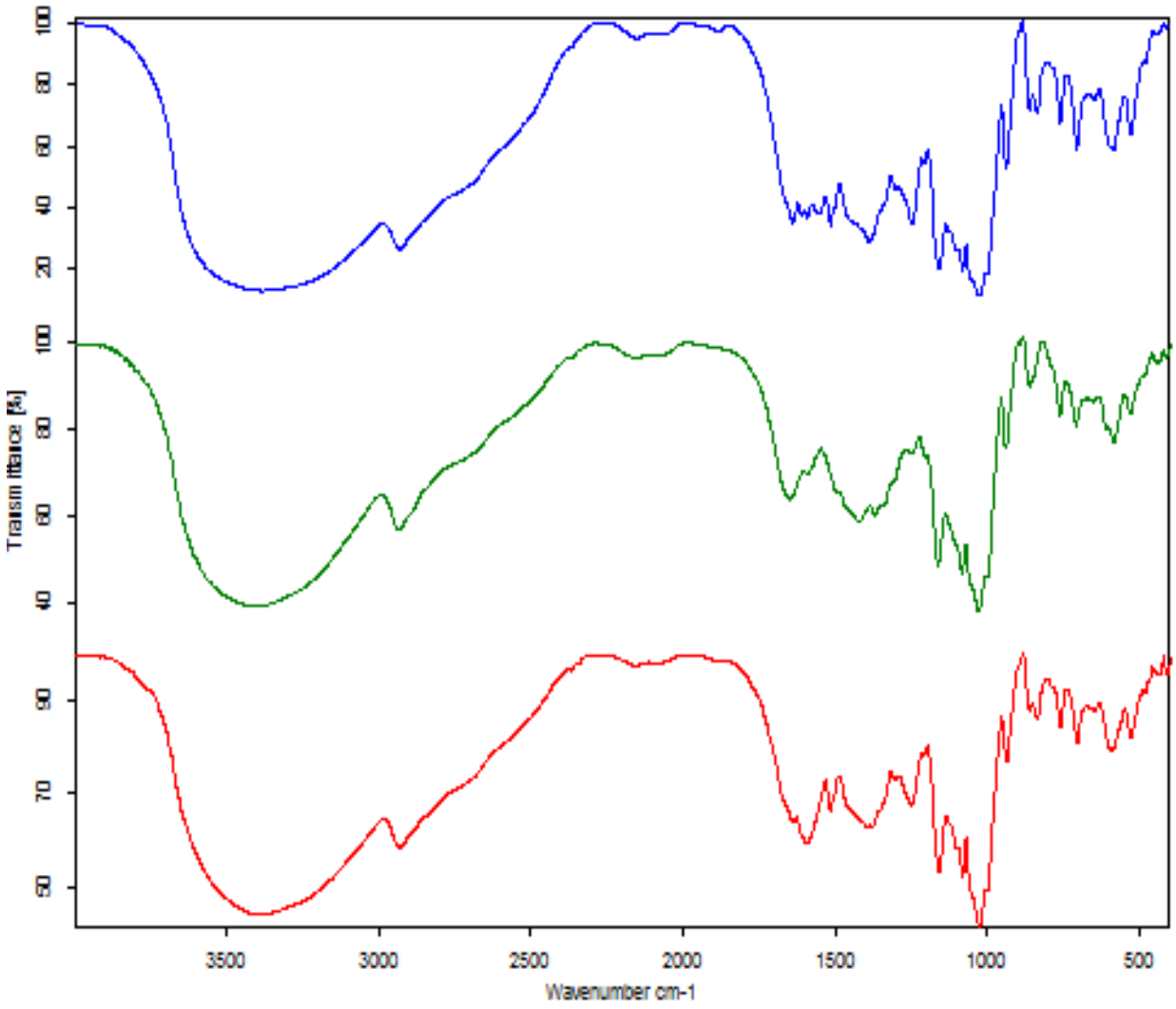

Figure S 12 :IR Spectra:  Blue-CIN@HDMOF, (1:8),green- CIN@HDMOF, Red-CIN@HDMOF

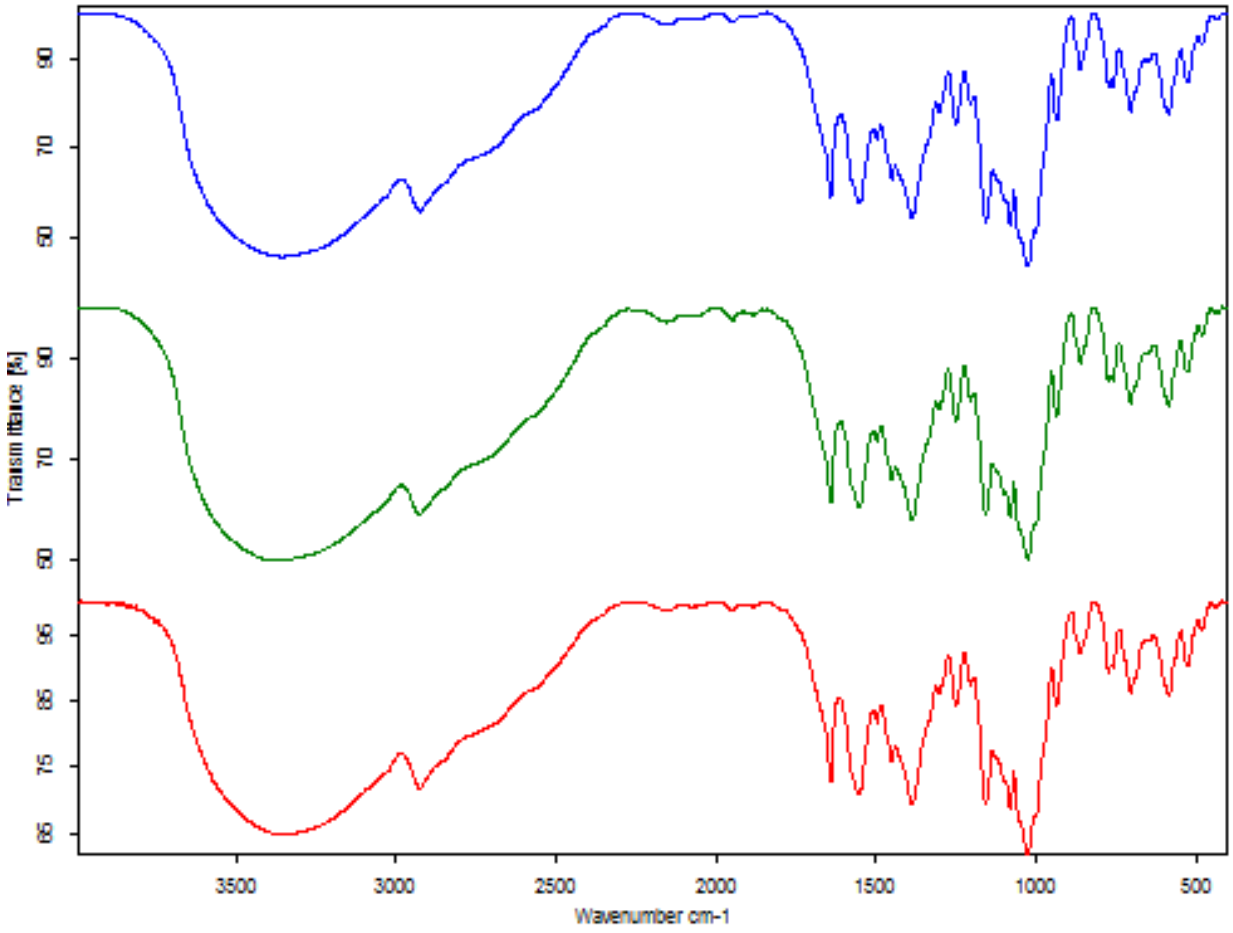

Figure S13 : UV spectrum  of Cinnamic acid

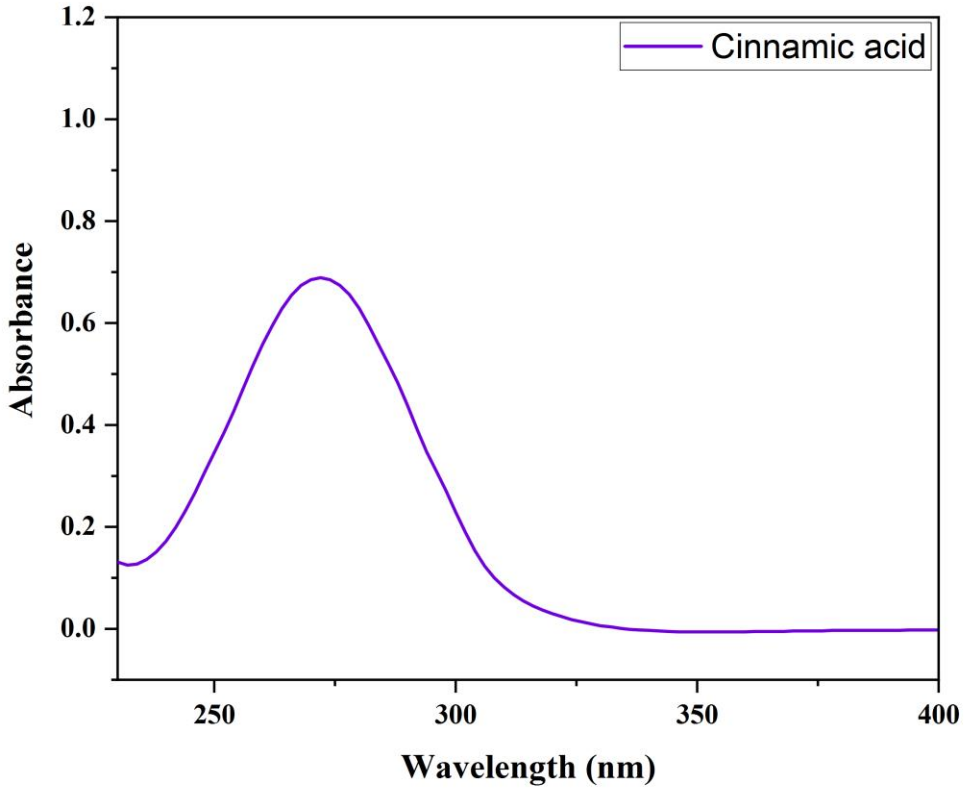

Figure S14 : UV spectrum  of p-coumaric acid

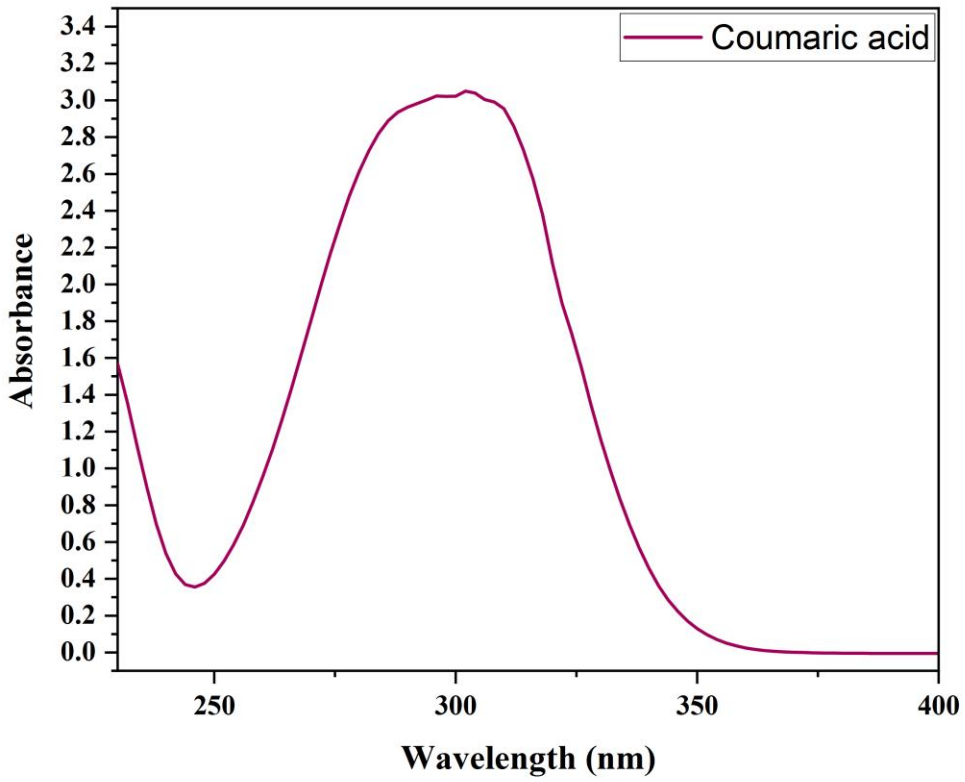

Figure S15 : UV spectrum  of Ferulic acid

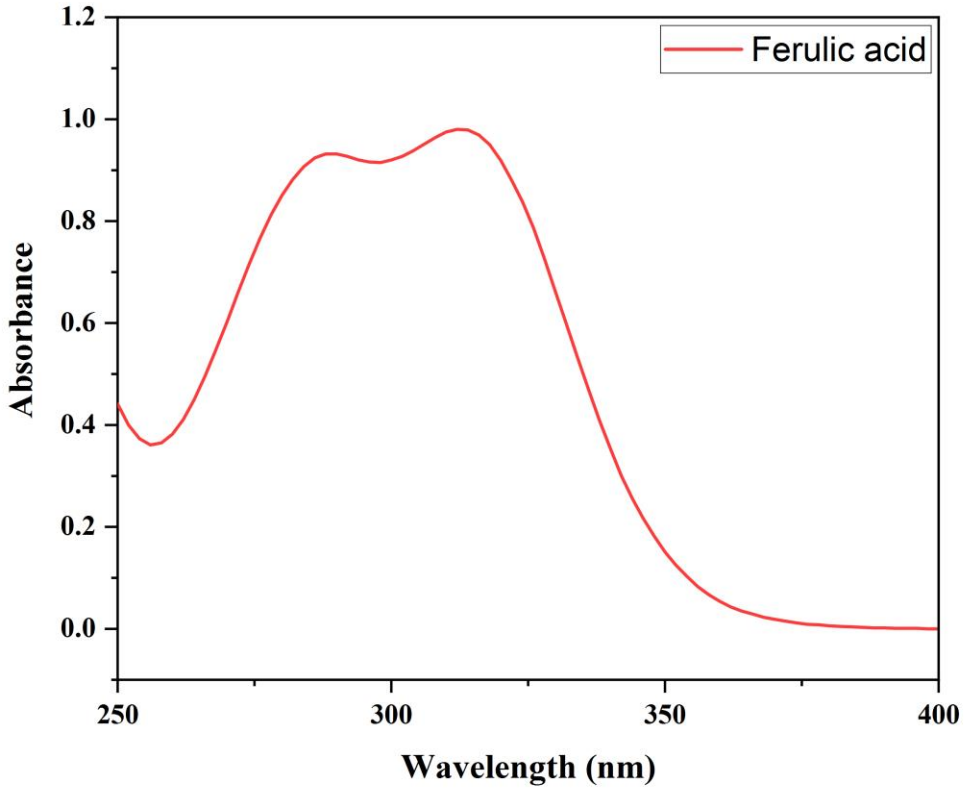

Figure S16: Stack plot of UV spectra; green-CIN@HDMOF(1:8), Red-CIN@HDMOF(1:16), blue- CIN@HDMOF(1:32)

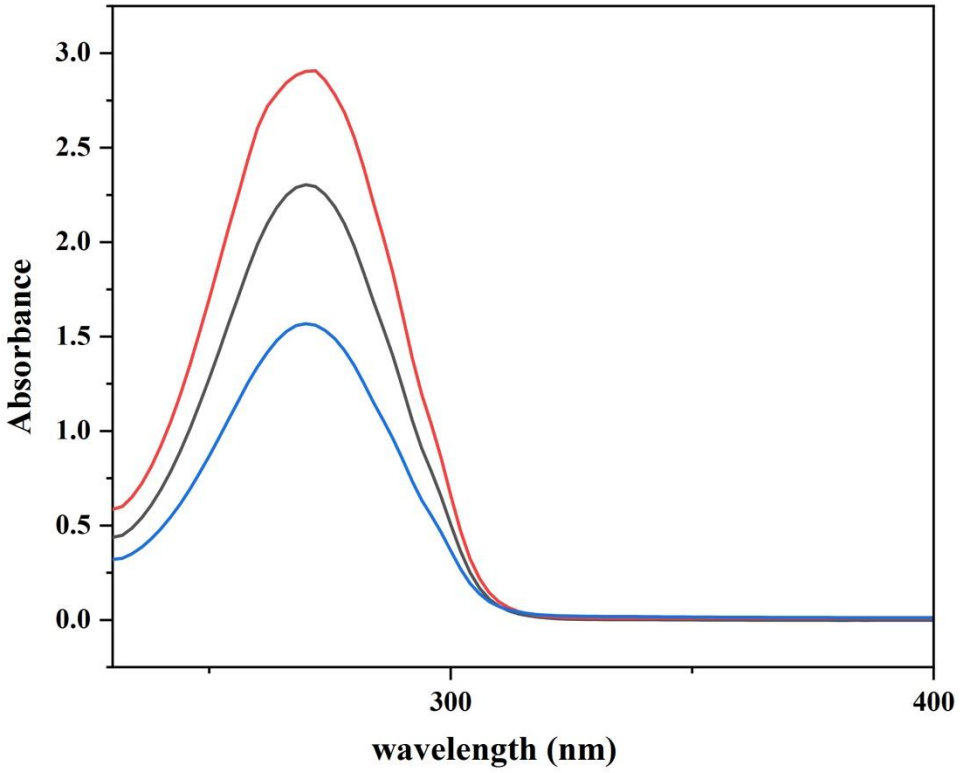

Figure S17: Stack plot of UV spectra; blue-COU@HDMOF(1:8), Red-COU@HDMOF(1:16), green- COU@HDMOF(1:32)

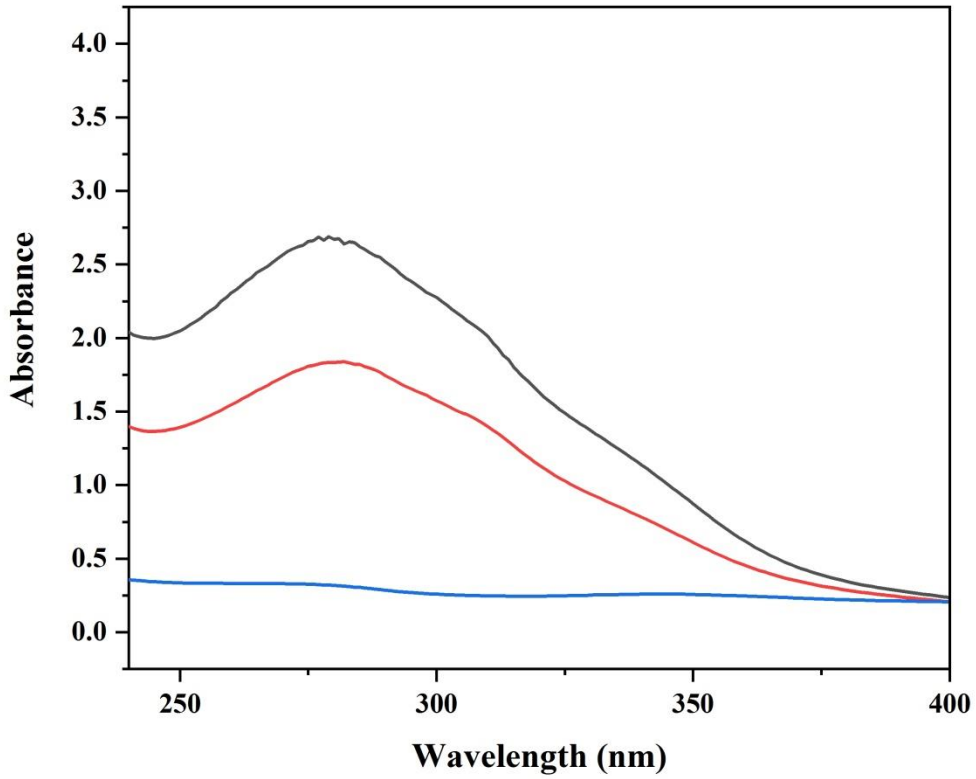

Figure S18: Stack plot of UV spectra; blue-FA@HDMOF(1:8), Red- FA@HDMOF(1:16), green-FA@HDMOF(1:32)

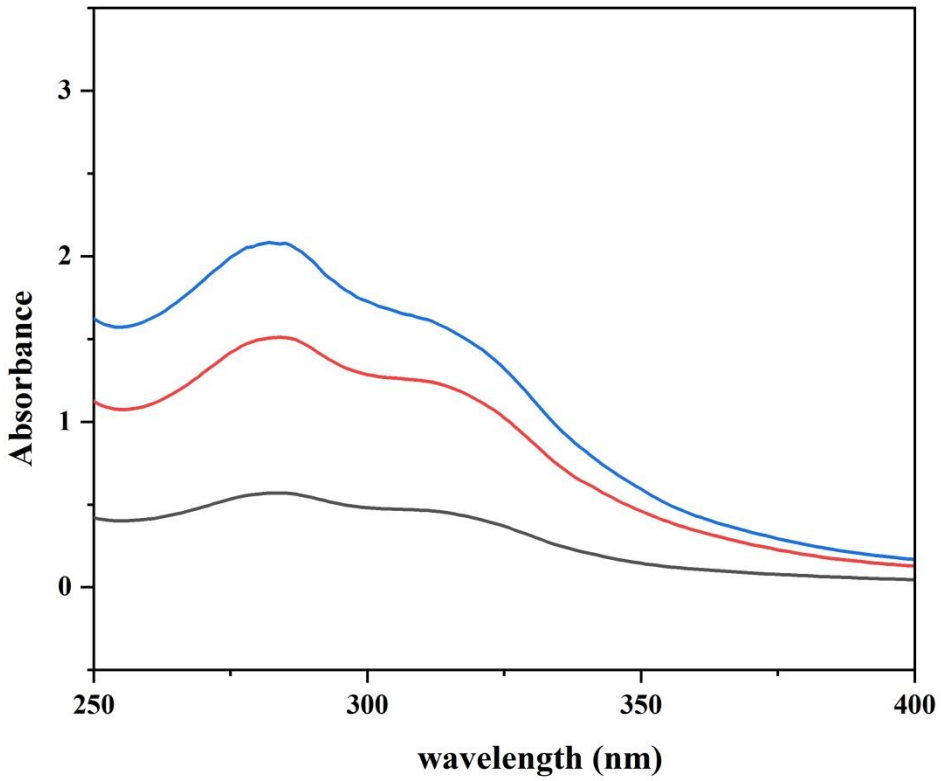

Figure S19: SEM  of FA@HDMOF(1:8)

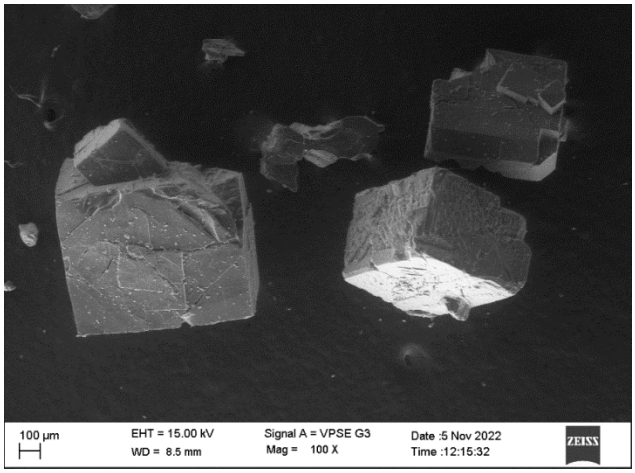


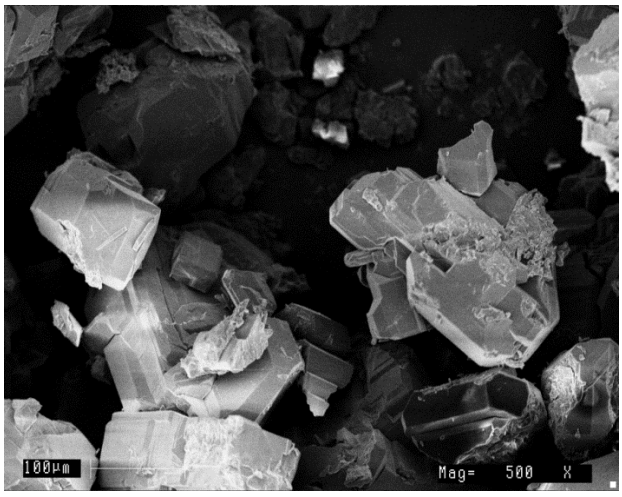

Figure S20: SEM of COU@HDMOF(1:8)

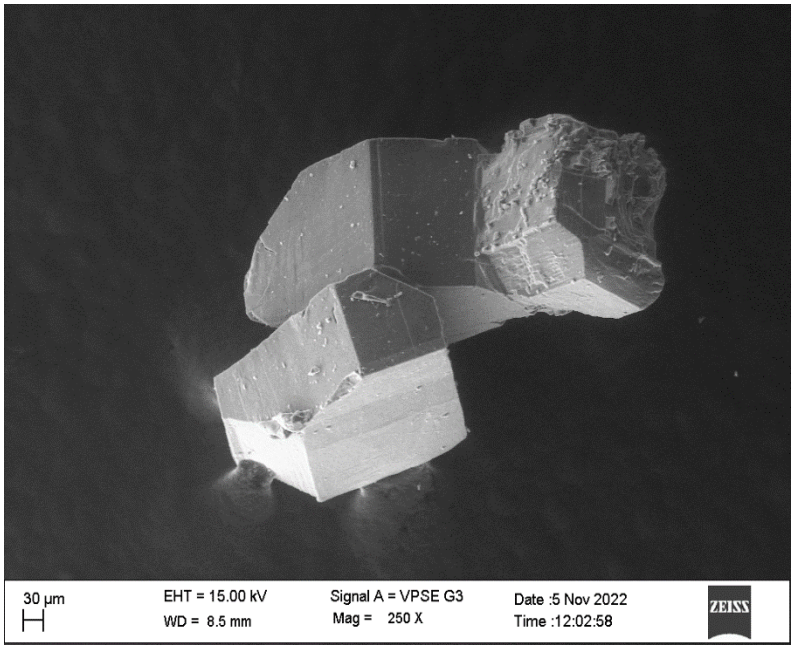

Figure S21: SEM of CIN@HDMOF(1:8)

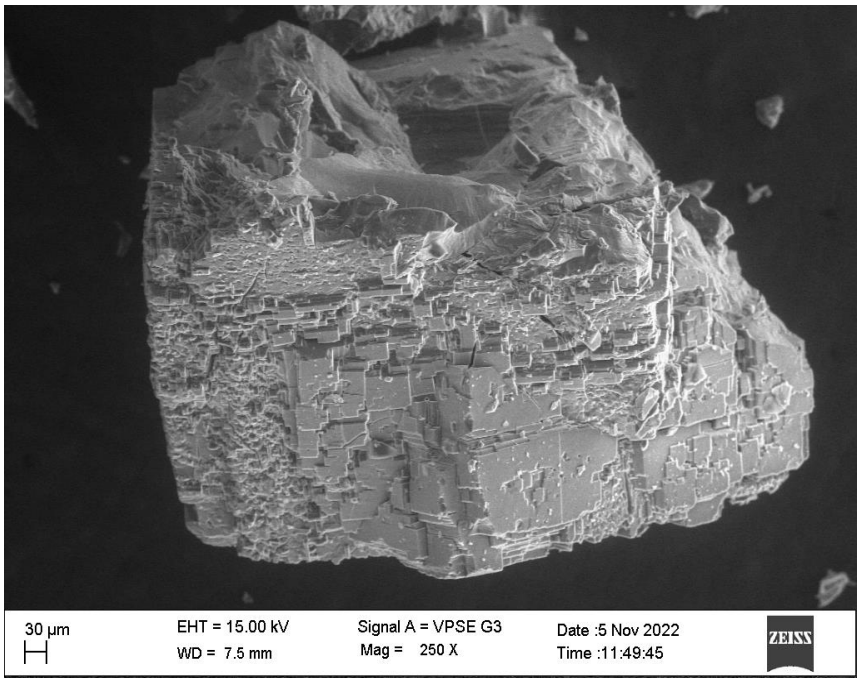

Figure S22: $^{1}$H NMR spectrum of CIN@HDMOF(1:8) crystals grown from ethanol solvent diffusion (CIN@HDMOF-0.9)

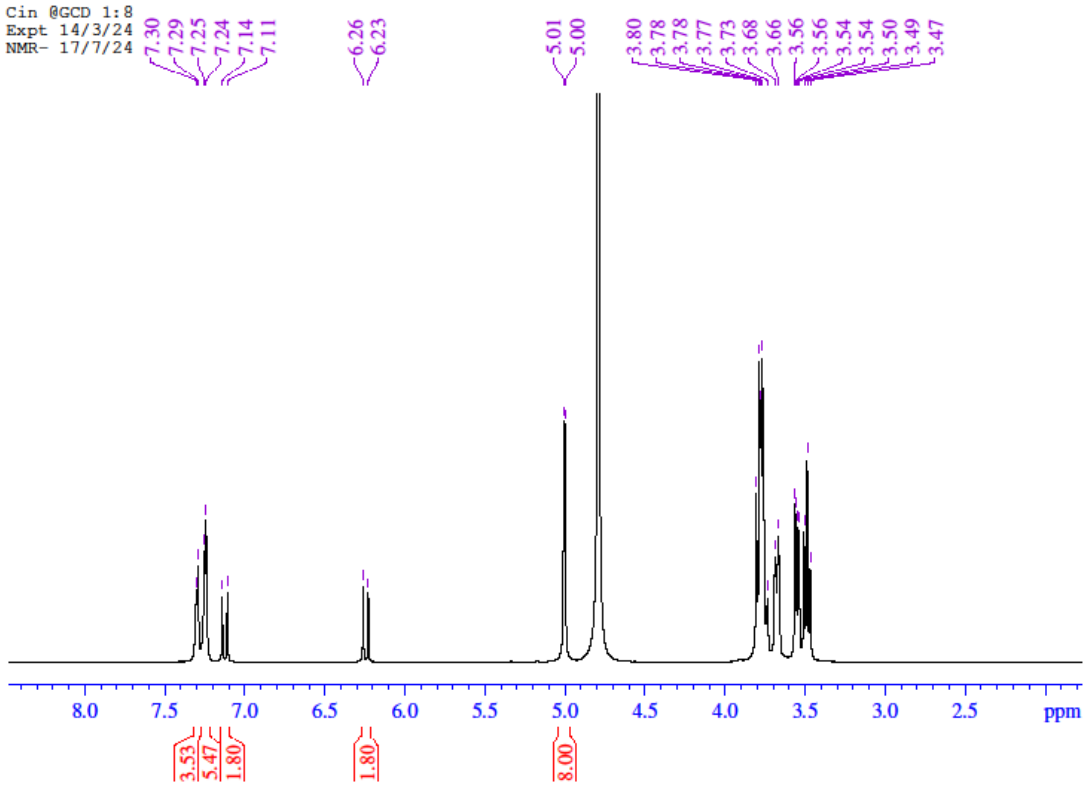

Figure S23: $^{13}C$ (inverse gated $^{1}H$ decoupled) NMR spectrum of CIN@HDMOF(1:8) crystals grown from ethanol solvent diffusion (CIN@HDMOF-1.1)

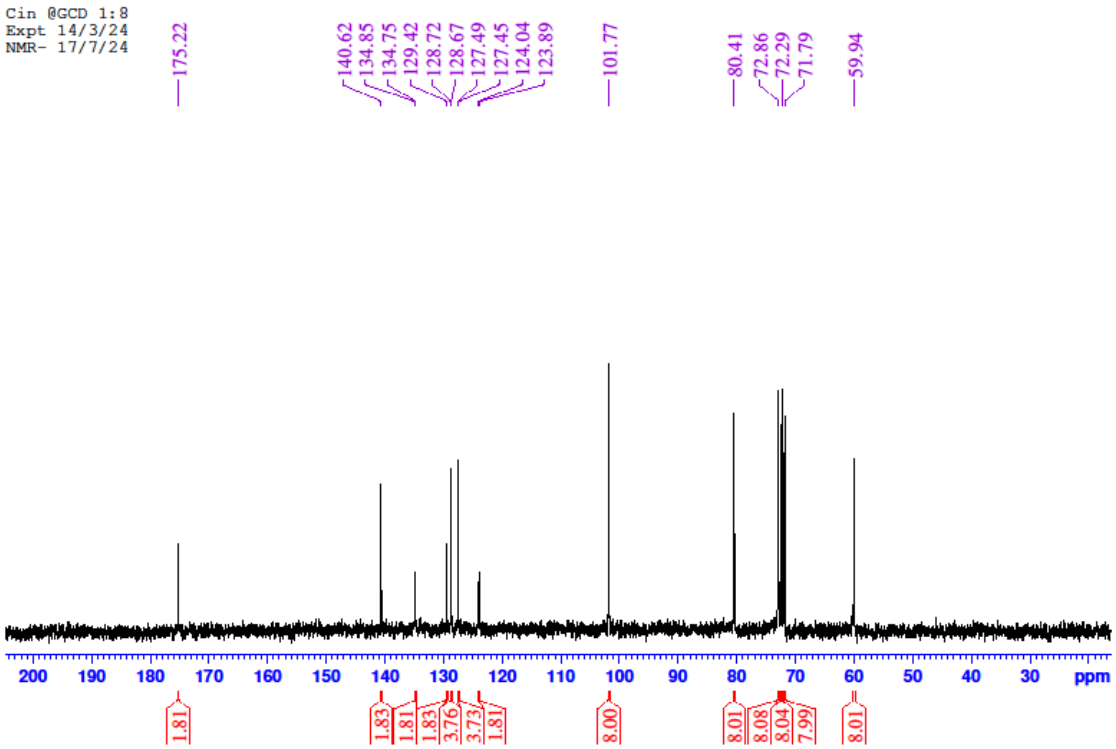

Figure S24: $^{1}$H NMR spectrum of CIN@HDMOF(1:16) crystals grown from ethanol solvent diffusion (CIN@HDMOF-1.1)

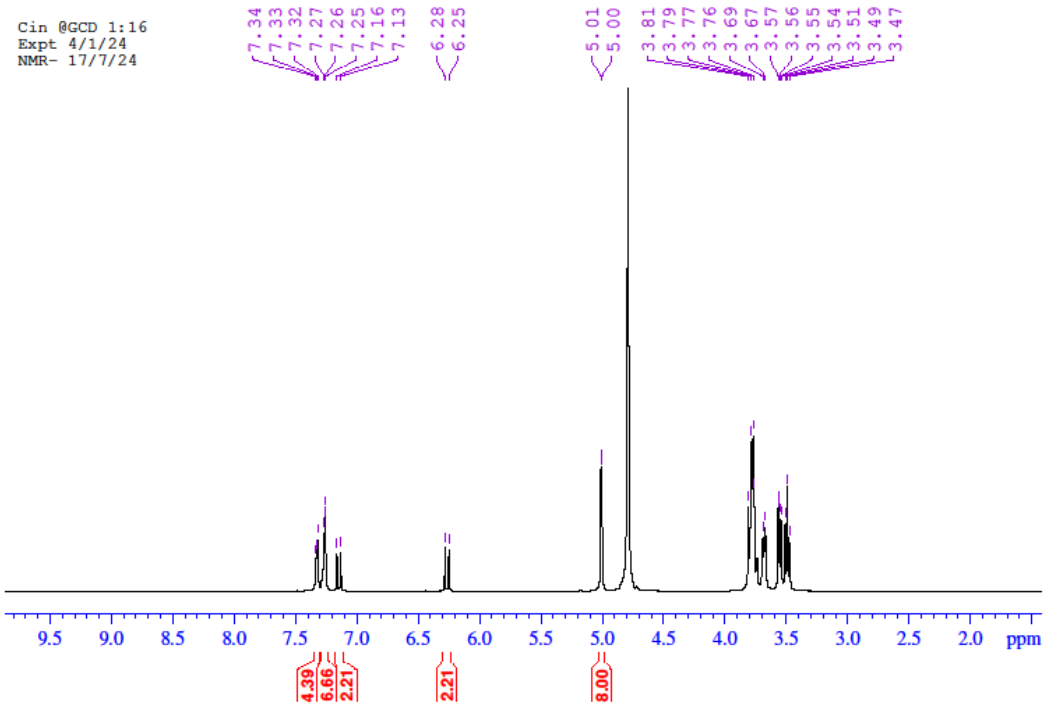

Figure S25: $^{13}C$ (inverse gated $^{1}H$ decoupled)NMR spectrum of CIN@HDMOF(1:6) crystals grown from ethanol solvent diffusion (CIN@HDMOF-1.1)

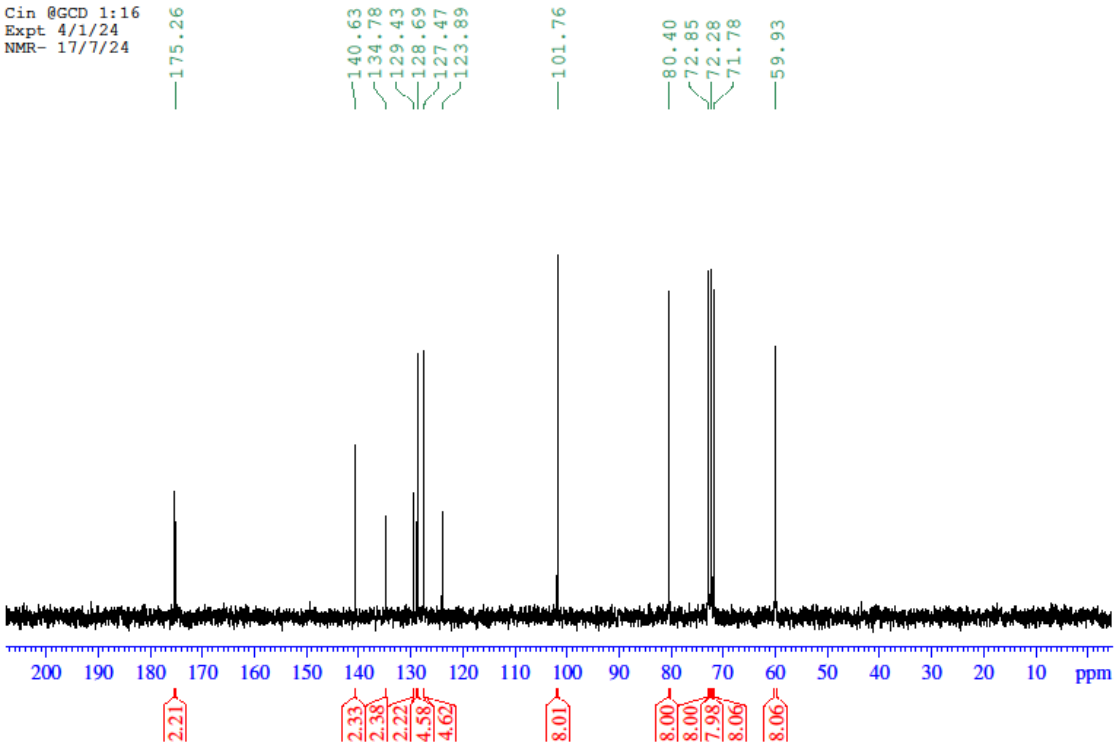

Figure S26: $^{1}$H NMR spectrum of CIN@HDMOF(1:32) crystals grown from ethanol solvent diffusion (CIN@HDMOF-1.1)

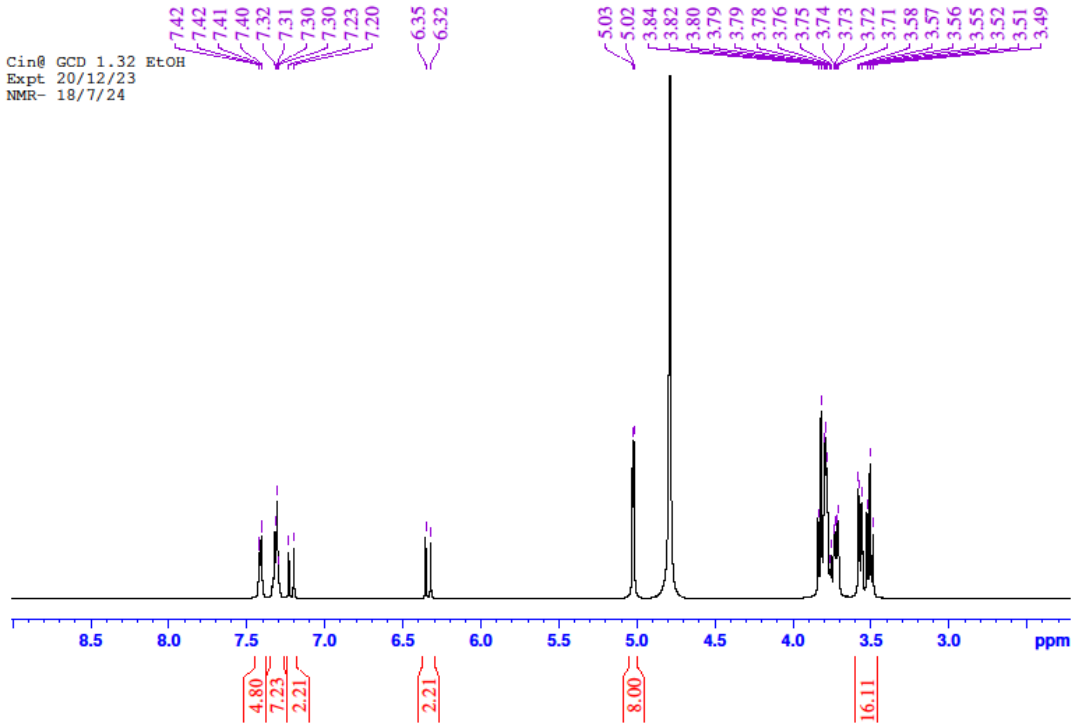

Figure S27: $^{13}C$ (inverse gated $^{1}H$ decoupled) NMR spectrum of CIN@HDMOF(1:32) crystals grown from ethanol solvent diffusion (CIN@HDMOF-1.1)

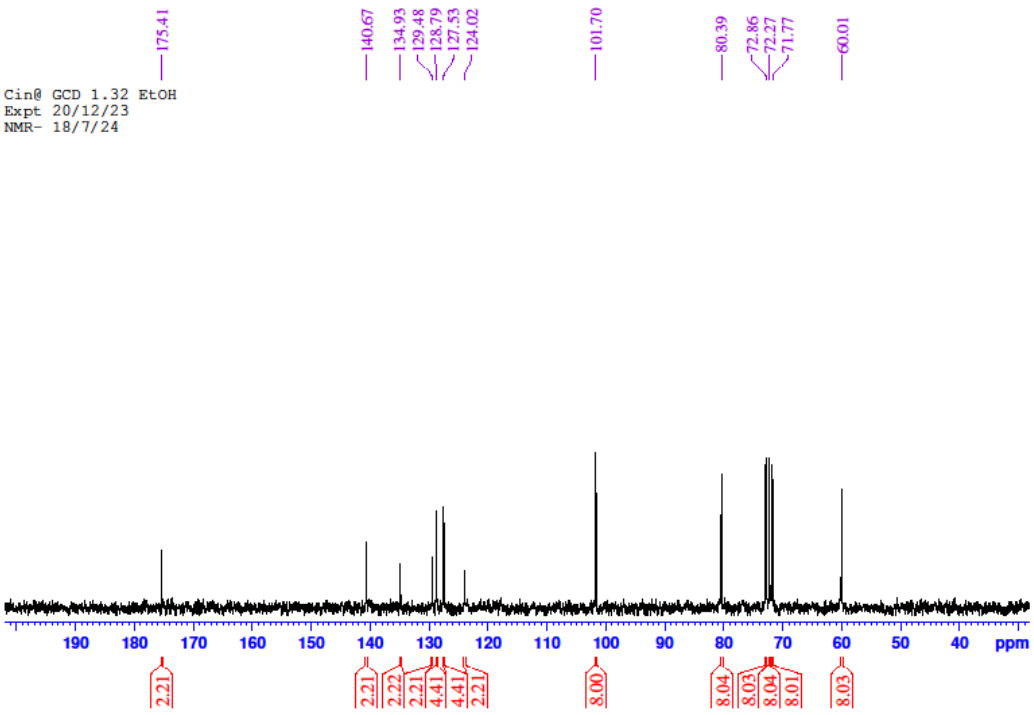

Figure S28: $^{1}$H NMR spectrum of COU@HDMOF(1:8) crystals grown from ethanol solvent diffusion (COU@HDMOF-0.9 )

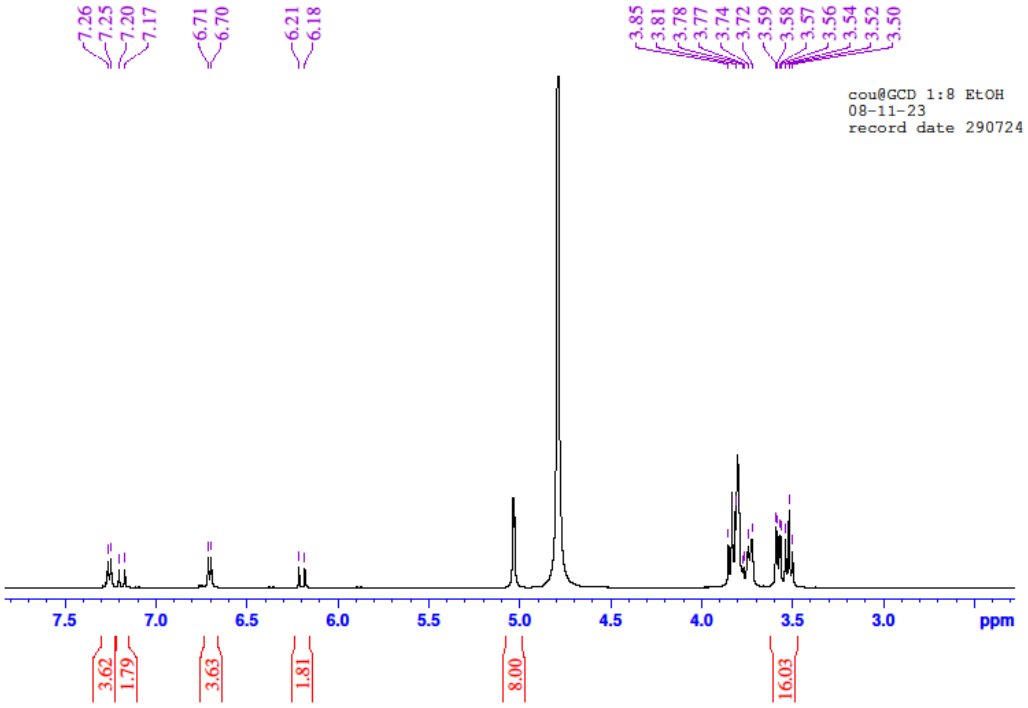

Figure S29: $^{13}C$ (inverse gated $^{1}H$ decoupled)NMR spectrum of COU@HDMOF(1:8) crystals grown from ethanol solvent diffusion (COU@HDMOF-0.9)

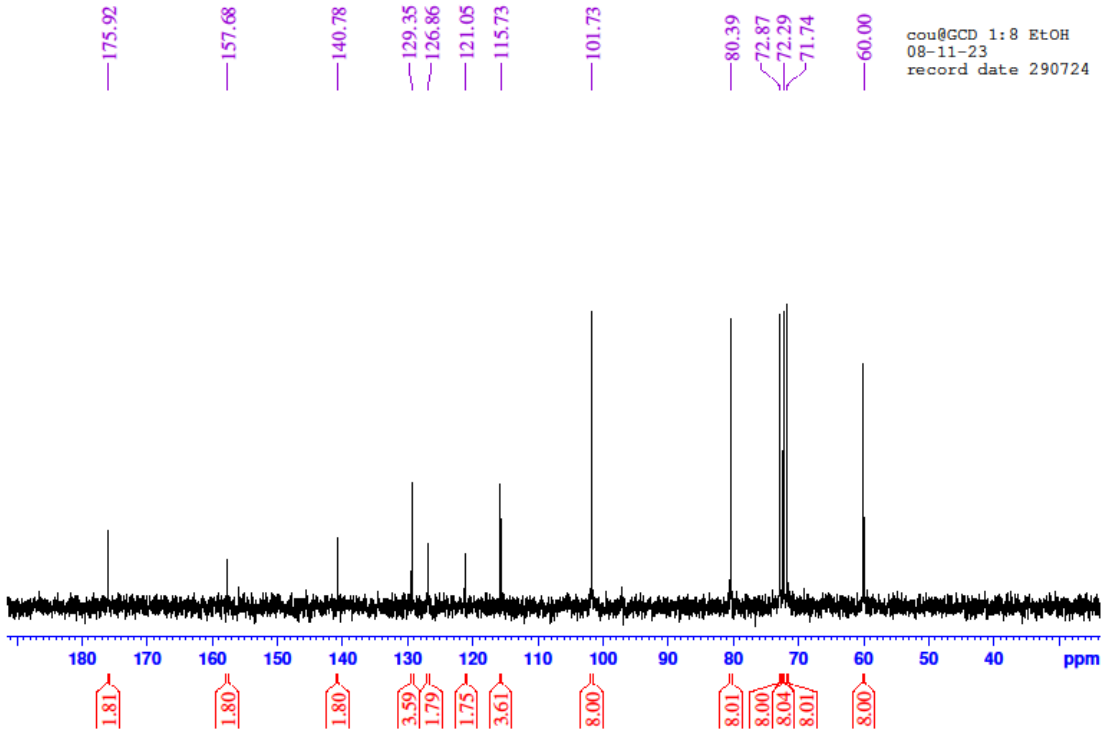

Figure S30: $^{1}$H NMR spectrum of COU@HDMOF(1:16) crystals grown from ethanol solvent diffusion (COU@HDMOF-1)

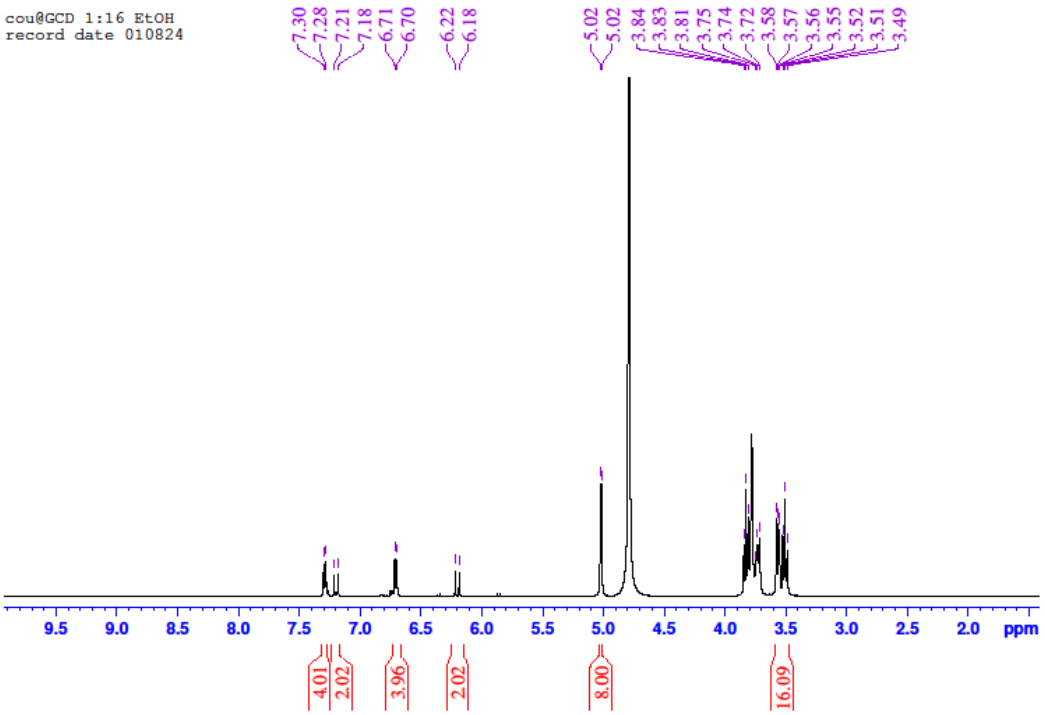

Figure S31: $^{13}C$ (inverse gated $^{1}H$ decoupled)NMR spectrum of COU@HDMOF(1:16) crystals grown from ethanol solvent diffusion (CIN@HDMOF-1)

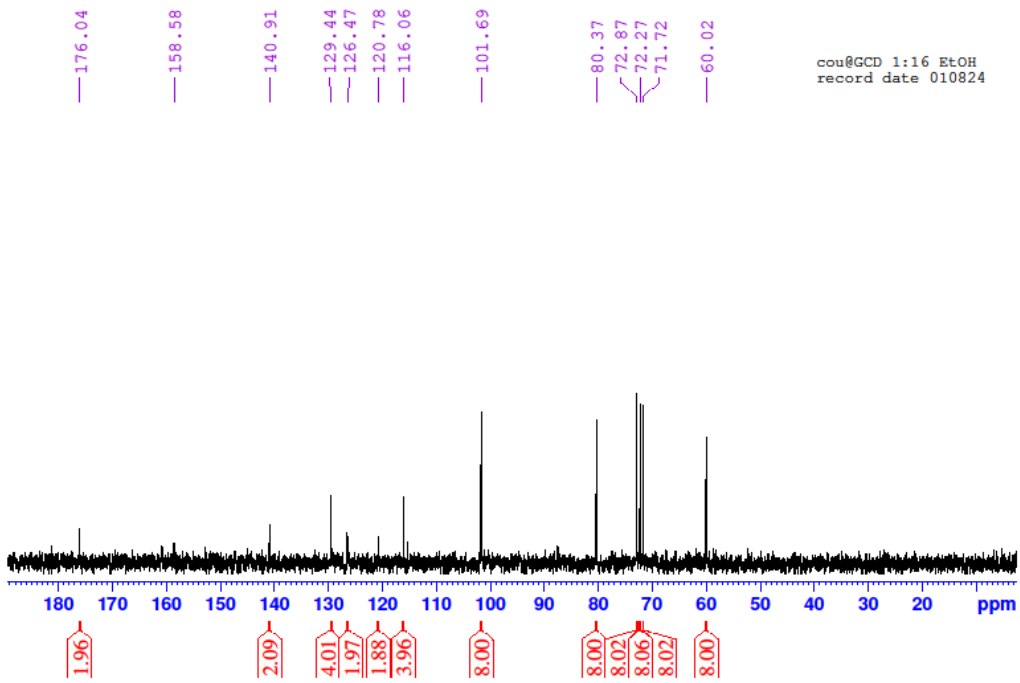

Figure S32: $^{1}$H NMR spectrum of COU@HDMOF(1:32) crystals grown from ethanol solvent diffusion (CIN@HDMOF-1.1)

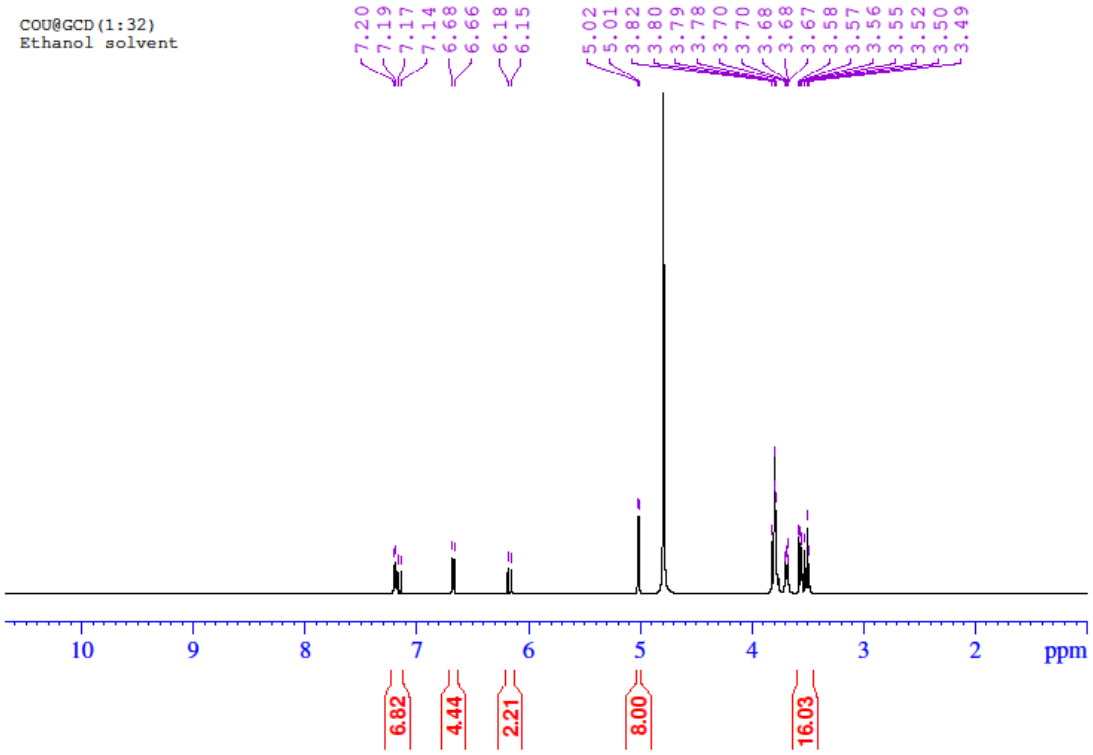

Figure S33: $^{13}C$ (inverse gated $^{1}H$ decoupled)NMR spectrum of COU@HDMOF(1:32) crystals grown from ethanol solvent diffusion (COU@HDMOF-1.1)

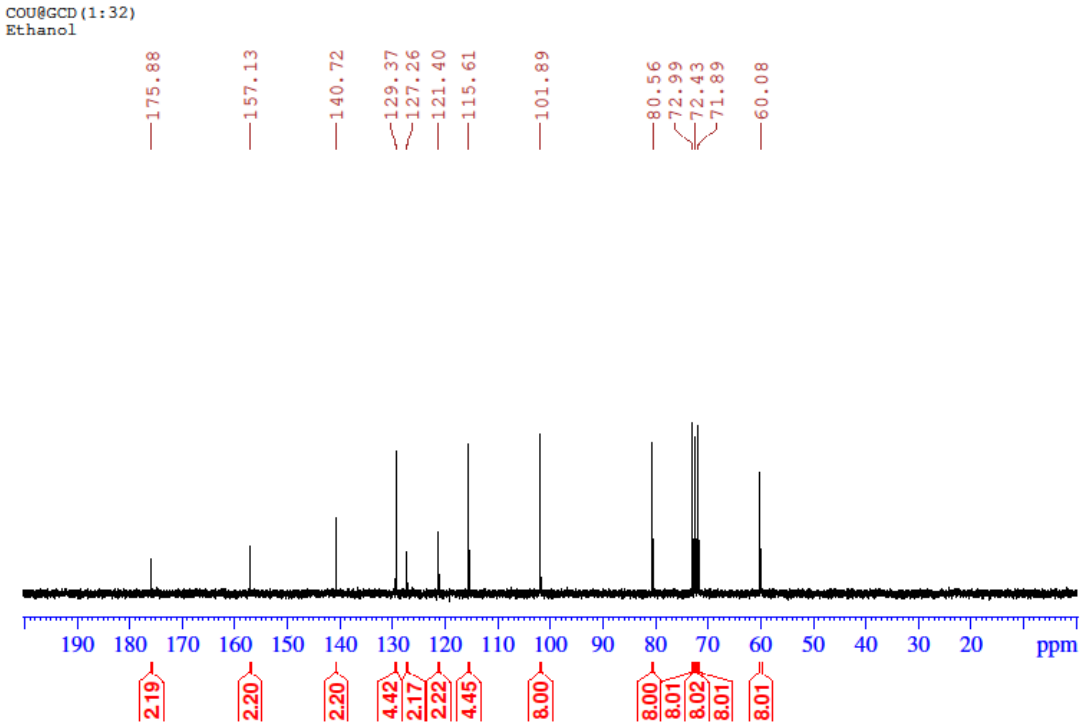

Figure S34: $^{1}$H NMR spectrum of FA@HDMOF(1:8) crystals grown from ethanol solvent diffusion (FA@HDMOF-0.65)

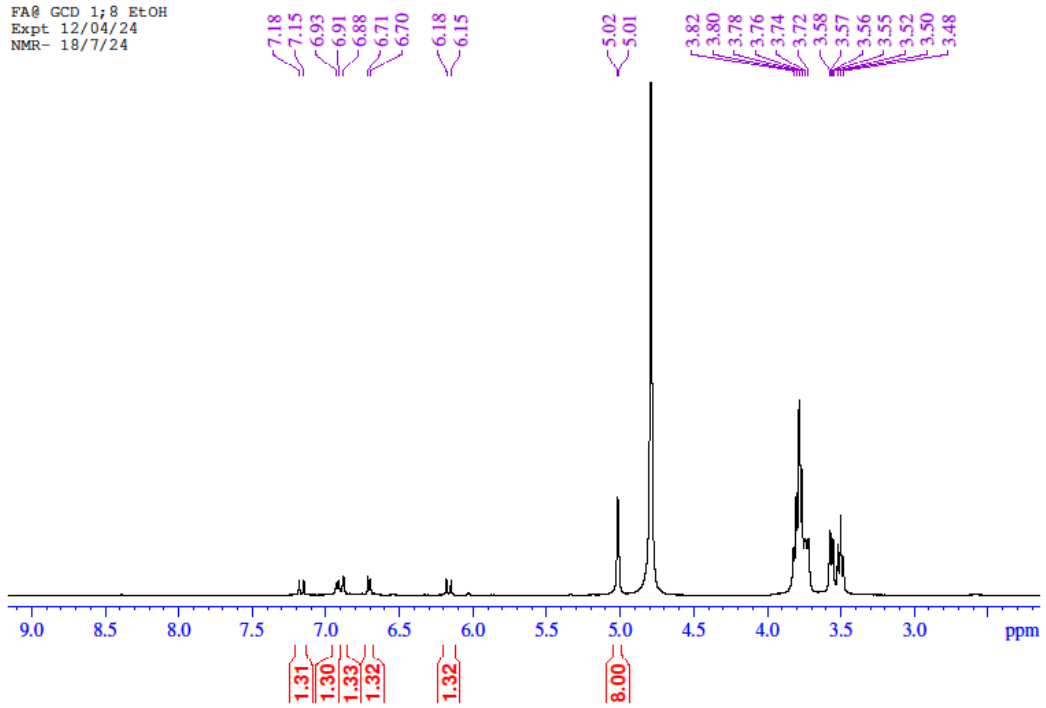

Figure S35: $^{13}C$ (inverse gated $^{1}H$ decoupled)NMR spectrum of FA@HDMOF(1:8) crystals grown from ethanol solvent diffusion (FA@HDMOF-0.65)

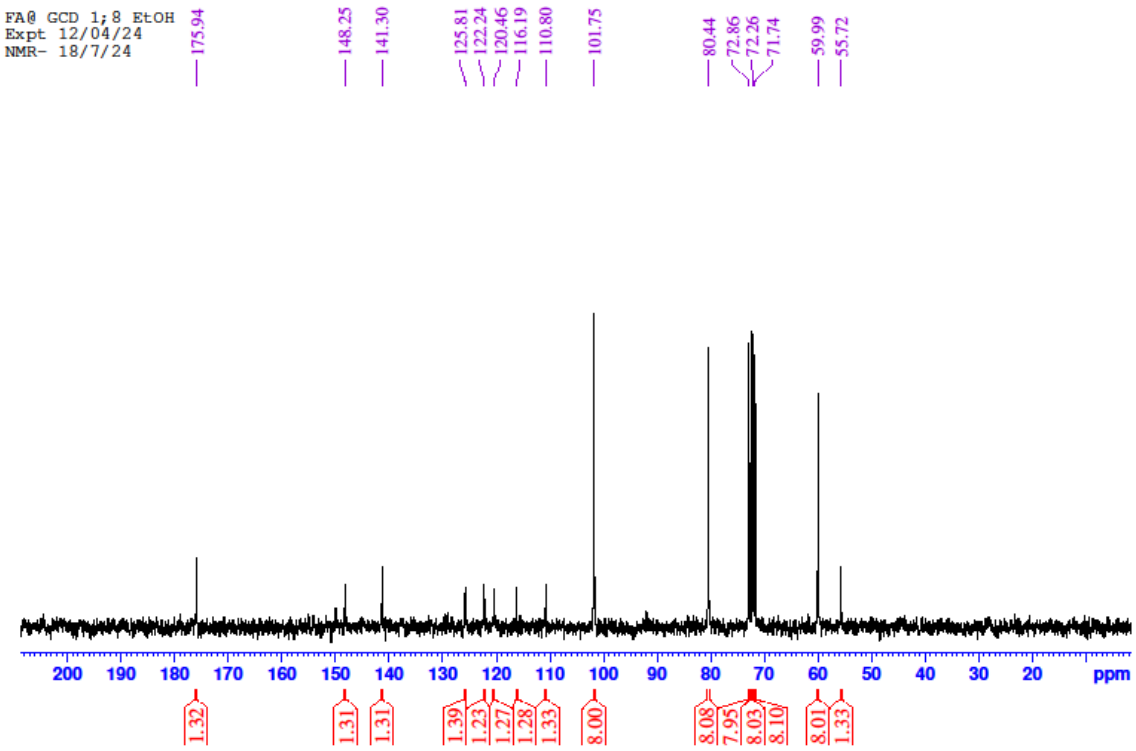

Figure S36: $^{1}$H NMR spectrum of FA@HDMOF(1:16) crystals grown from ethanol solvent diffusion (FA@HDMOF-0.75)

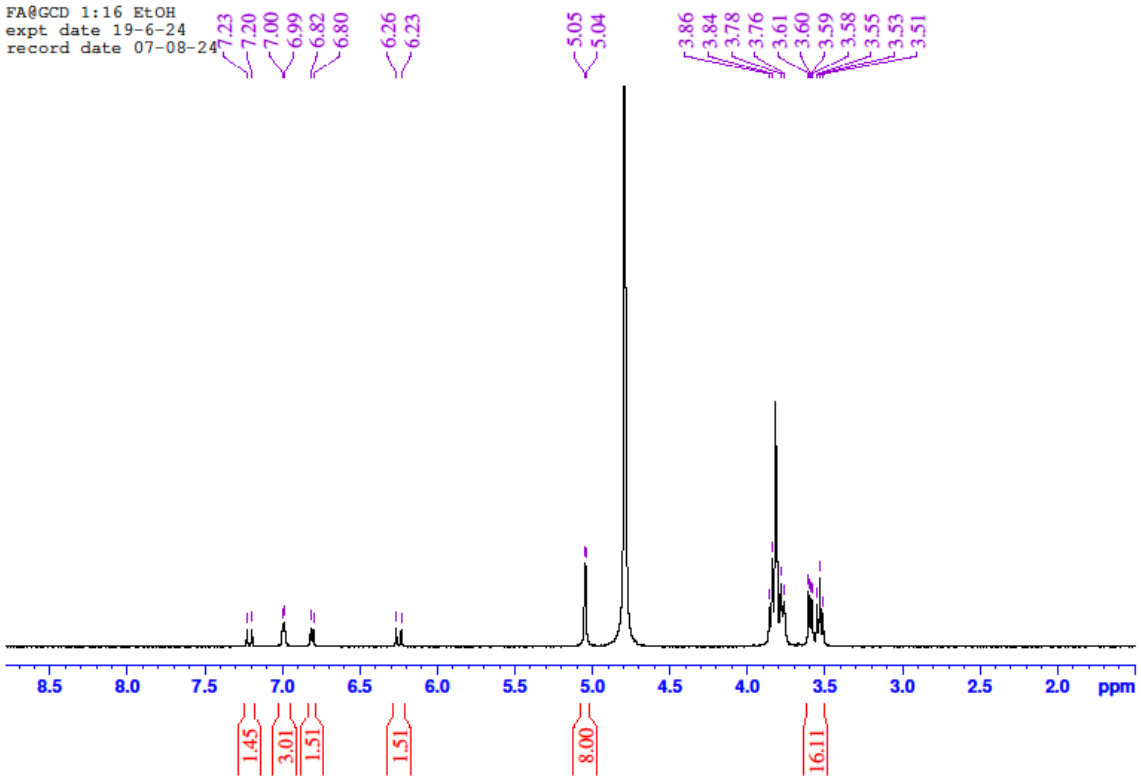

Figure S37: $^{13}C$ (inverse gated $^{1}H$ decoupled)NMR spectrum of FA@HDMOF(1:16) crystals grown from ethanol solvent diffusion (FA@HDMOF-0.75)

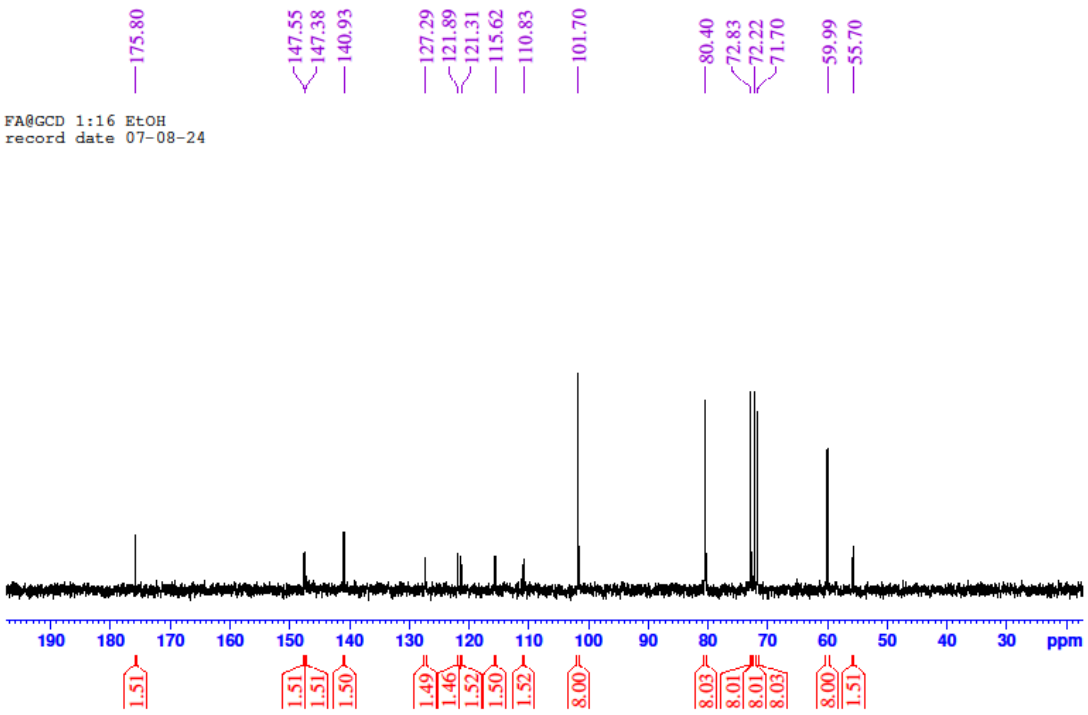

Figure S38: $^{1}$H NMR spectrum of FA@HDMOF(1:32) crystals grown from ethanol solvent diffusion (FA@HDMOF-0.65)

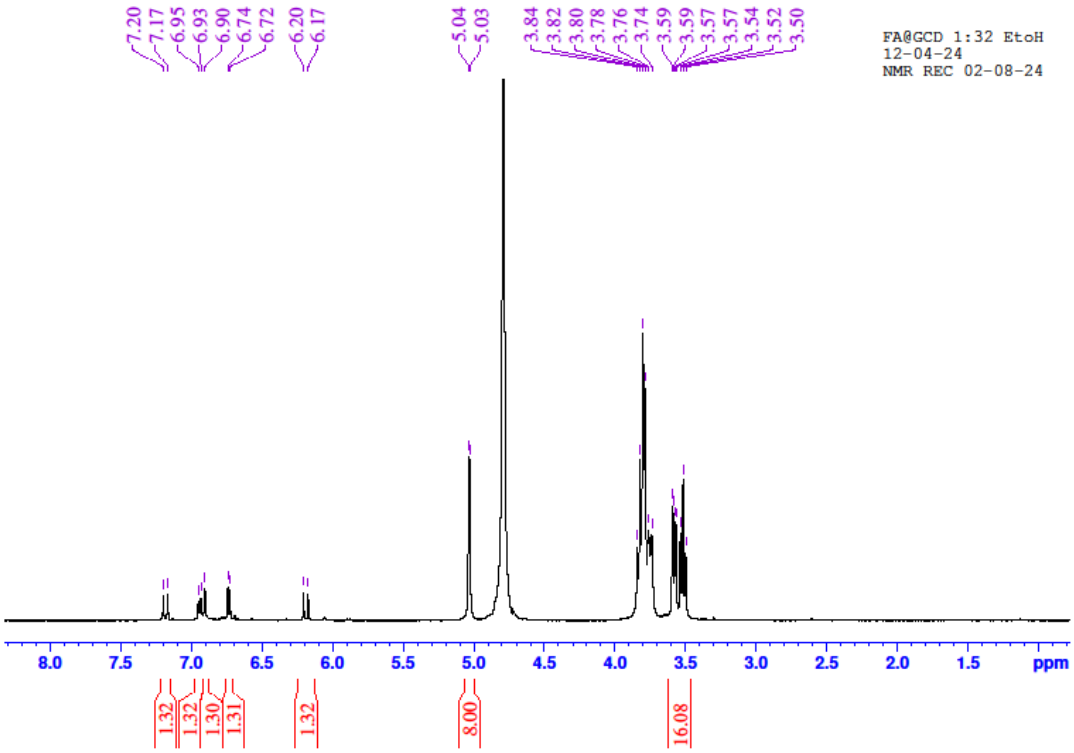

Figure S39: $^{13}C$ (inverse gated $^{1}H$ decoupled) NMR spectrum of FA@HDMOF(1:32) crystals grown from ethanol solvent diffusion (FA@HDMOF-0.65 )

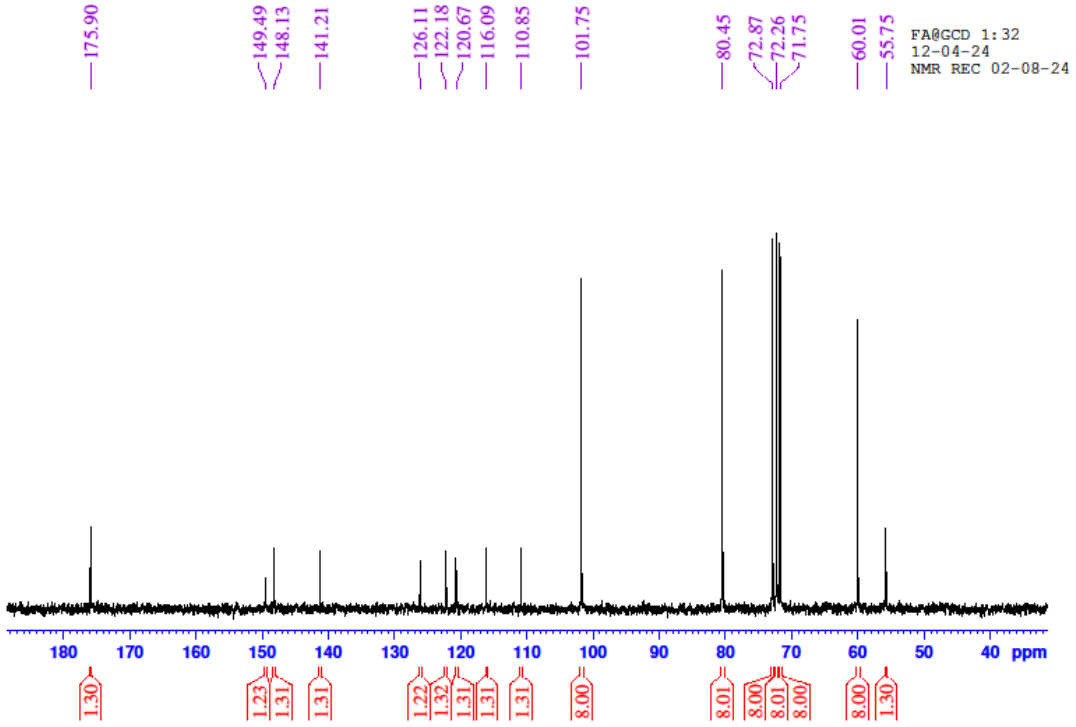

Figure S40: $^{1}$H NMR spectrum of CIN@HDMOF(1:8) crystals grown from methanol solvent diffusion (CIN@HDMOF-1.1)

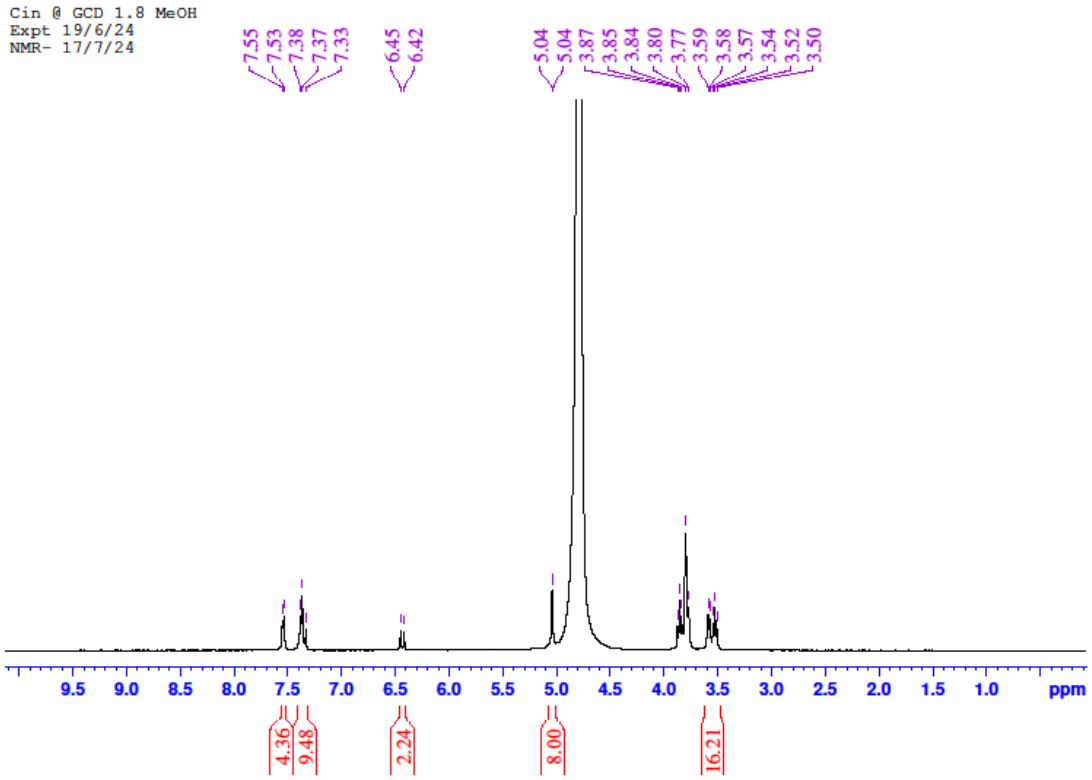

Figure S41: $^{13}C$ (inverse gated $^{1}H$ decoupled)NMR spectrum of CIN@HDMOF(1:8) crystals grown from methanol solvent diffusion (CIN@HDMOF-1.1)

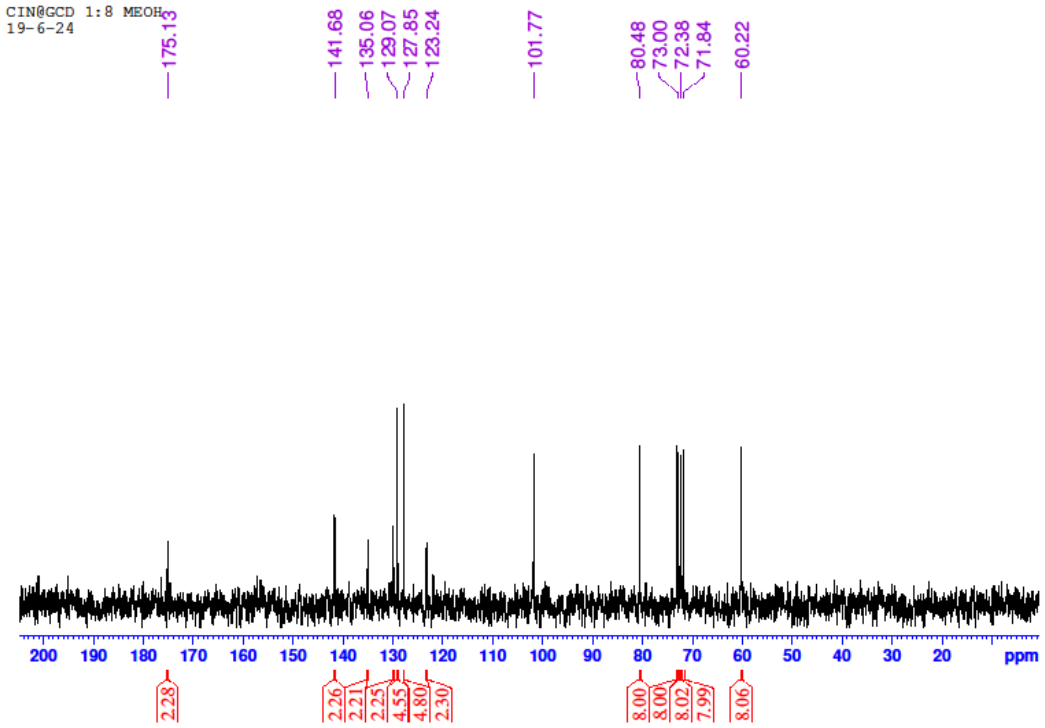

Figure S42: $^{1}$H NMR spectrum of CIN@HDMOF(1:16) crystals grown from methanol solvent diffusion (CIN@HDMOF-1.3)

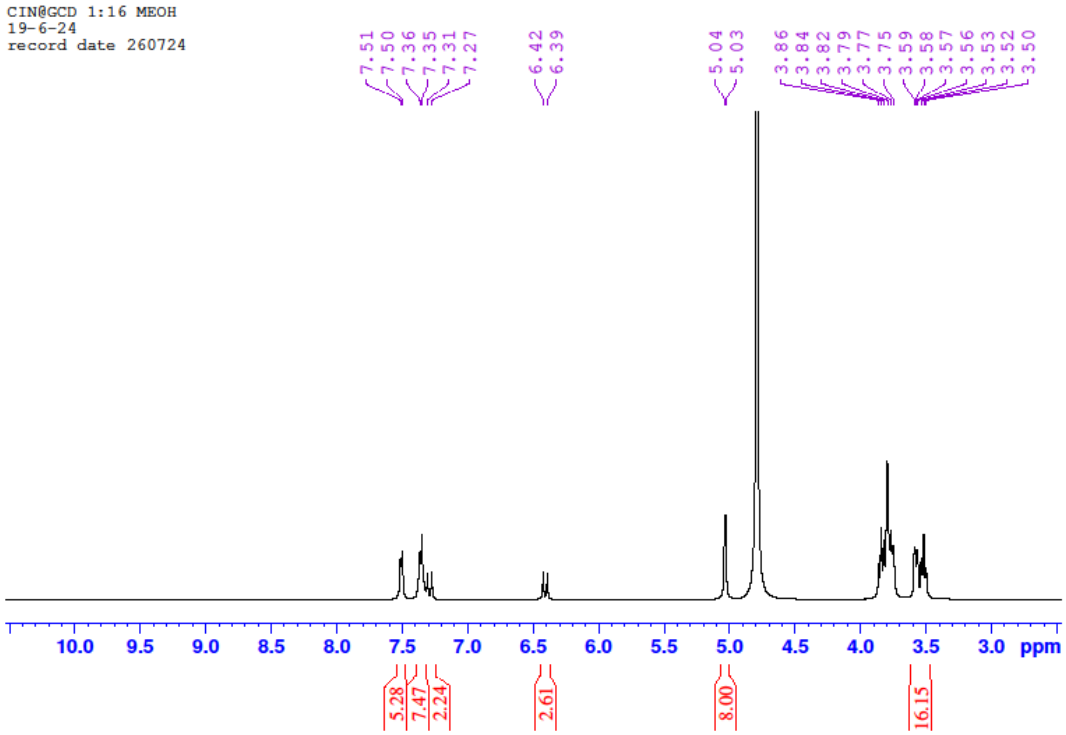

Figure S43: $^{13}C$ (inverse gated $^{1}H$ decoupled) NMR spectrum of CIN@HDMOF(1:6) crystals grown from methanol solvent diffusion (CIN@HDMOF-1.3)

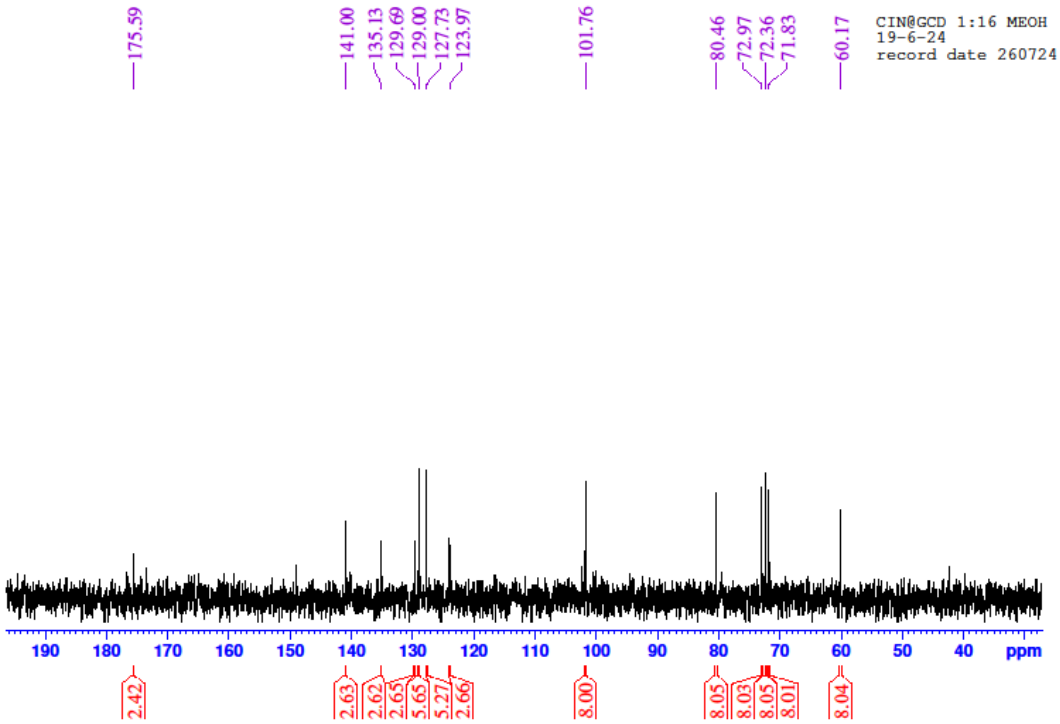

Figure S44: $^{1}$H NMR spectrum of CIN@HDMOF(1:32) crystals grown from methanol solvent diffusion (CIN@HDMOF-1.1)

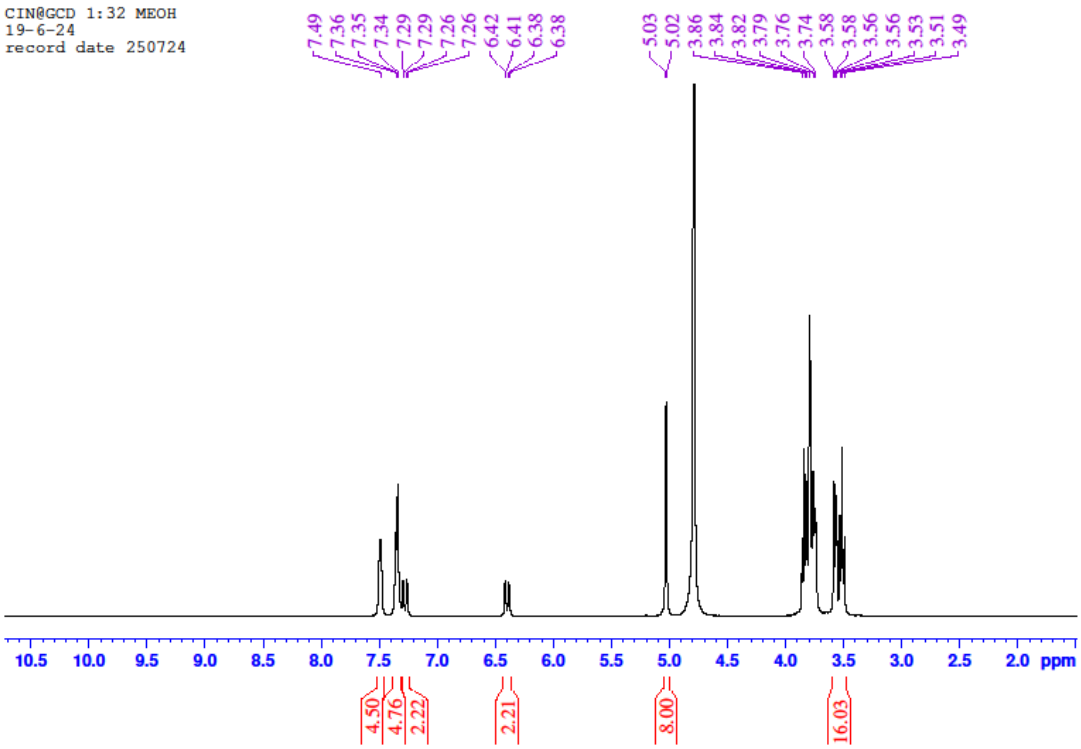

Figure S45: $^{13}C$ (inverse gated $^{1}H$ decoupled) NMR spectrum of CIN@HDMOF(1:32) crystals grown from methanol solvent diffusion (CIN@HDMOF-1.1)

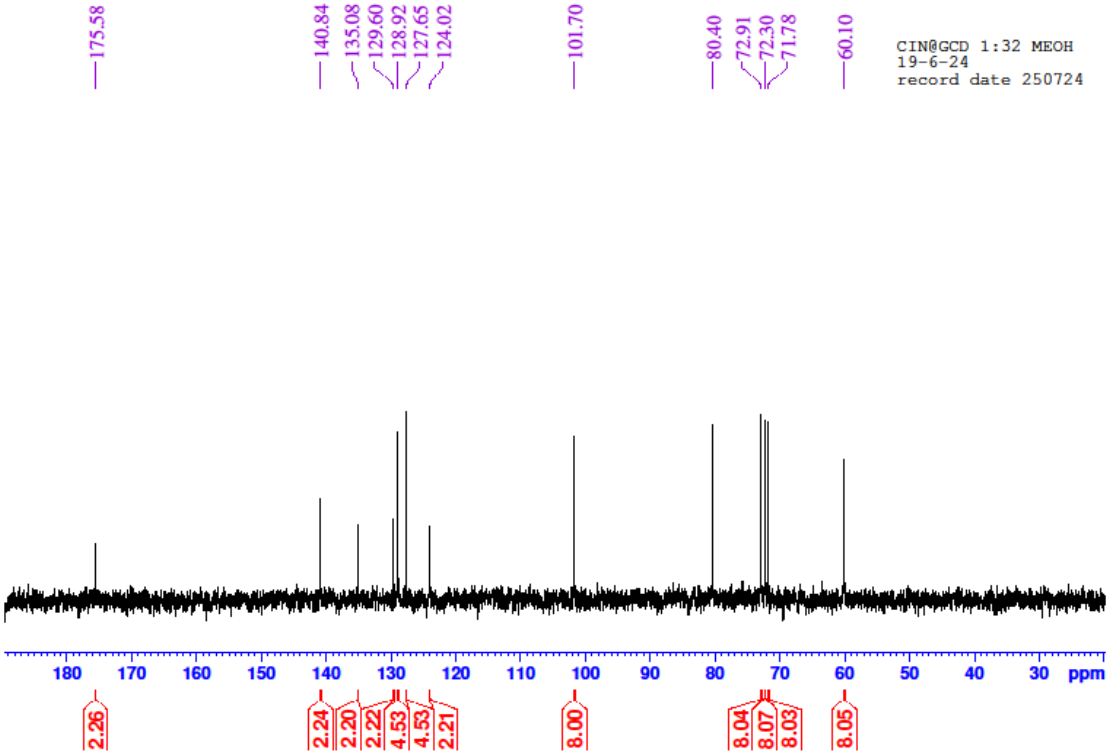

Figure S46: $^{1}$H NMR spectrum of COU@HDMOF(1:8) crystals grown from methanol solvent diffusion (COU@HDMOF-0.9 )

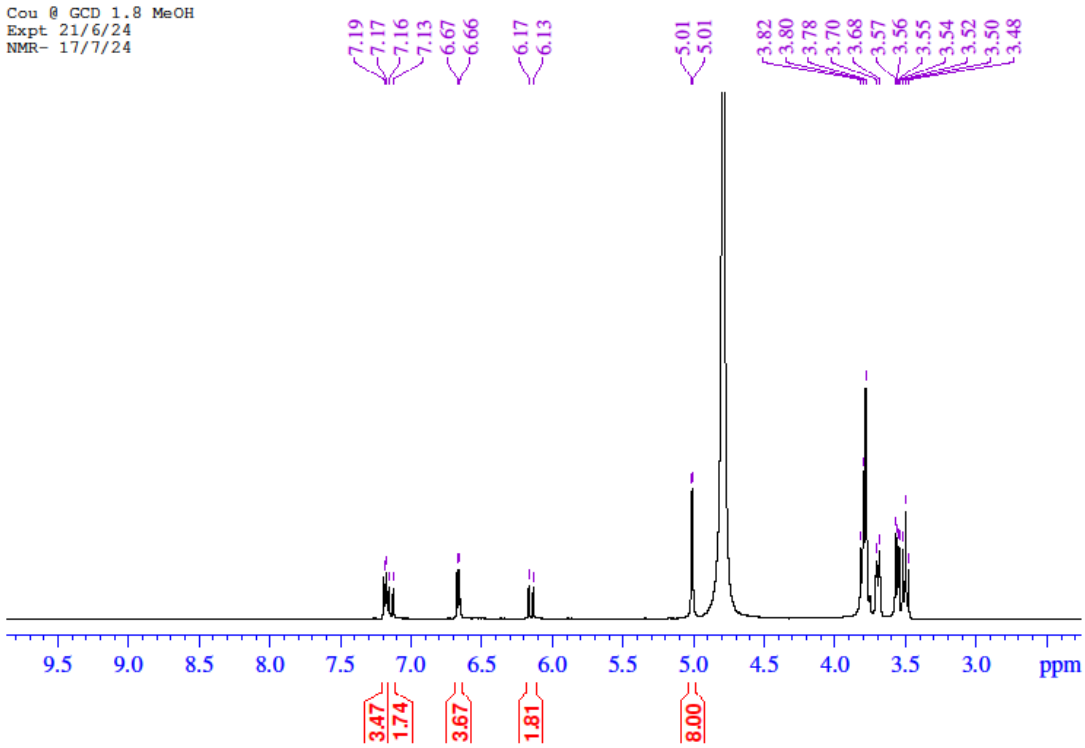

Figure S47: $^{13}C$ (inverse gated $^{1}H$ decoupled)NMR spectrum of COU@HDMOF(1:8) crystals grown from methanol solvent diffusion (COU@HDMOF-0.9)

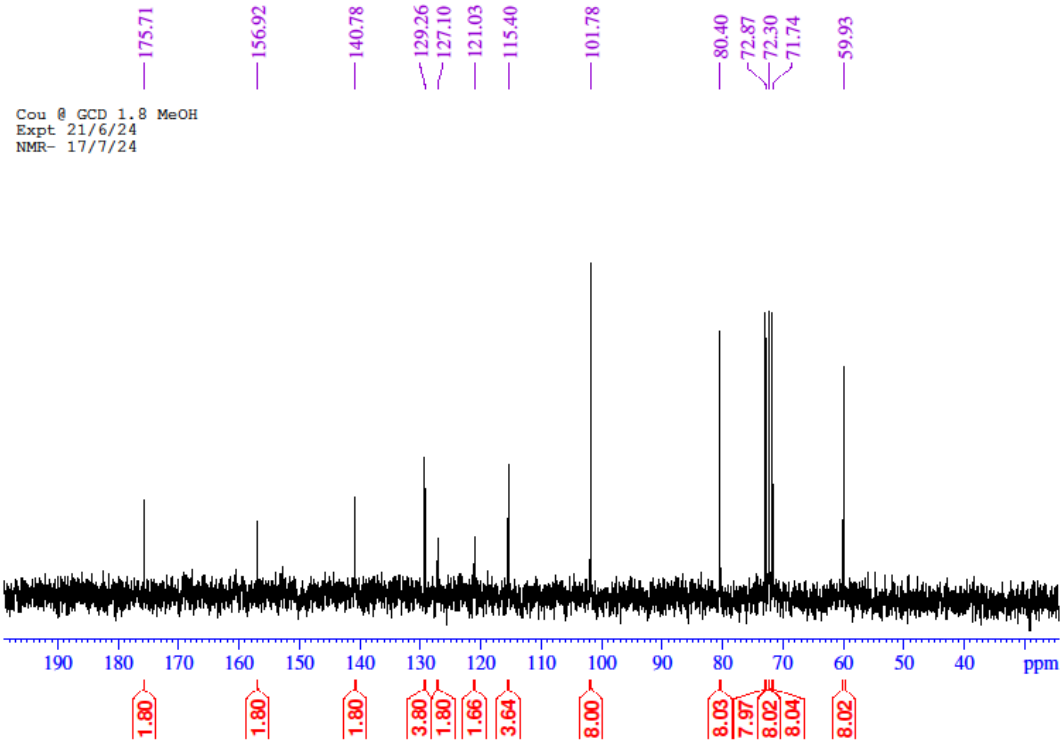

Figure S48: $^{1}$H NMR spectrum of COU@HDMOF(1:16) crystals grown from methanol solvent diffusion (COU@HDMOF-1)

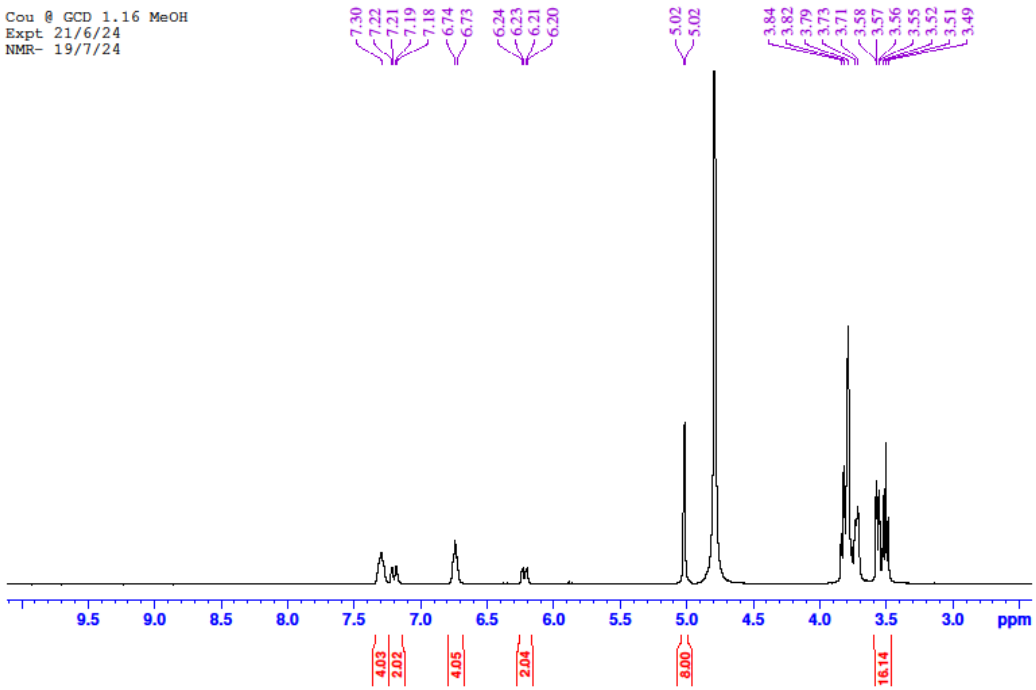

Figure S49: $^{13}C$ (inverse gated $^{1}H$ decoupled)NMR spectrum of COU@HDMOF(1:16) crystals grown from methanol solvent diffusion (CIN@HDMOF-1)

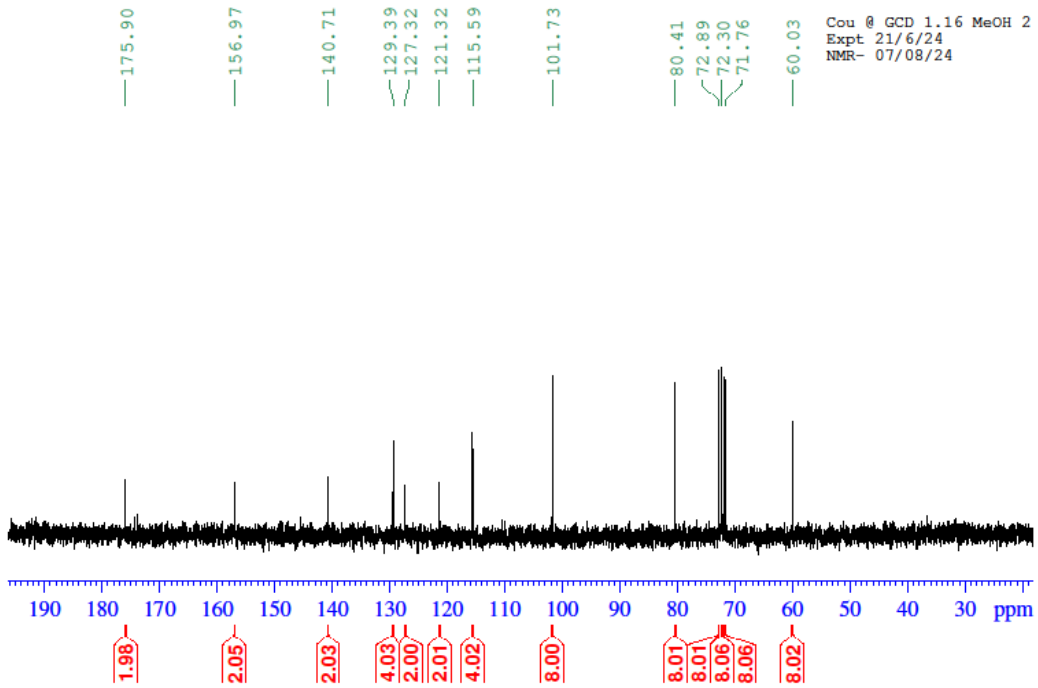

Figure S50: $^{1}$H NMR spectrum of COU@HDMOF(1:32) crystals grown from methanol solvent diffusion (CIN@HDMOF-1.1)

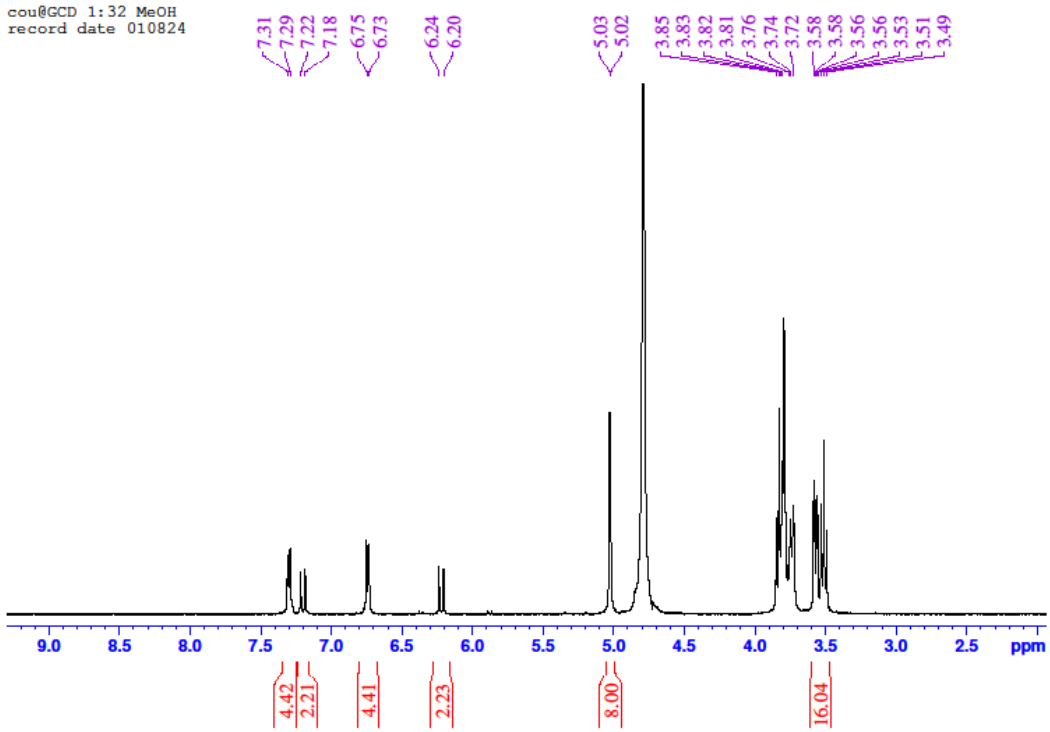

Figure S51: $^{13}C$ (inverse gated $^{1}H$ decoupled)NMR spectrum of COU@HDMOF(1:32) crystals grown from methanol solvent diffusion (COU@HDMOF-1.1)

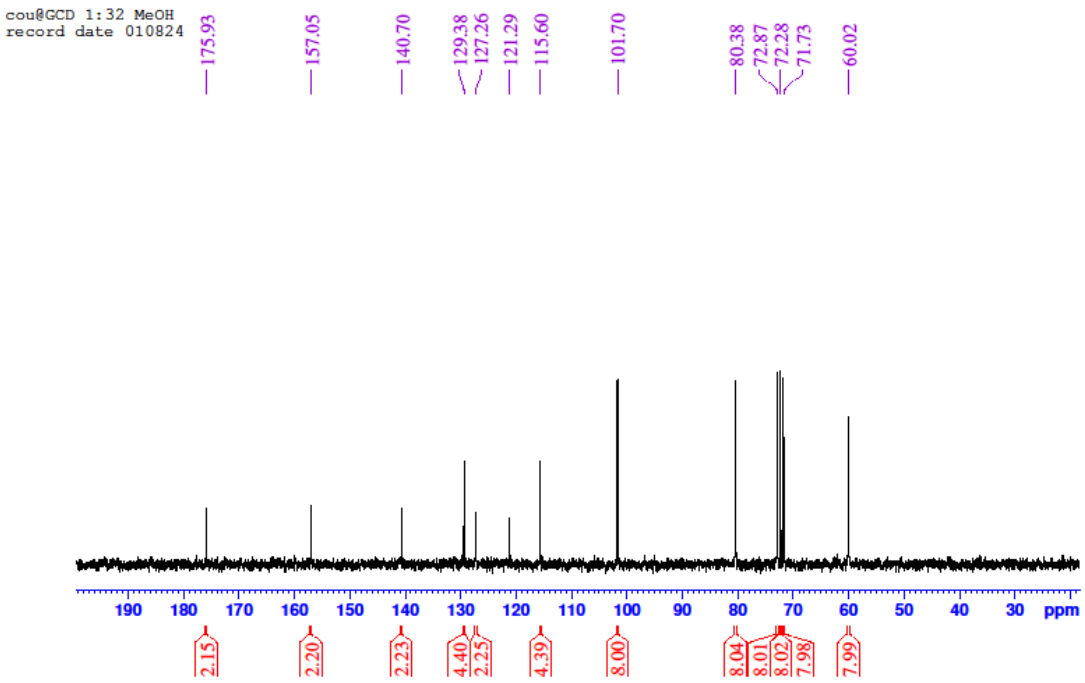

Figure S52: $^{1}$H NMR spectrum of FA@HDMOF(1:8) crystals grown from methanol solvent diffusion (FA@HDMOF-0.85)

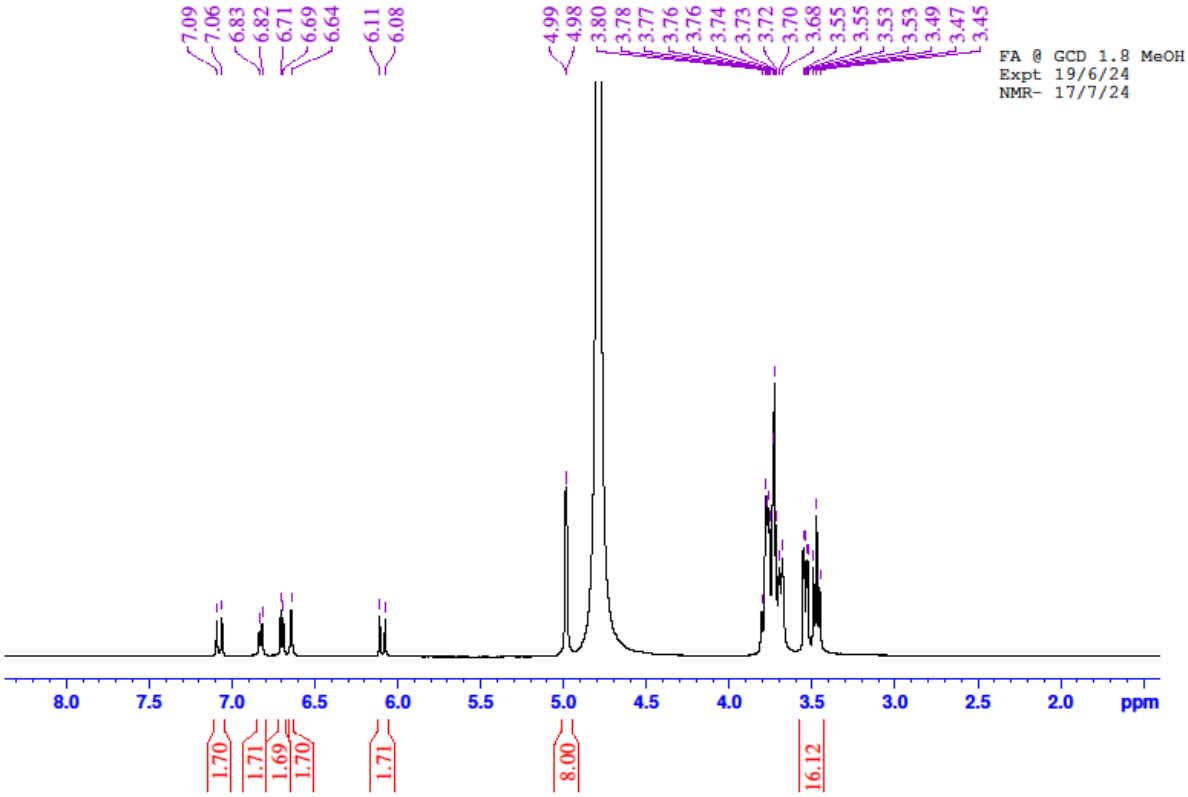

Figure S53: $^{13}C$ (inverse gated $^{1}H$ decoupled) NMR spectrum of FA@HDMOF(1:8) crystals grown from methanol solvent diffusion (FA@HDMOF-0.85)

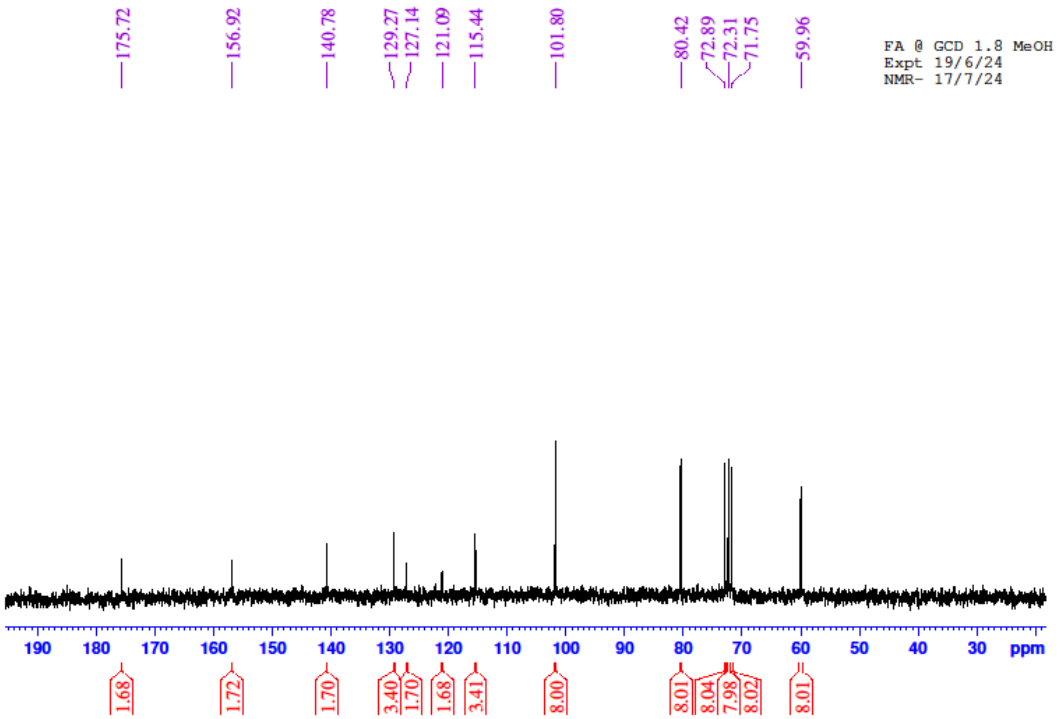

Figure S54: $^{1}$H NMR spectrum of FA@HDMOF(1:16) crystals grown from methanol solvent diffusion (FA@HDMOF-1.2)

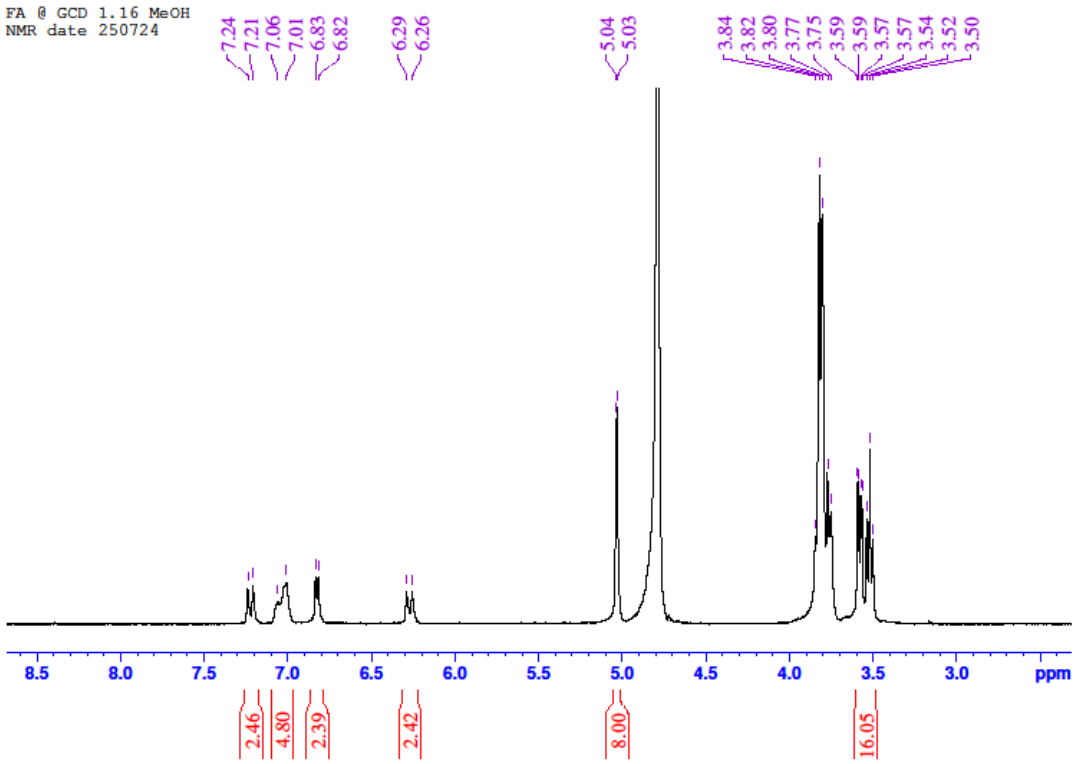

Figure S55: $^{13}C$ (inverse gated $^{1}H$ decoupled) NMR spectrum of FA@HDMOF(1:16) crystals grown from methanol solvent diffusion (FA@HDMOF-1.2)

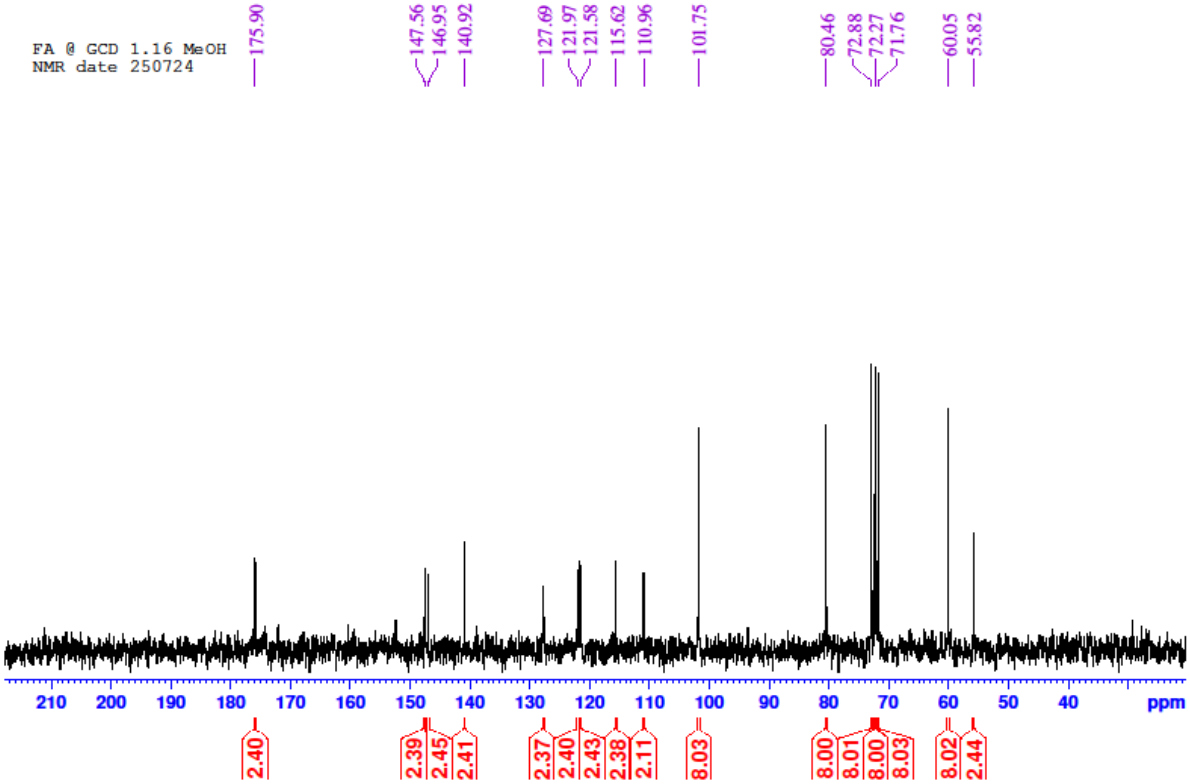

Figure S56: $^{1}$H NMR spectrum of FA@HDMOF(1:32) crystals grown from methanol solvent diffusion (FA@HDMOF-1.2.)

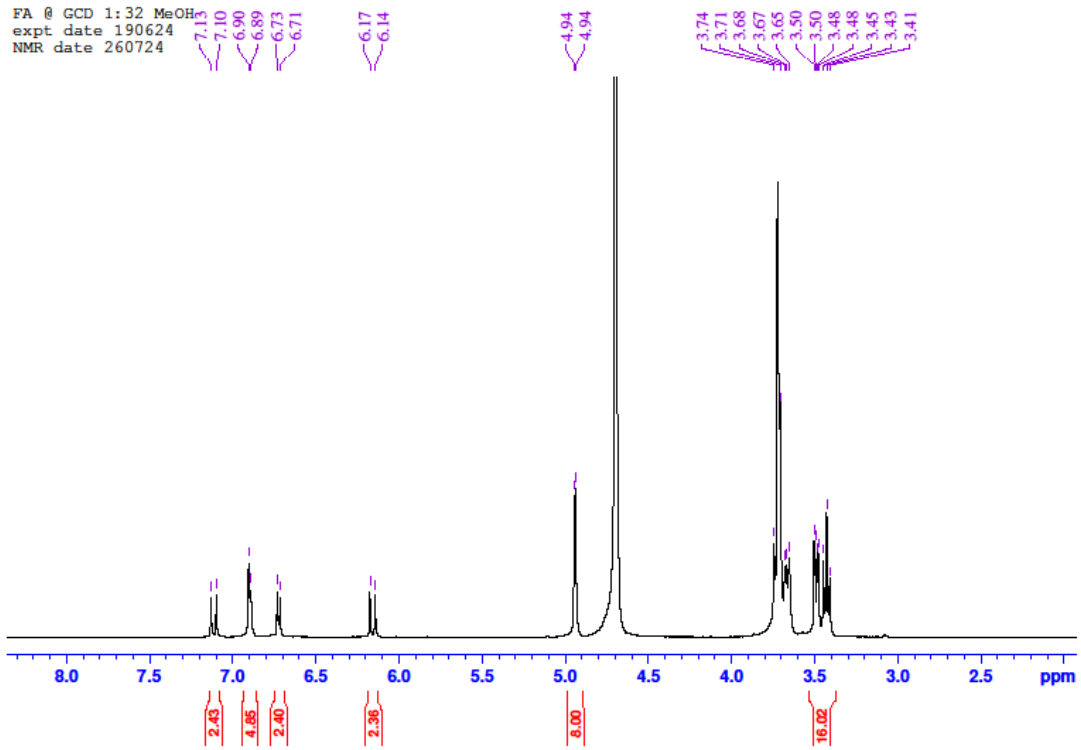

Figure S57: $^{13}C$ (inverse gated $^{1}H$ decoupled) NMR spectrum of CIN@HDMOF(1:32) crystals grown from methanol solvent diffusion (FA@HDMOF-1.2 )

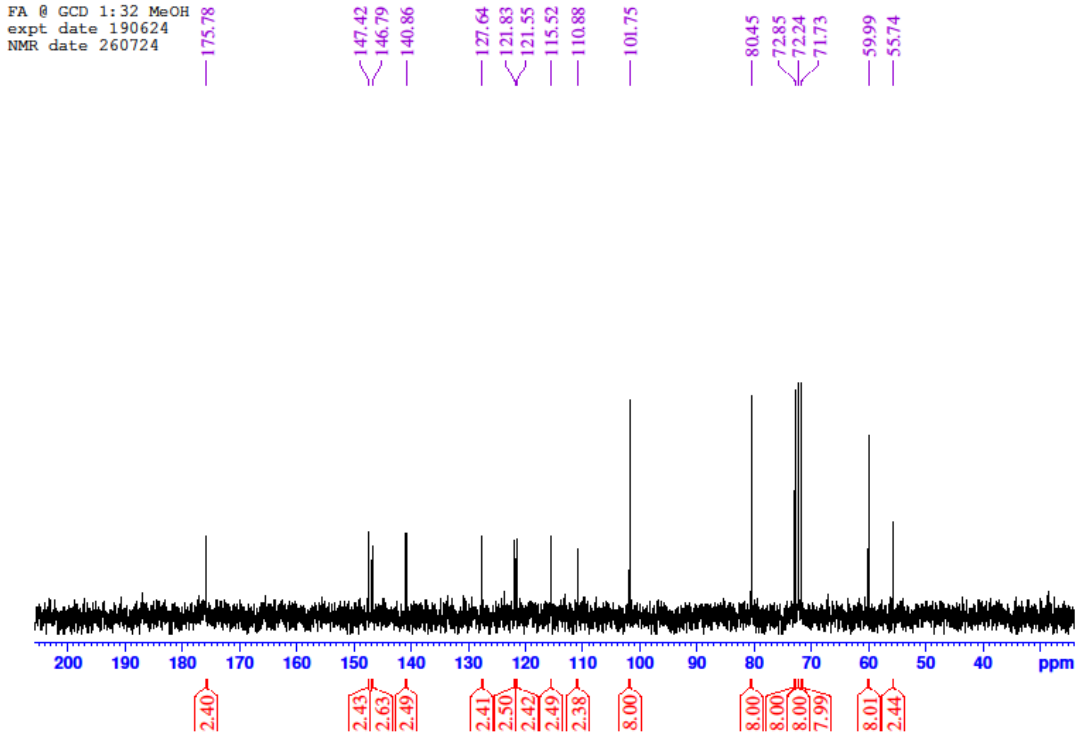

Figure S58: PXRD data of γ-CD

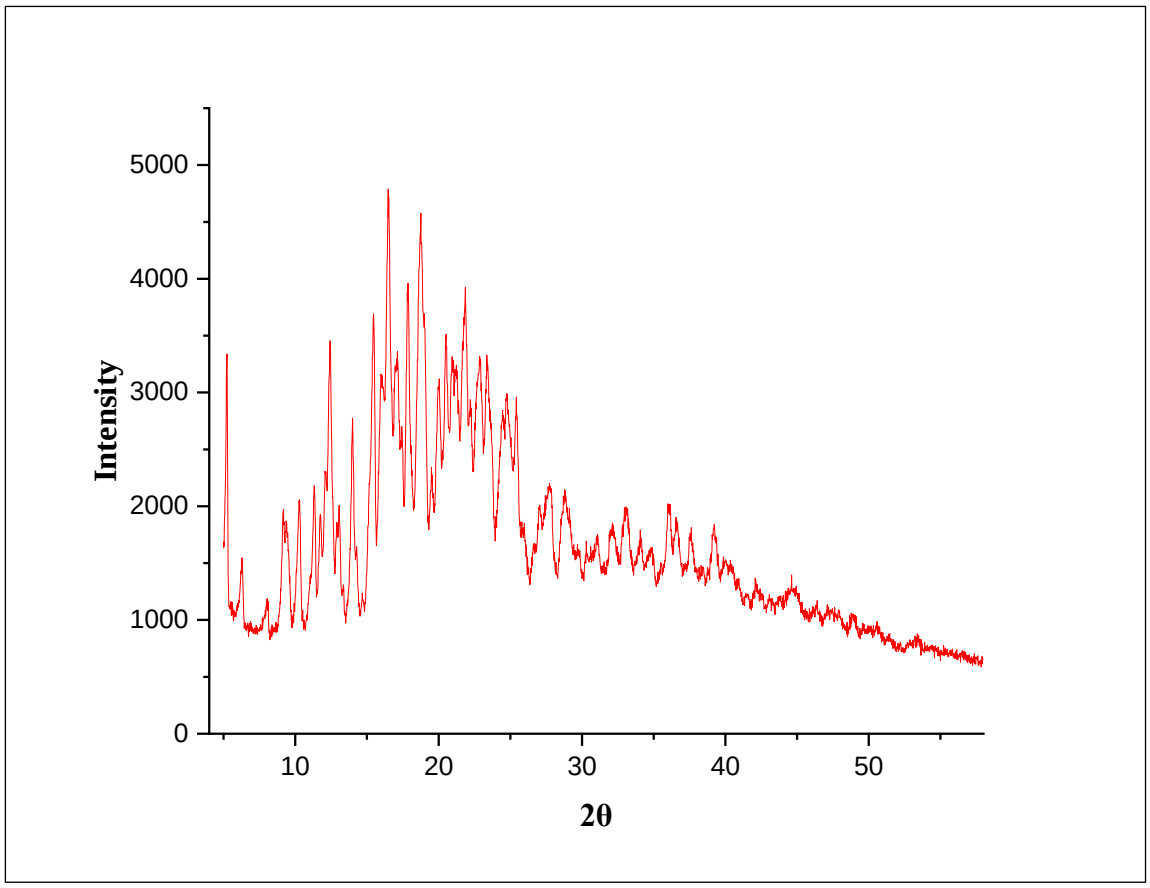

Figure S59: PXRD data of CIN@HDMOF(1:8) crystals grown from ethanol solvent diffusion (CIN@HDMOF-0.9)

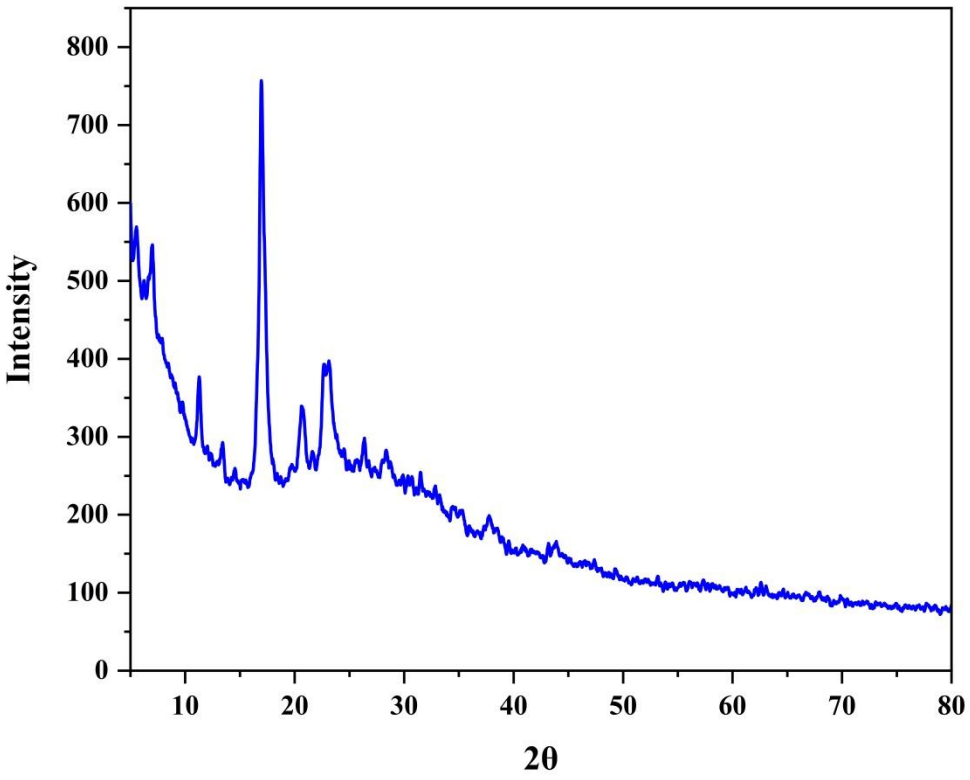

Figure S60: PXRD data of CIN@HDMOF(1:16) crystals grown from ethanol solvent diffusion (CIN@HDMOF-1.1)

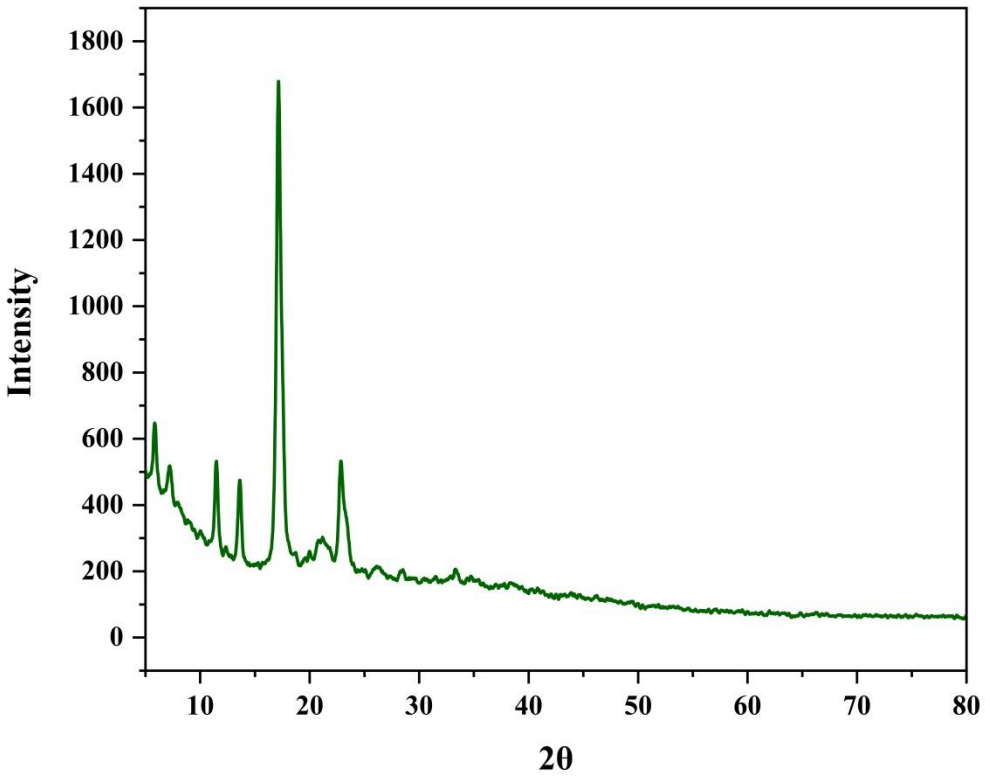

Figure S61: PXRD data of CIN@HDMOF(1:32) crystals grown from ethanol solvent diffusion (CIN@HDMOF-1.1)

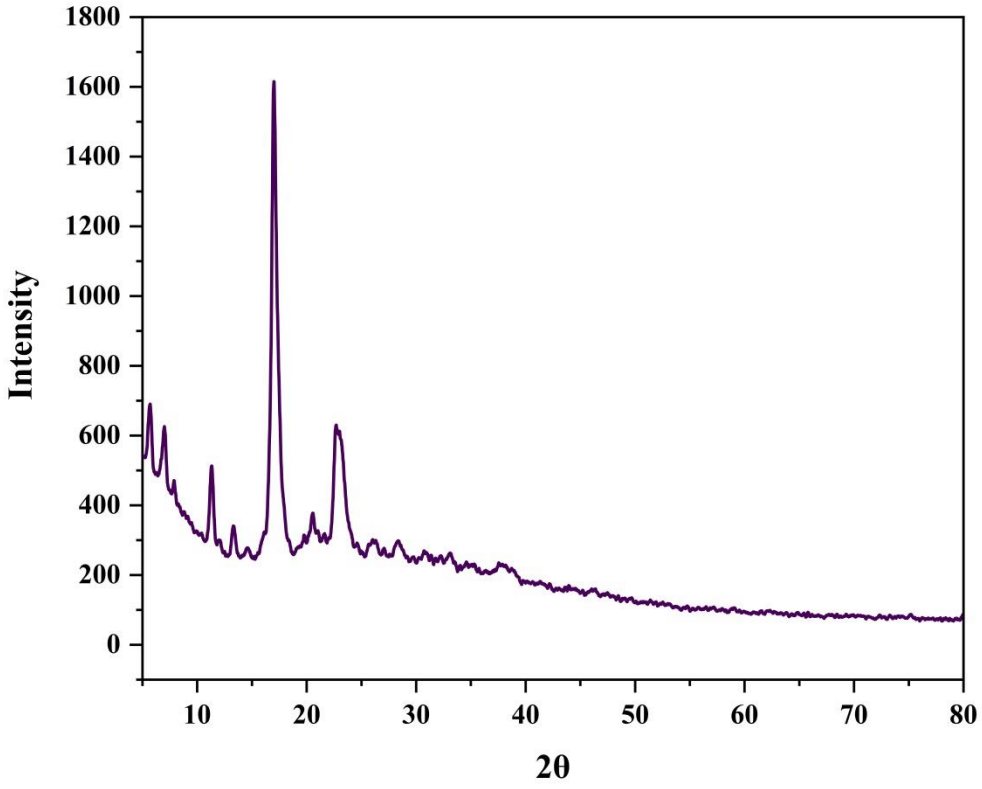

Figure S62: PXRD data of COU@HDMOF(1:8) crystals grown from ethanol solvent diffusion (COU@HDMOF-0.9 )

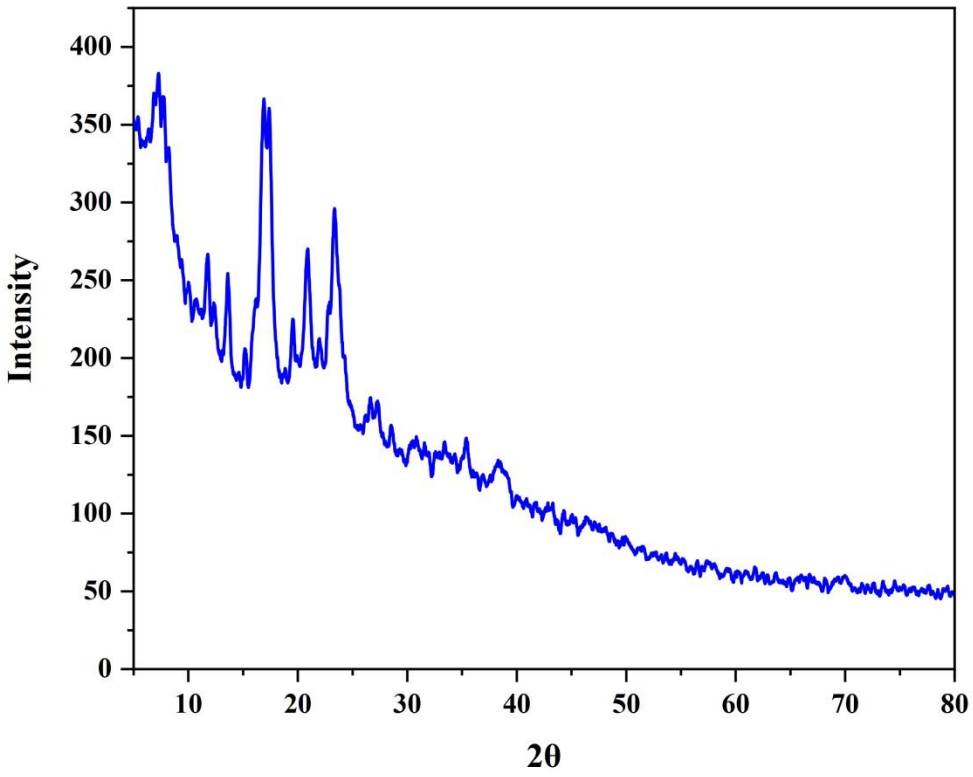

Figure S63: PXRD data of COU@HDMOF(1:16) crystals grown from ethanol solvent diffusion (COU@HDMOF-1)

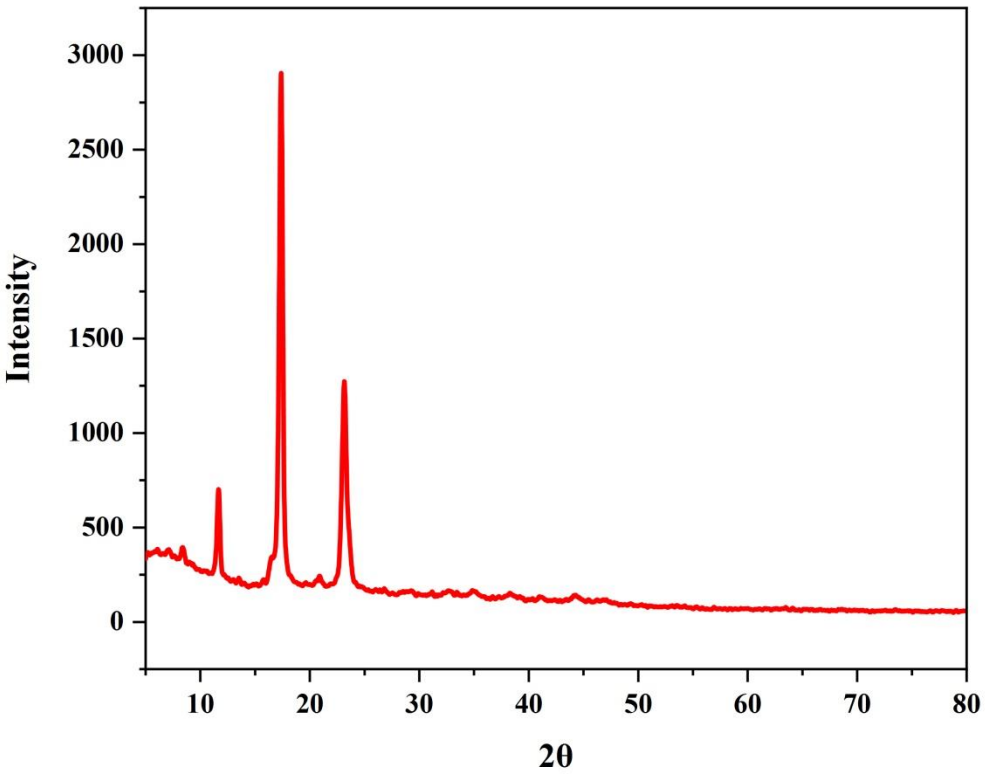

Figure S64: PXRD data of COU@HDMOF(1:32) crystals grown from ethanol solvent diffusion (CIN@HDMOF-1.1)

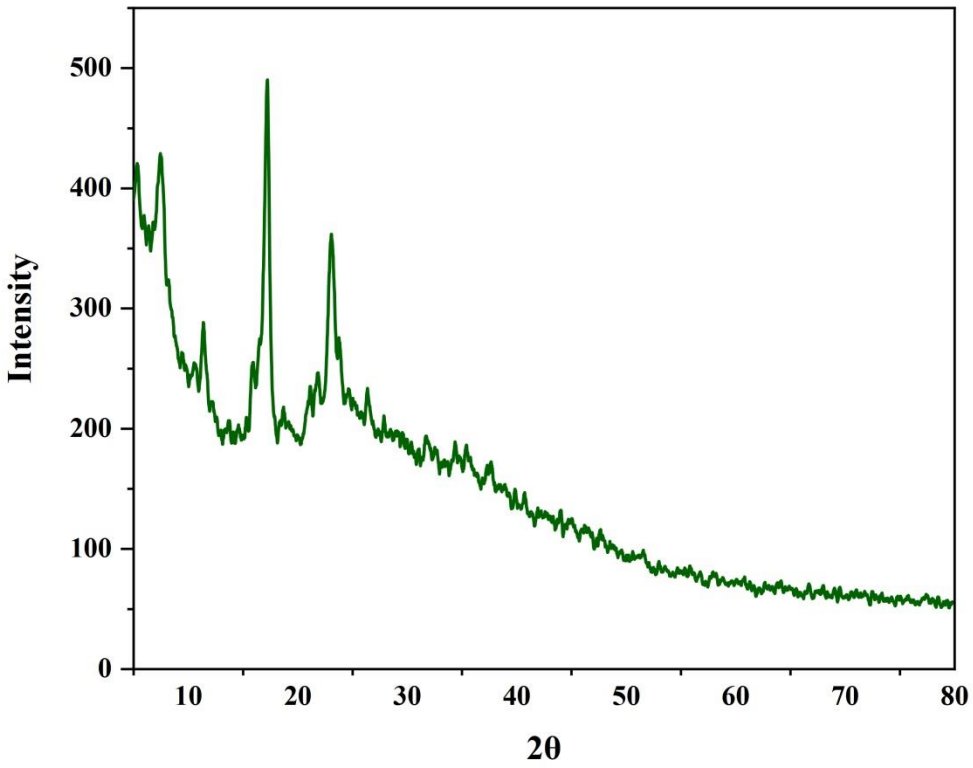

Figure S65: PXRD data of FA@HDMOF(1:8) crystals grown from ethanol solvent diffusion (FA@HDMOF-0.65)

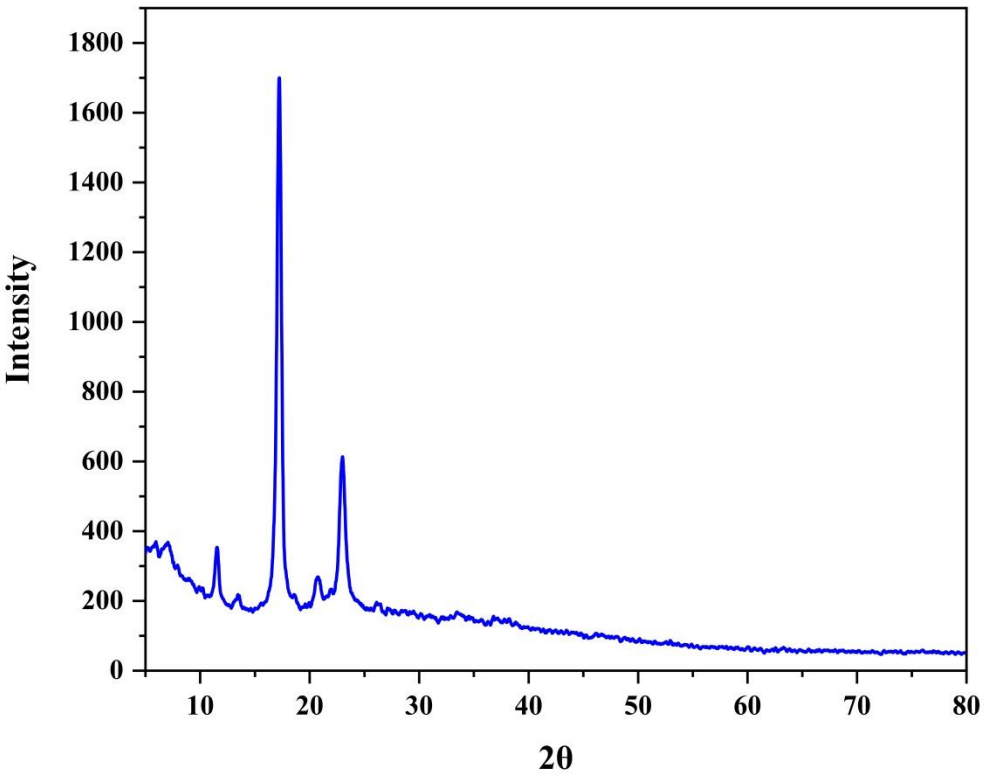

Figure S66: PXRD data of FA@HDMOF(1:16) crystals grown from ethanol solvent diffusion (FA@HDMOF-0.75)

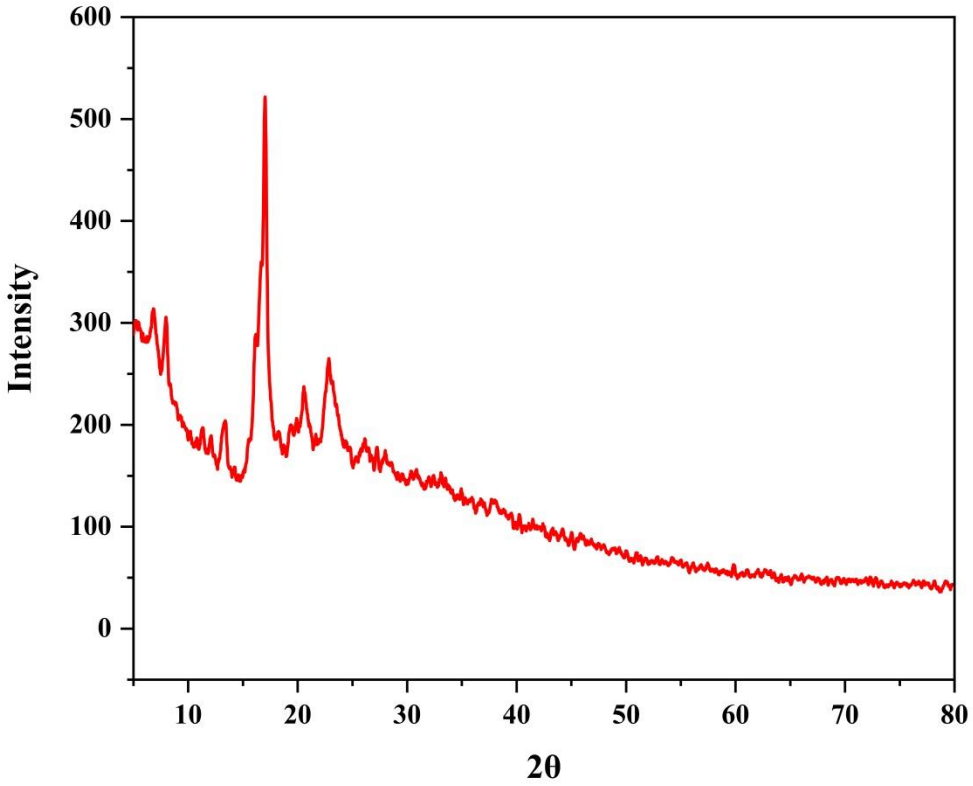

Figure S67: PXRD data of FA@HDMOF(1:32) crystals grown from ethanol solvent diffusion (FA@HDMOF-0.65)

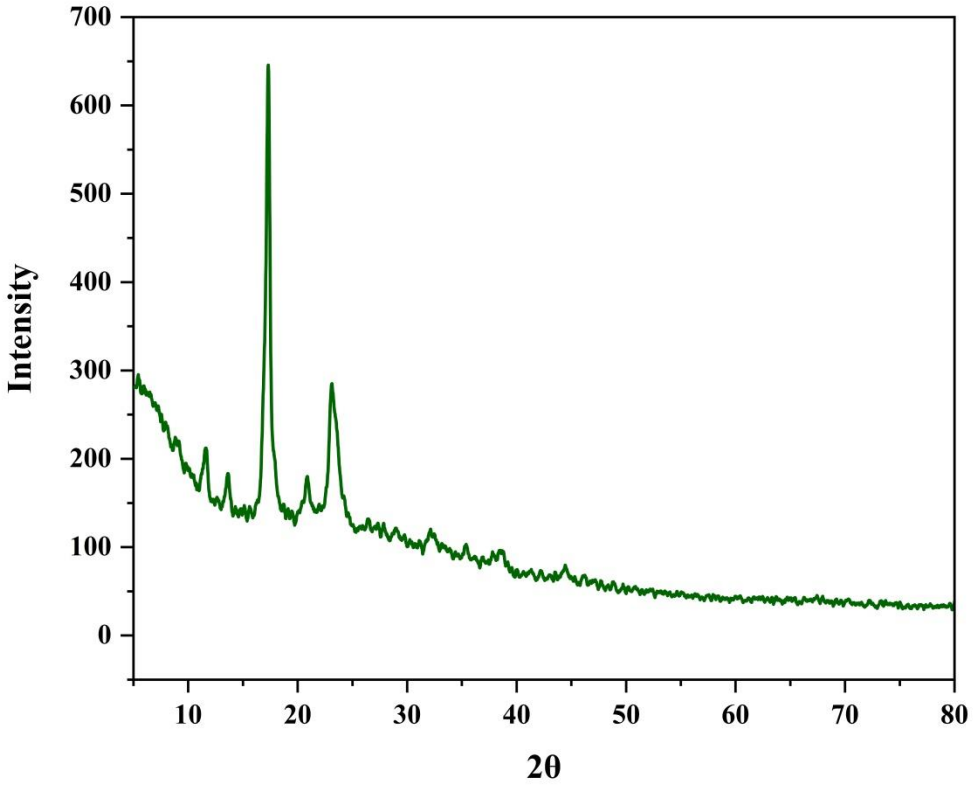

Figure S68: PXRD data of CIN@HDMOF(1:8) crystals grown from methanol solvent diffusion (CIN@HDMOF-1.1)

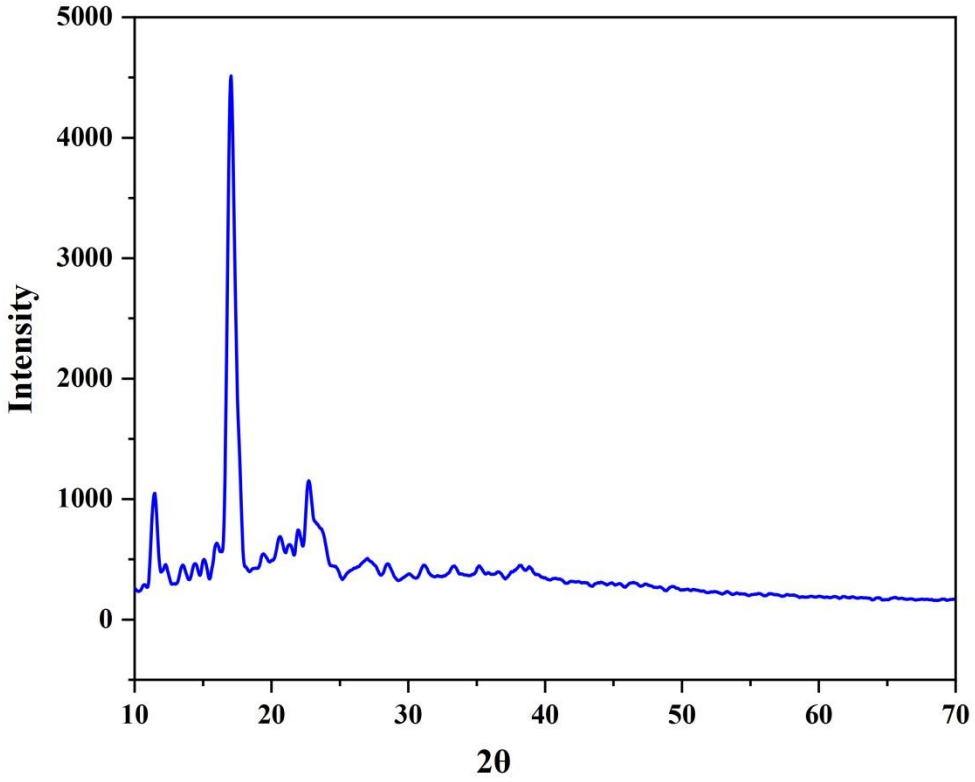

Figure S69: PXRD data of CIN@HDMOF(1:16) crystals grown from methanol solvent diffusion (CIN@HDMOF-1.3)

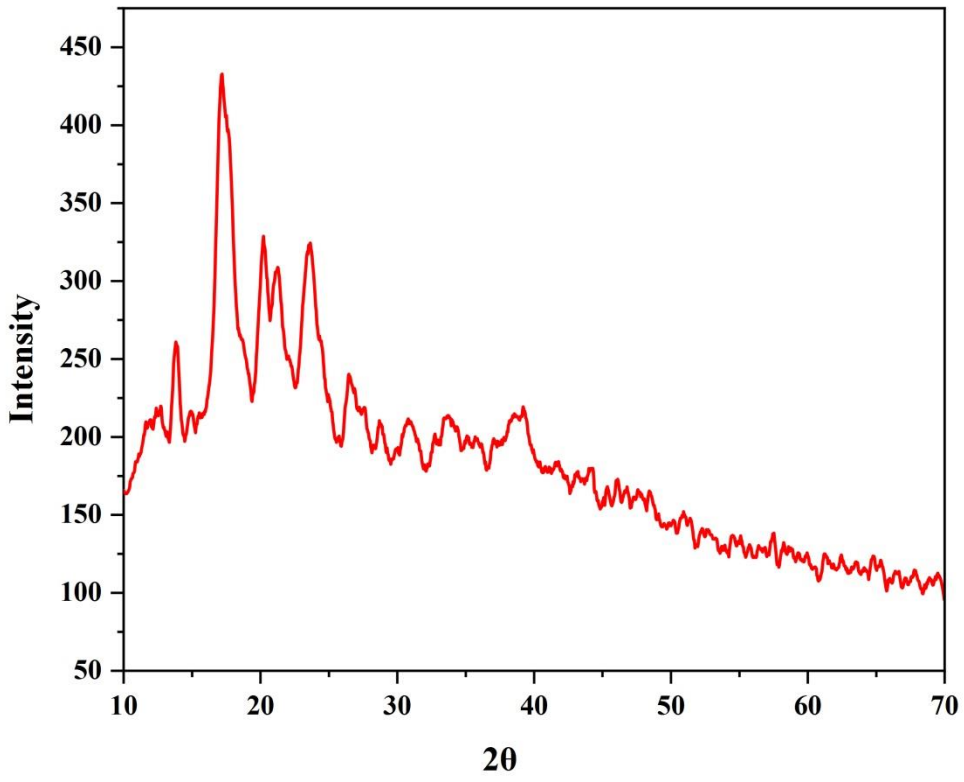

Figure S70: PXRD data of CIN@HDMOF(1:32) crystals grown from methanol solvent diffusion (CIN@HDMOF-1.1)

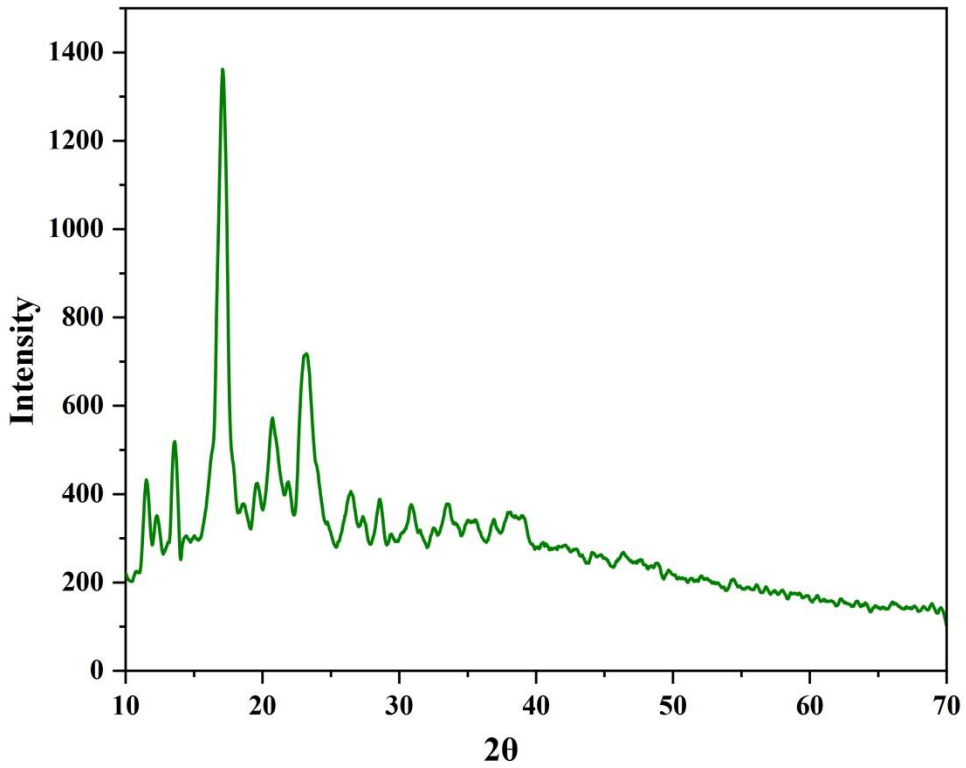

Figure S71: PXRD data of COU@HDMOF(1:8) crystals grown from methanol solvent diffusion (COU@HDMOF-0.9 )

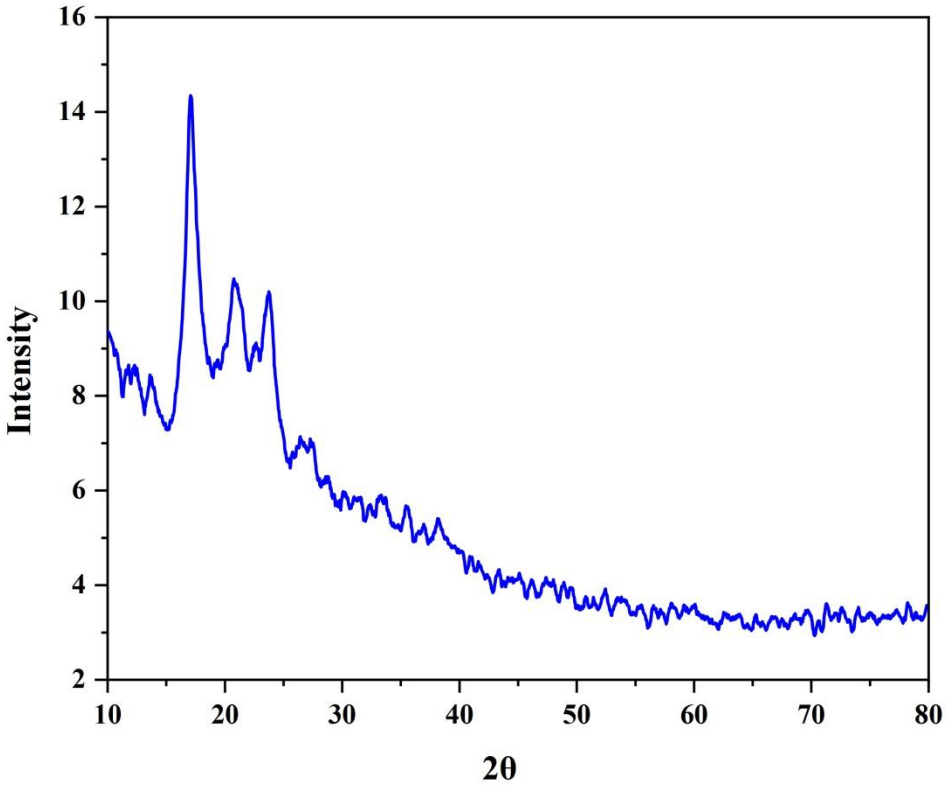

Figure S72: PXRD data of COU@HDMOF(1:16) crystals grown from methanol solvent diffusion (COU@HDMOF-1)

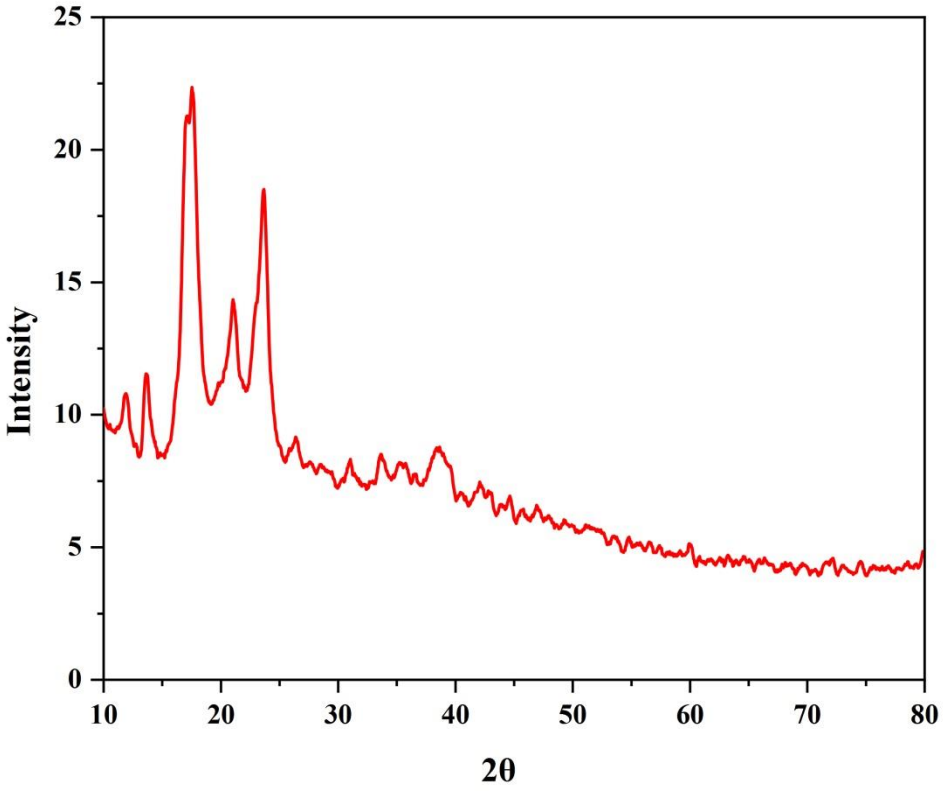

Figure S73: PXRD data of COU@HDMOF(1:32) crystals grown from methanol solvent diffusion (CIN@HDMOF-1.1)

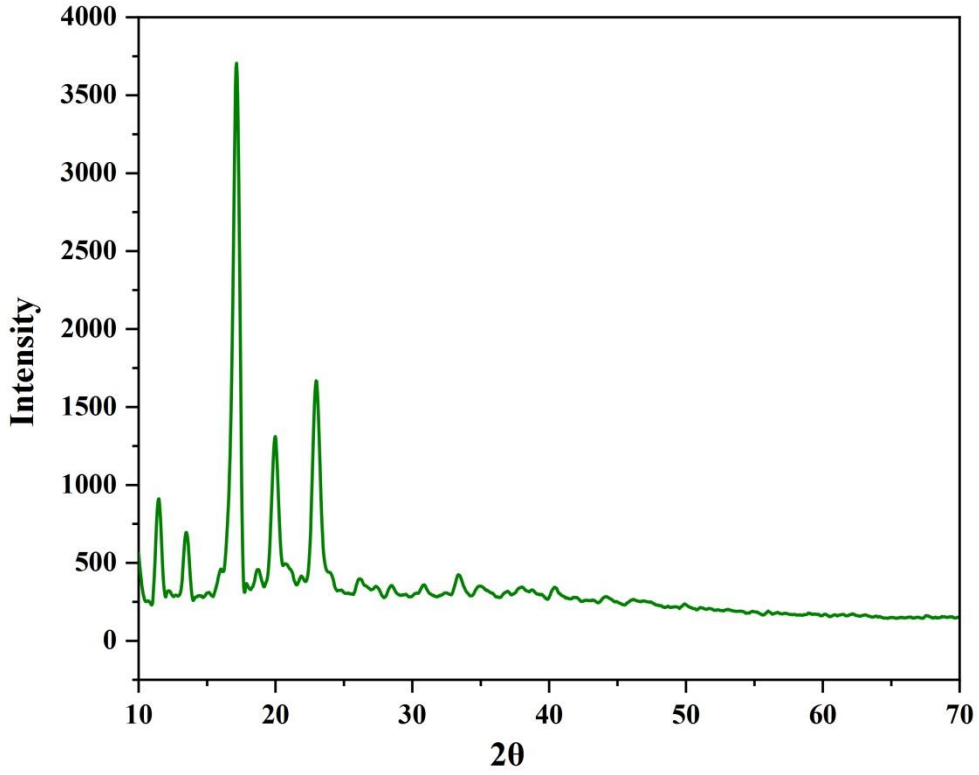

Figure S74: PXRD data of FA@HDMOF(1:8) crystals grown from methanol solvent diffusion (FA@HDMOF-0.85)

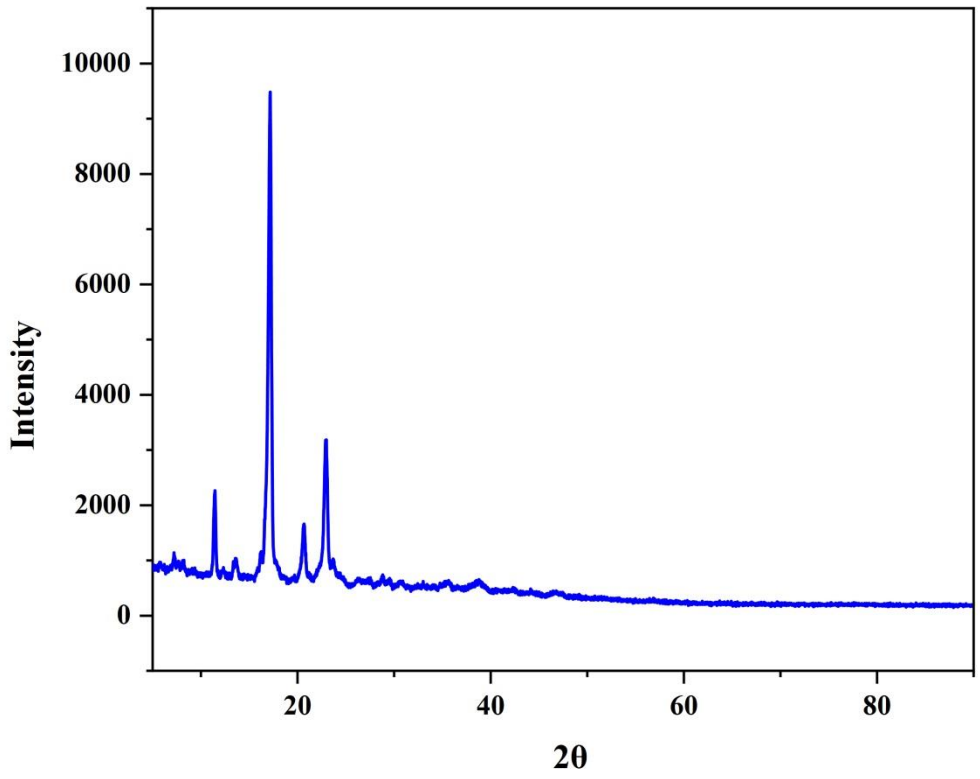

Figure S75: PXRD data of FA@HDMOF(1:16) crystals grown from methanol solvent diffusion (FA@HDMOF-1.2)

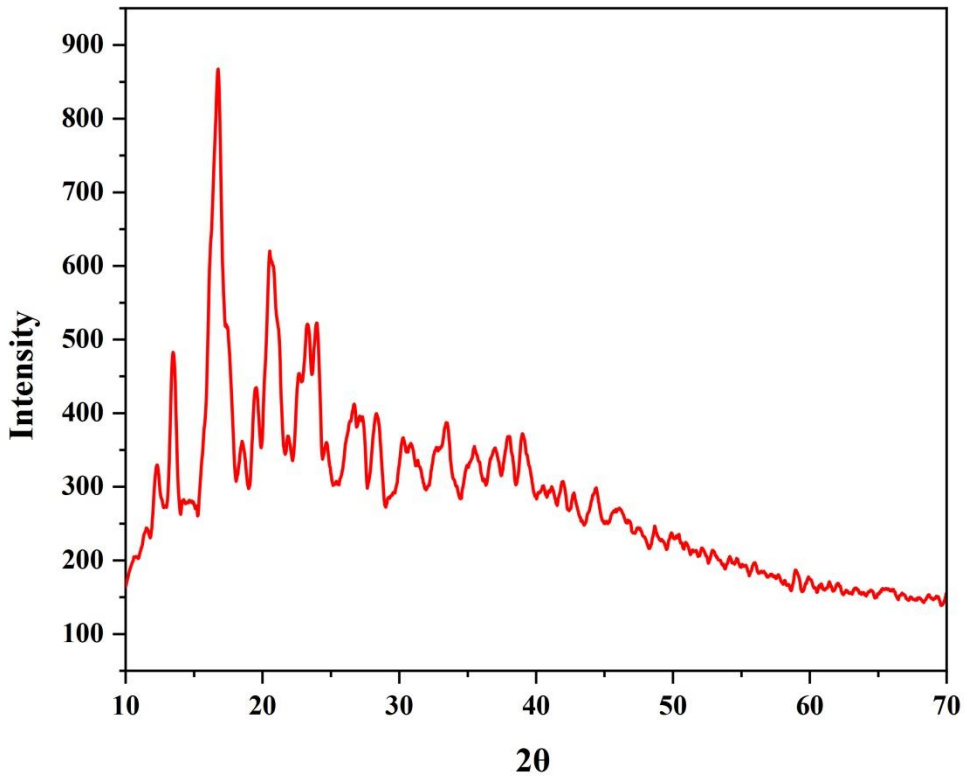

Figure S76: PXRD data of FA@HDMOF(1:32) crystals grown from methanol solvent diffusion (FA@HDMOF-1.2.)

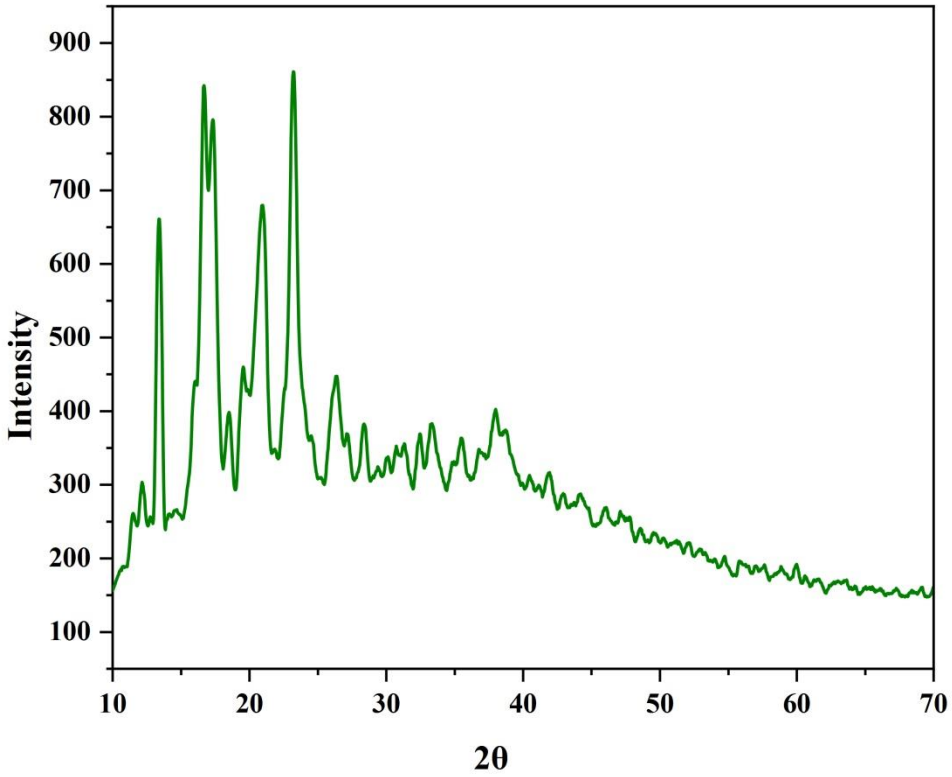

Figure S77: PXRD data of cinnamic acid

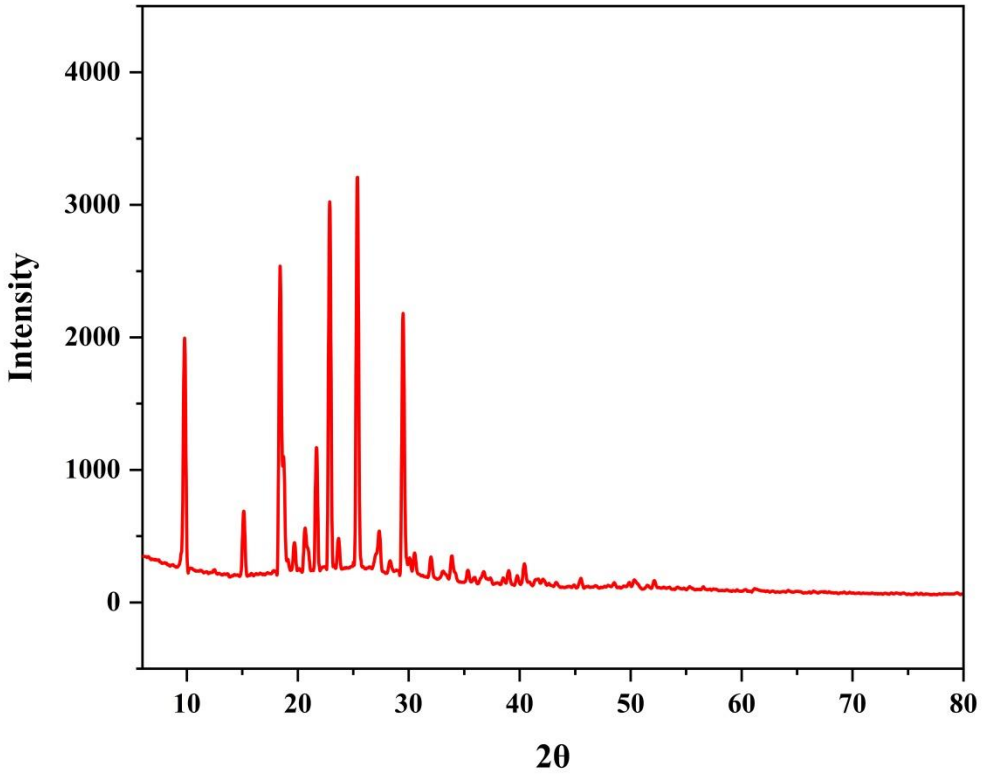

Figure S78: PXRD data of potassium cinnamate

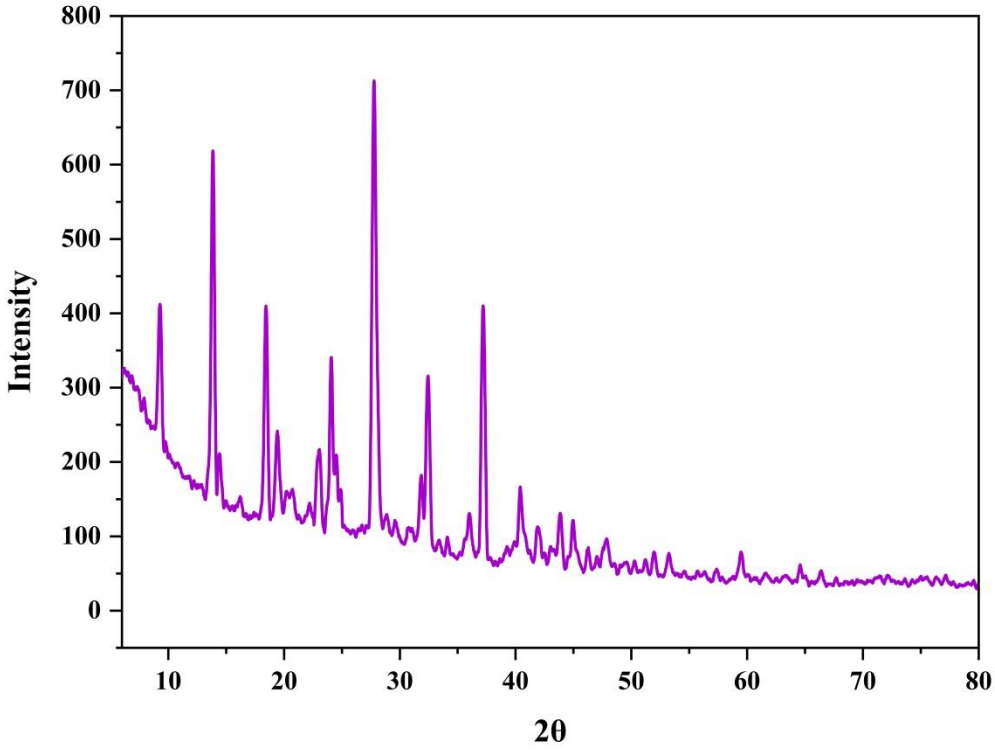

Figure S79: PXRD data of p-coumaric acid

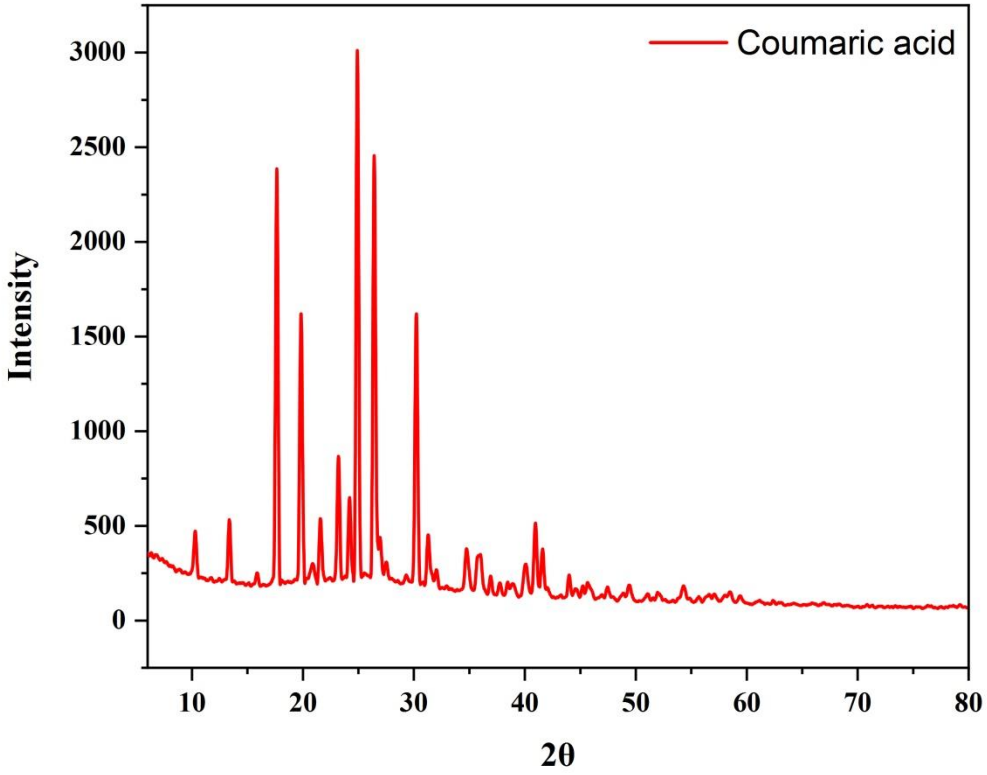

Figure S80: PXRD data of potassium coumarate

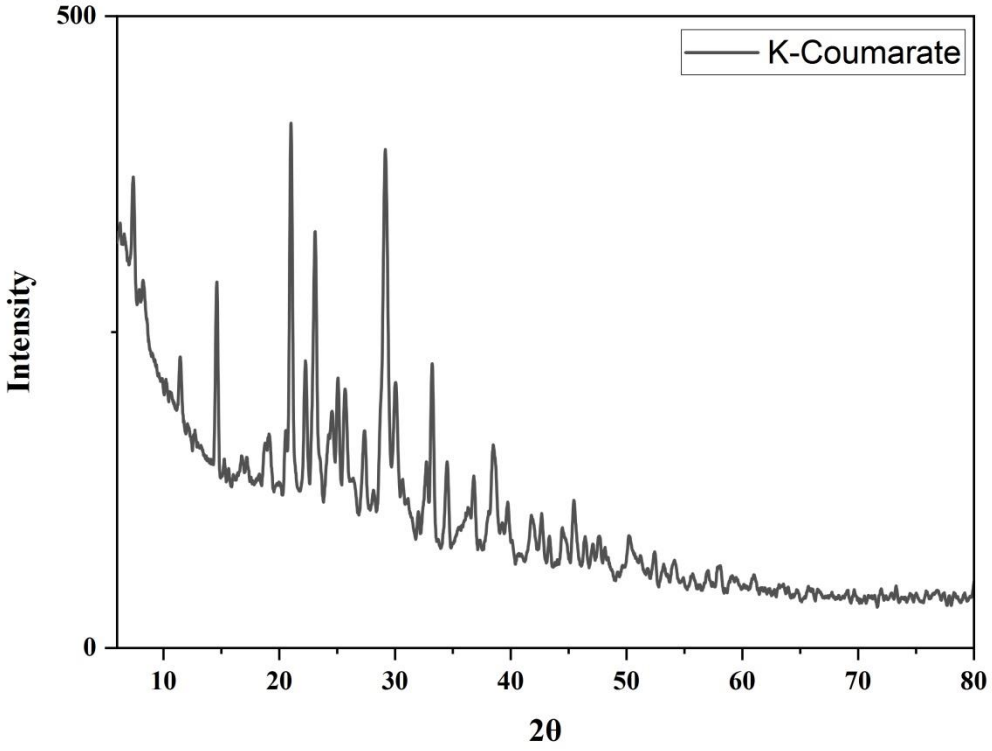

Figure S81: PXRD data of ferulic acid

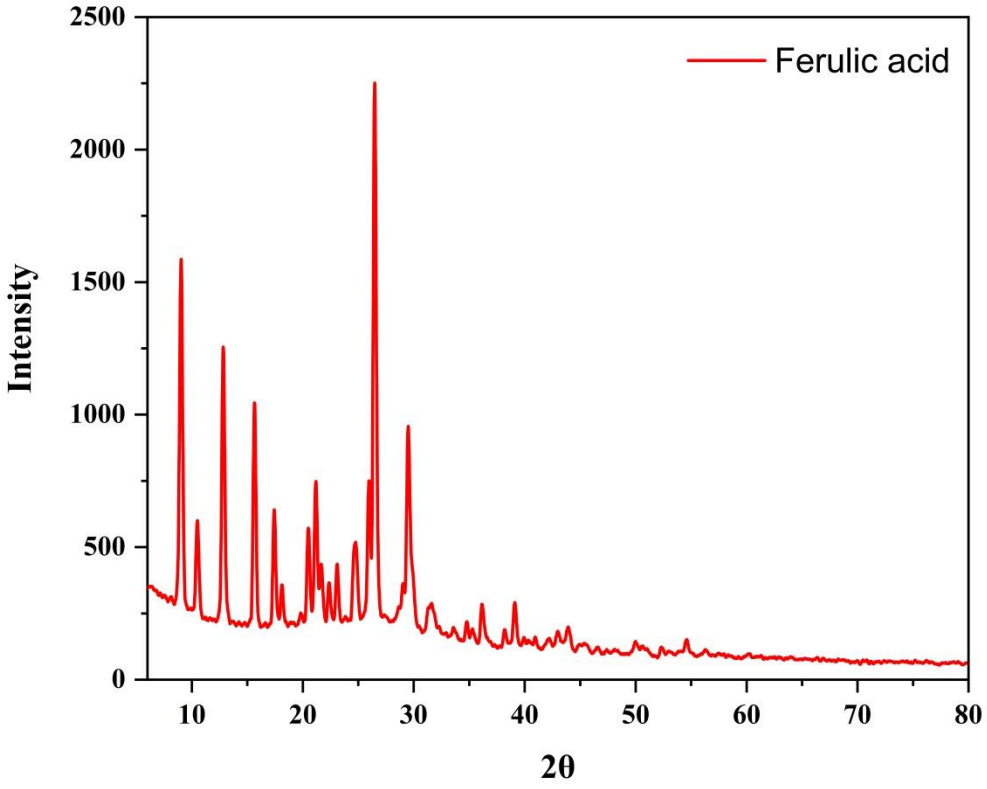

Figure S82: PXRD data of potassium ferulate

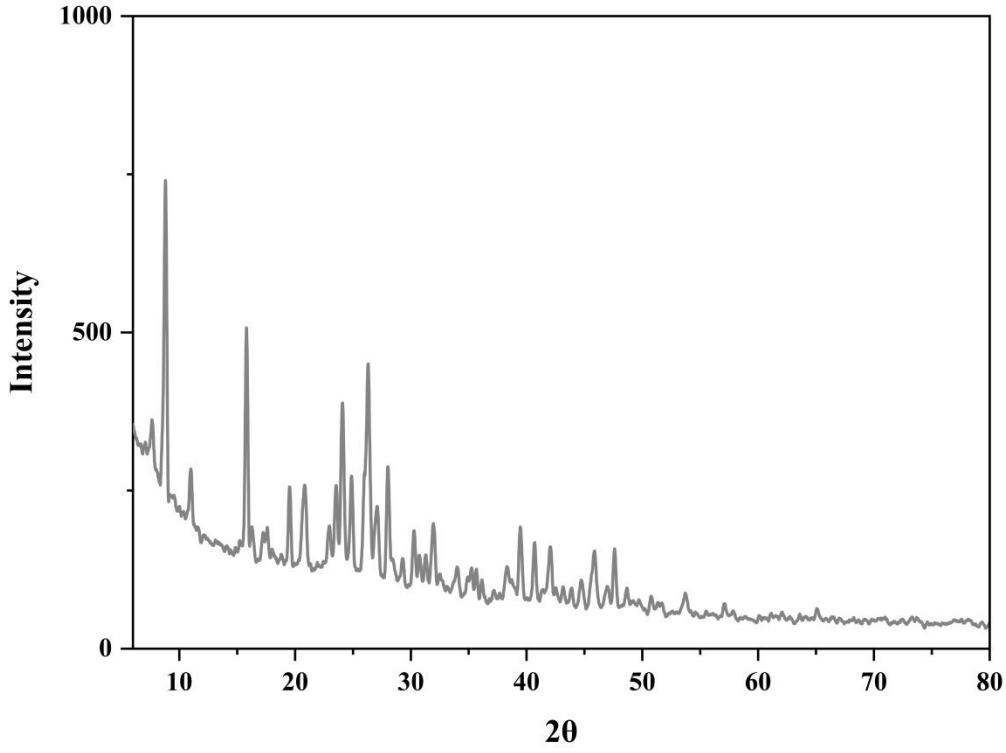

Figure S83: The FT-IR spectra of blue: AgNp^FA@HDMOF(1:8), Red: AgNp^FA@HDMOF(1:16), Pink- AgNp^FA@HDMOF (1:32),

Figure S84: The FT-IR spectra of blue: AgNp^COU@HDMOF(1:8), Red: AgNp^COU@HDMOF(1:16), Pink:AgNp^COU@HDMOF (1:32)

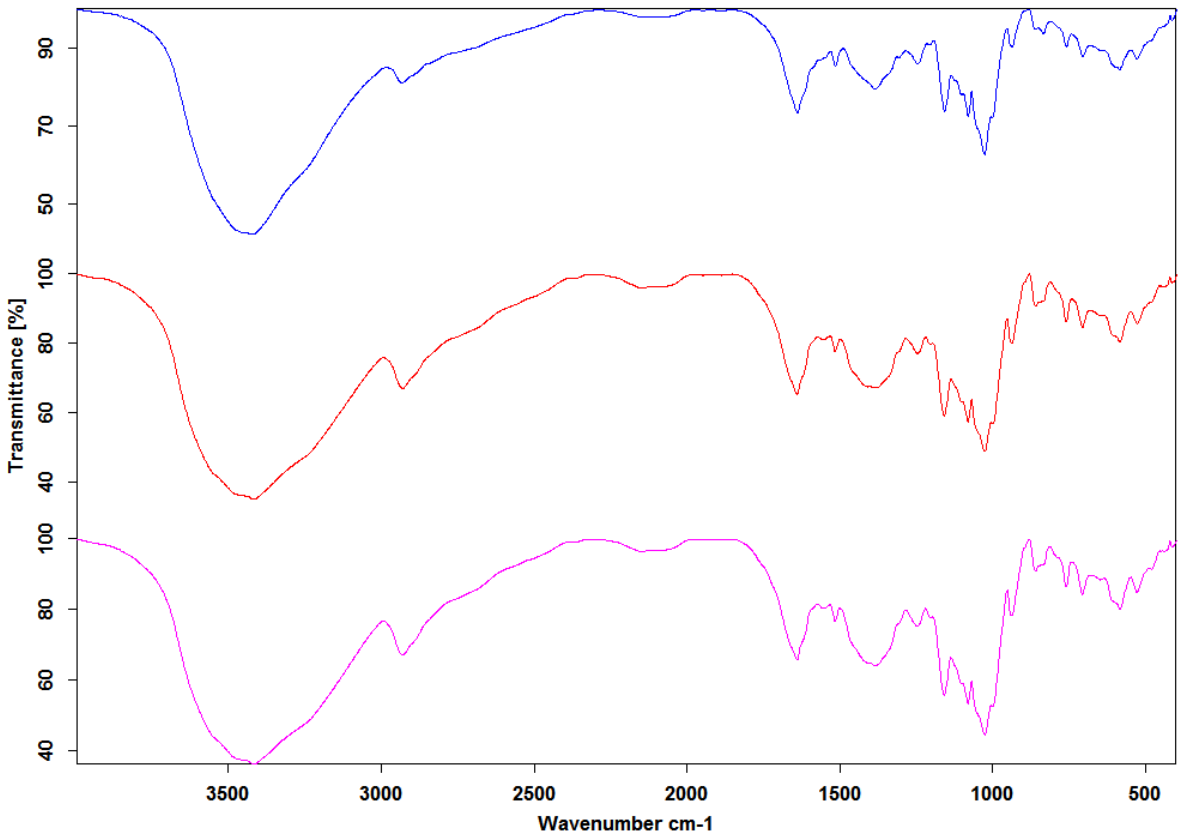

Figure S85: UV spectra of blue:AgNp^COU@HDMOF(1:8), red: AgNp^COU@HDMOF(1:16), green: AgNp^COU@HDMOF(1:32),

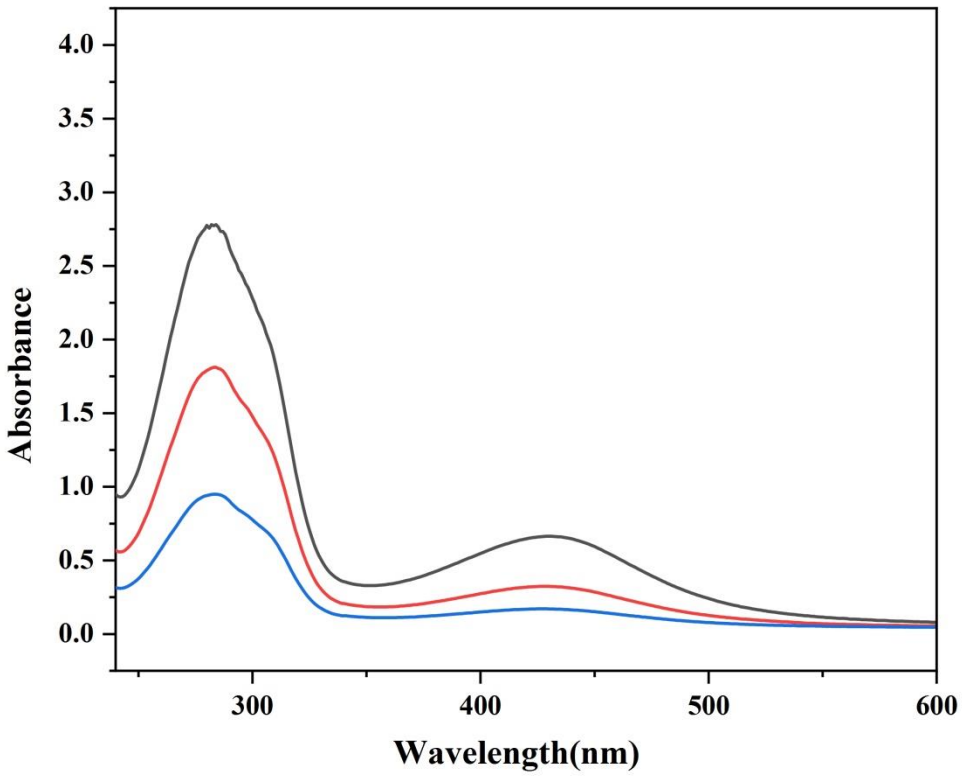

Figure S86: UV spectra of green:AgNp^FA@HDMOF(1:8), red: AgNp^FA@HDMOF(1:16), blue: AgNp^FA@HDMOF(1:32),

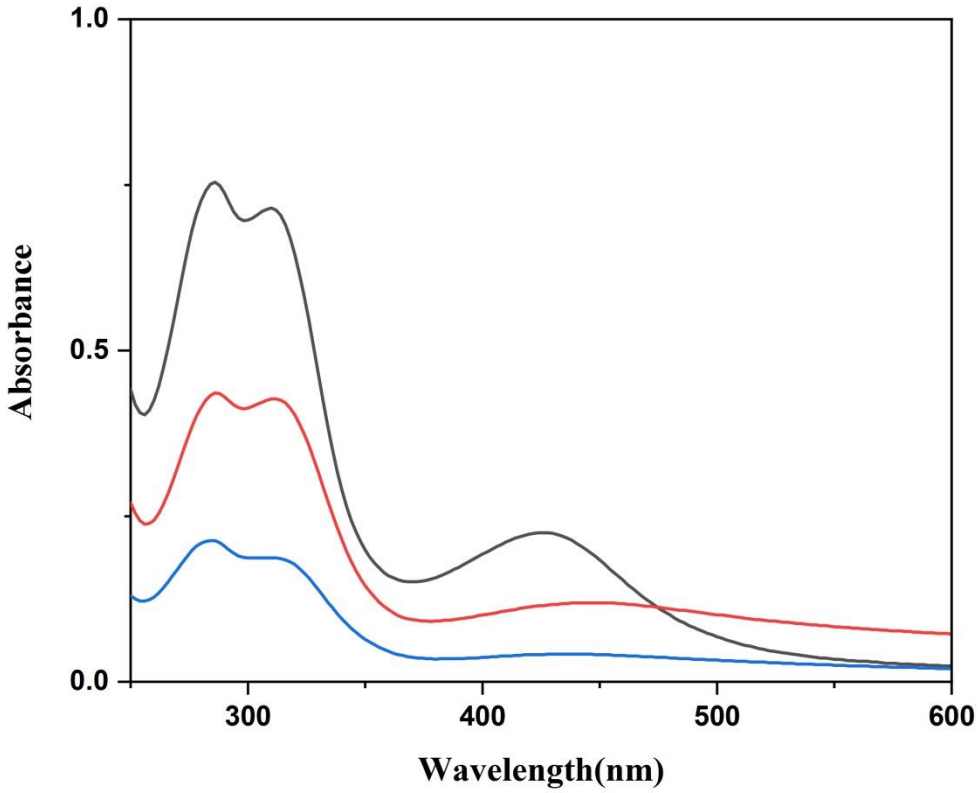

Figure S87: PXRD patterns of black:AgNp^COU@HDMOF(1:8), red: AgNp^COU@HDMOF(1:16), blue: AgNp^COU@HDMOF(1:32),

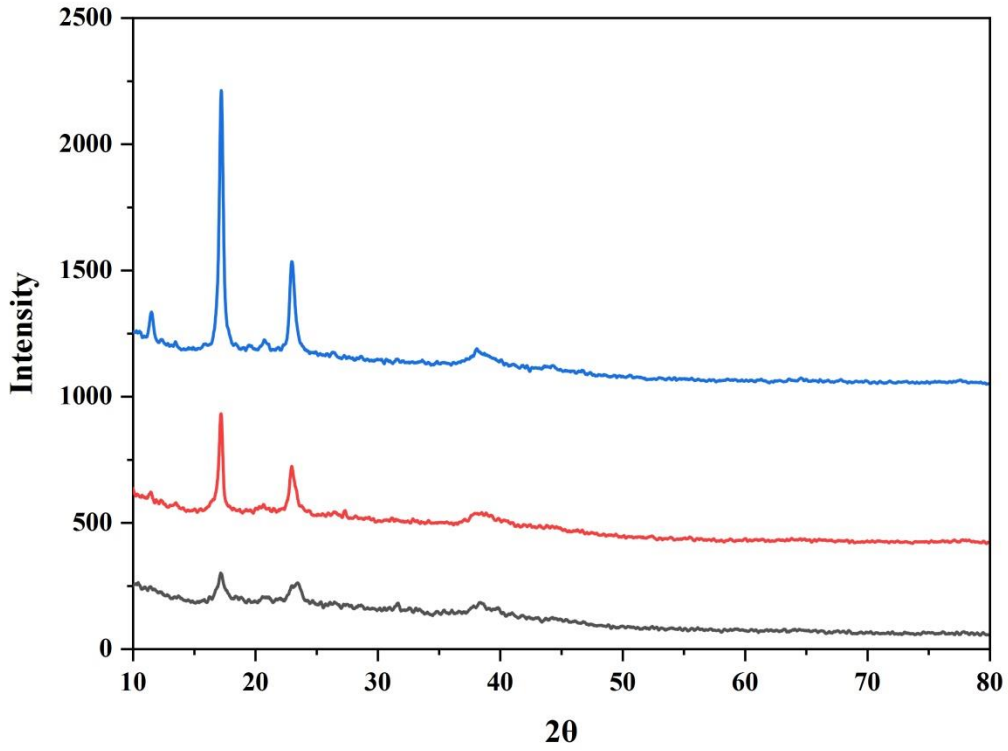

Figure S88: PXRD patterns of black:AgNp^FA@HDMOF(1:8), red: AgNp^FA@HDMOF(1:16), blue: AgNp^FA@HDMOF(1:32)

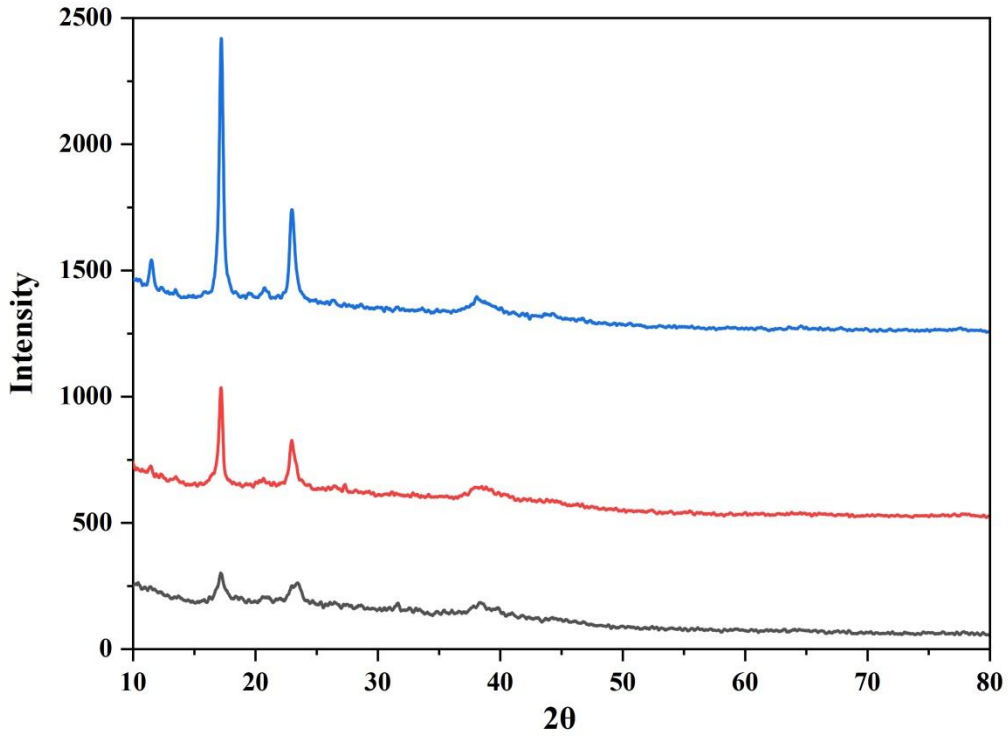

Figure S89: PXRD patterns of PXRD pattern of blue:AgNp^COU@HDMOF(1:32) red: AgNp^FA@HDMOF(1:16), black: AgNp^FA@HDMOF(1:32). The precursor hybrid CDMOFs were grown in MeOH solvent

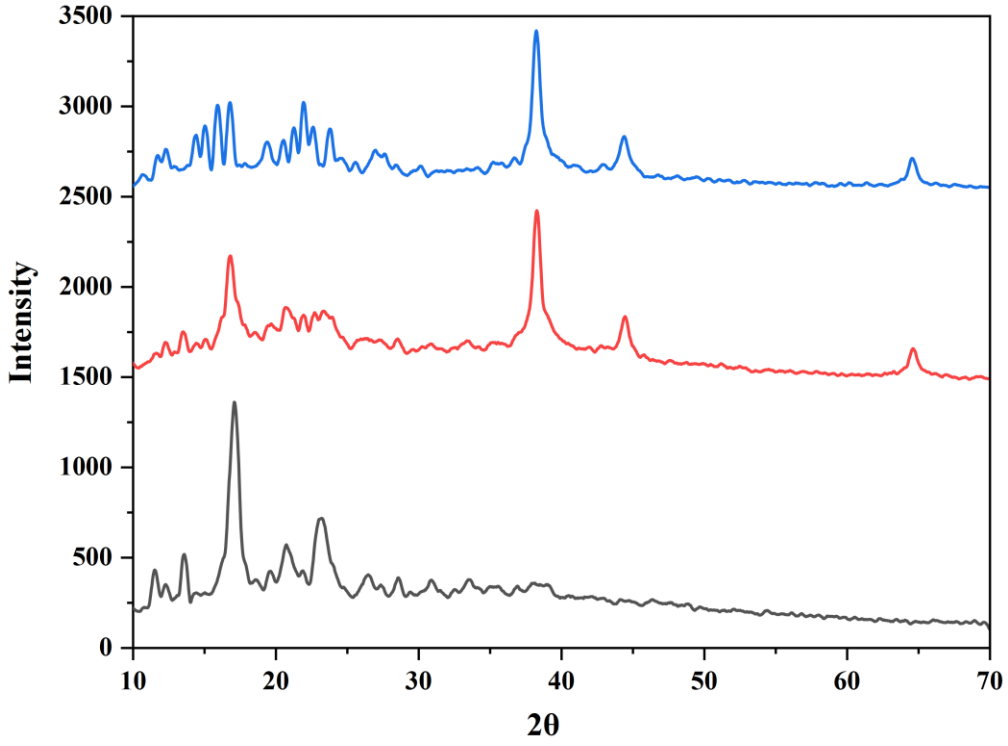

Figure S90: PXRD pattern of blue:AgNp^FA@HDMOF(1:8) red: AgNp^FA@HDMOF(1:16), black: AgNp^FA@HDMOF(1:32). The precursor hybrid CDMOFs were grown in MeOH solvent

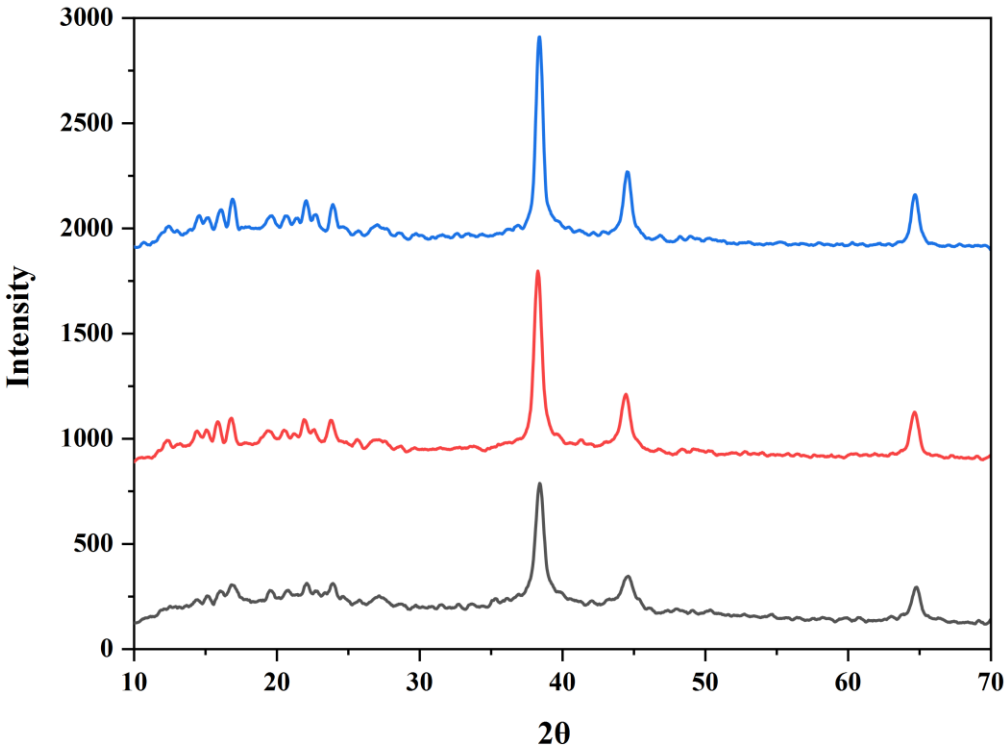

Figure S91: PXRD patterns of reaction product of CIN@HDMOF dipped in $AgNO_3$ PXRD pattern of blue: CIN@HDMOF(1:32), red: CIN@HDMOF(1:16), black: CIN@HDMOF(1:8) The precursor HDMOFs were grown in MeOH solvent

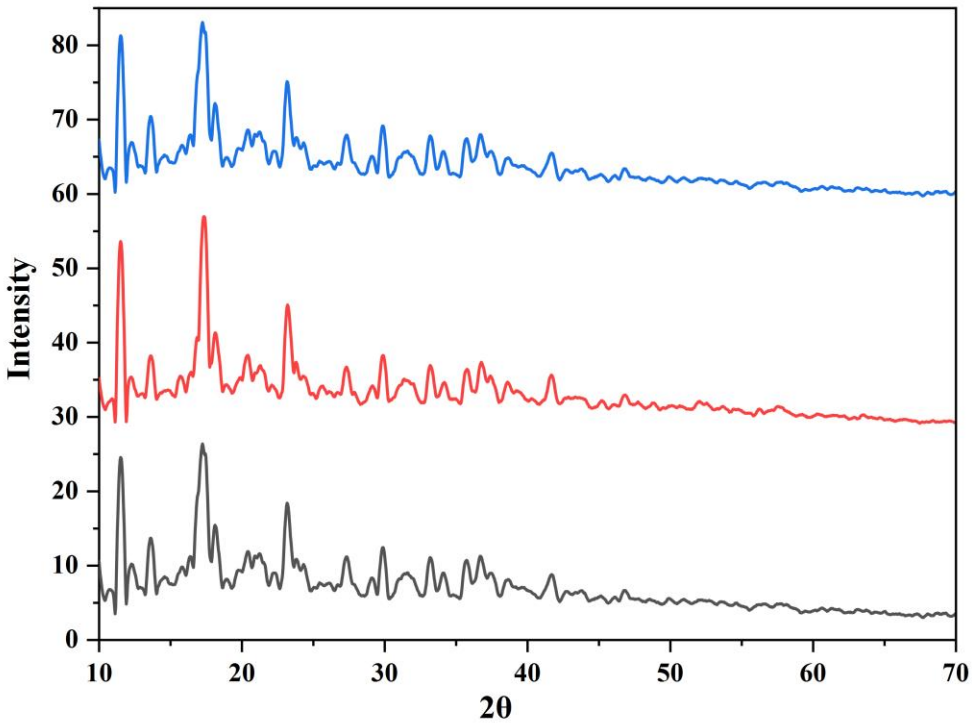

Figure S92: PXRD patterns of reaction product of CIN@HDMOF dipped in $AgNO_3$. blue: CIN@HDMOF(1:32), red: CIN@HDMOF(1:16), black: CIN@HDMOF(1:8) The precursor HDMOFs were grown in ethanol solvent.

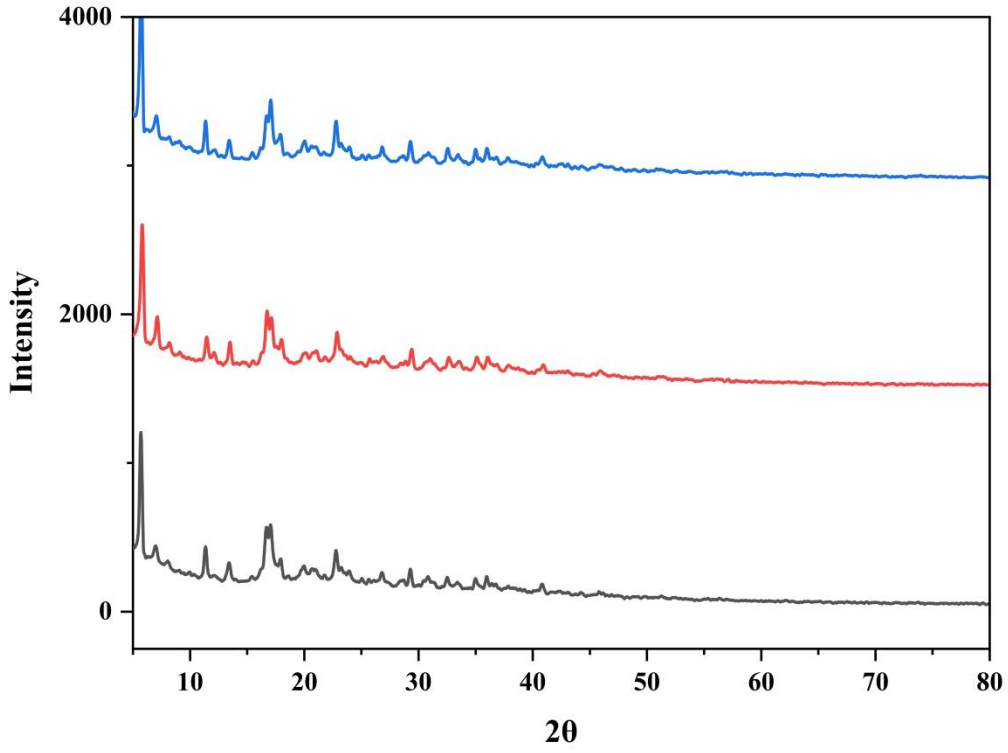

Figure S93: UV spectra of reaction product of CIN@HDMOF dipped in $AgNO_3$.
black: CIN@HDMOF(1:8), red: CIN@HDMOF(1:16), blue: CIN@HDMOF(1:32)
The precursor HDMOFs were grown in ethanol solvent.

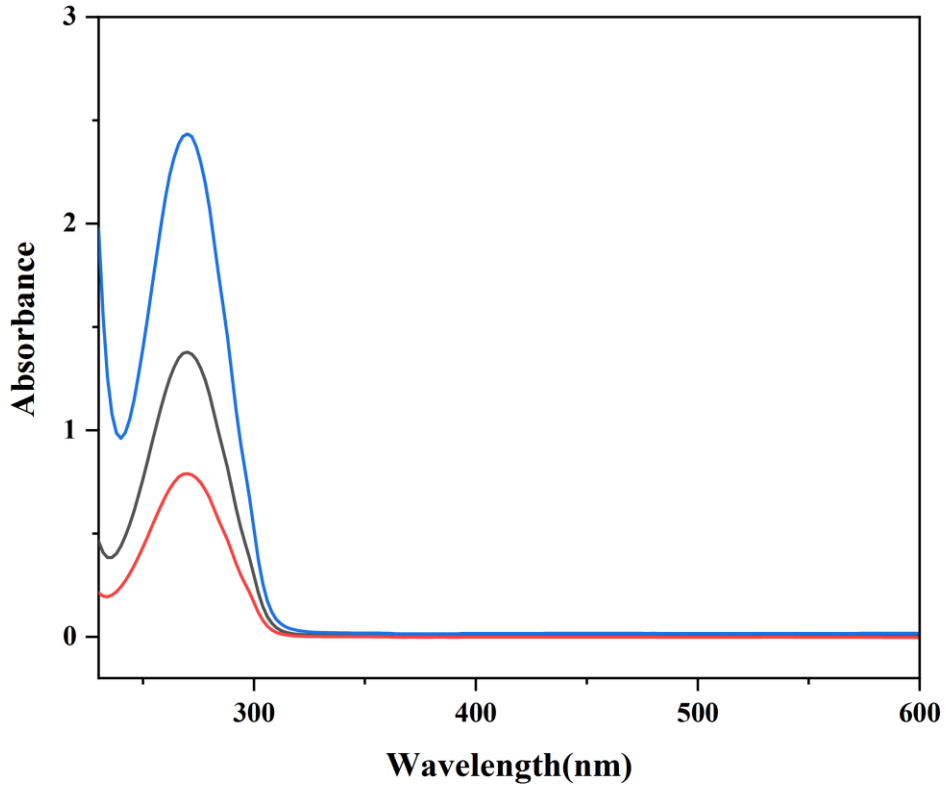

Figure S94: UV spectra of reaction product of CIN@HDMOF dipped in $AgNO_3$.
black: CIN@HDMOF(1:8), red: CIN@HDMOF(1:16), blue: CIN@HDMOF(1:32)
The precursor HDMOFs were grown in methanol solvent.

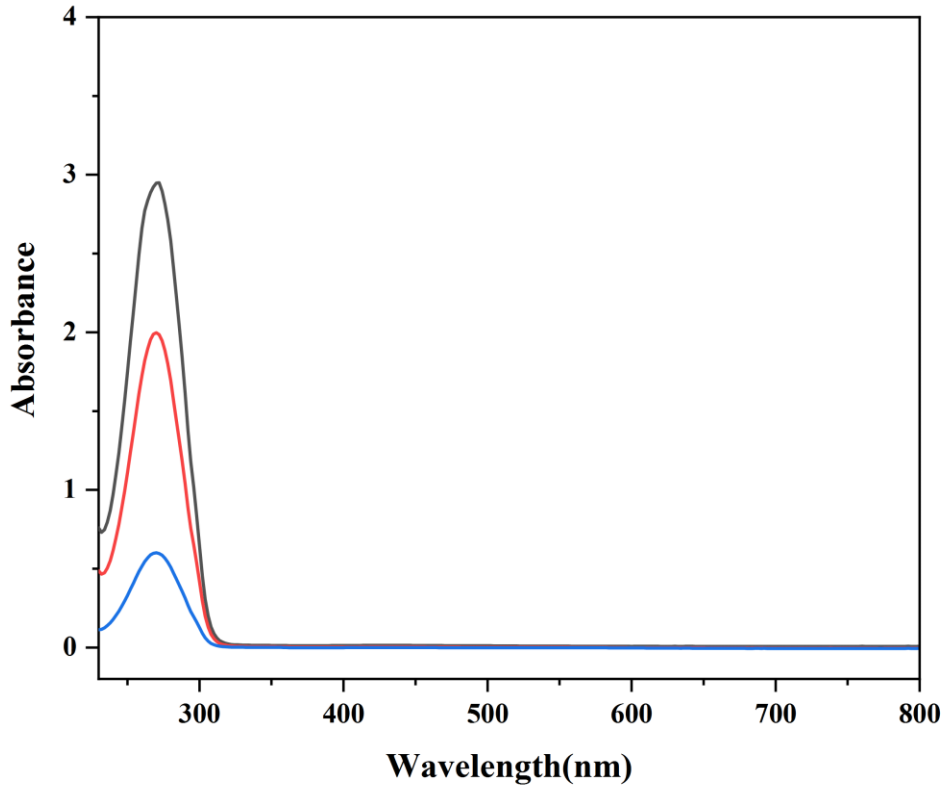

Figure S95: SEM of AgNp^COU@HDMOF(1:8),

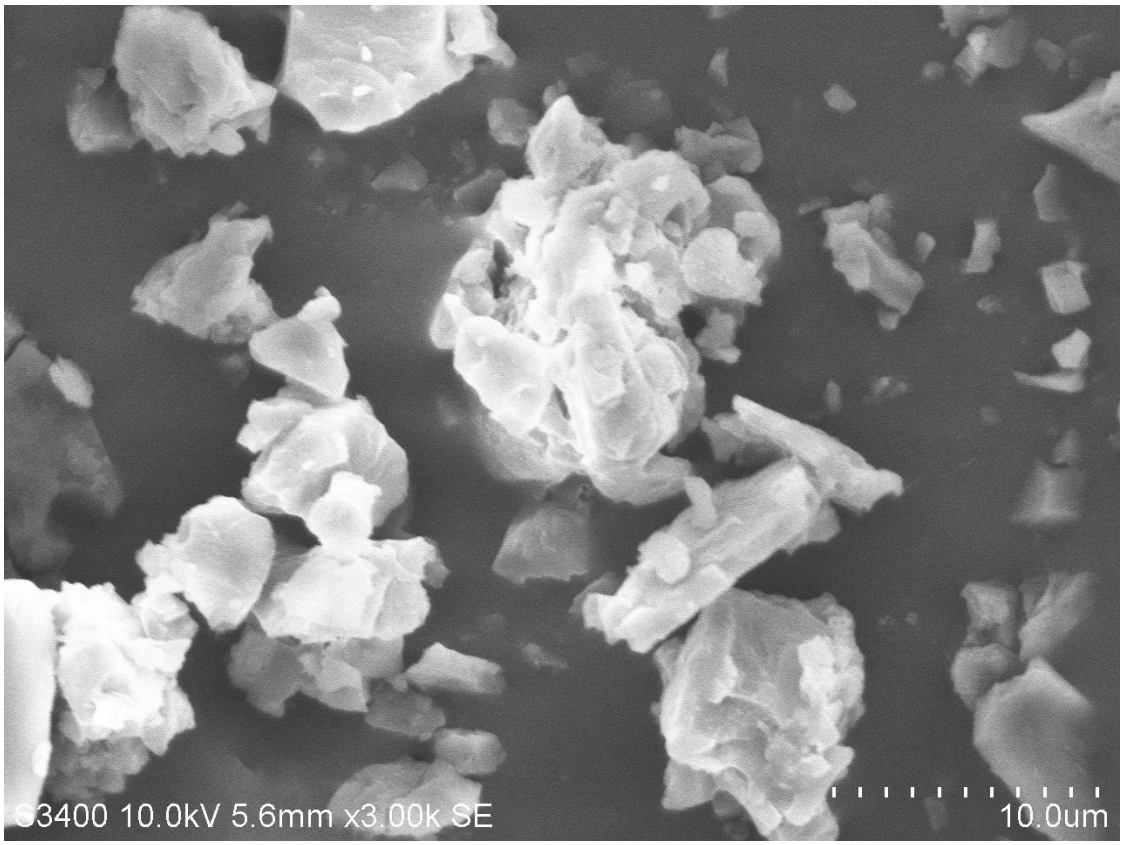

Figure S96: AgNp^FA@HDMOF(1:8)

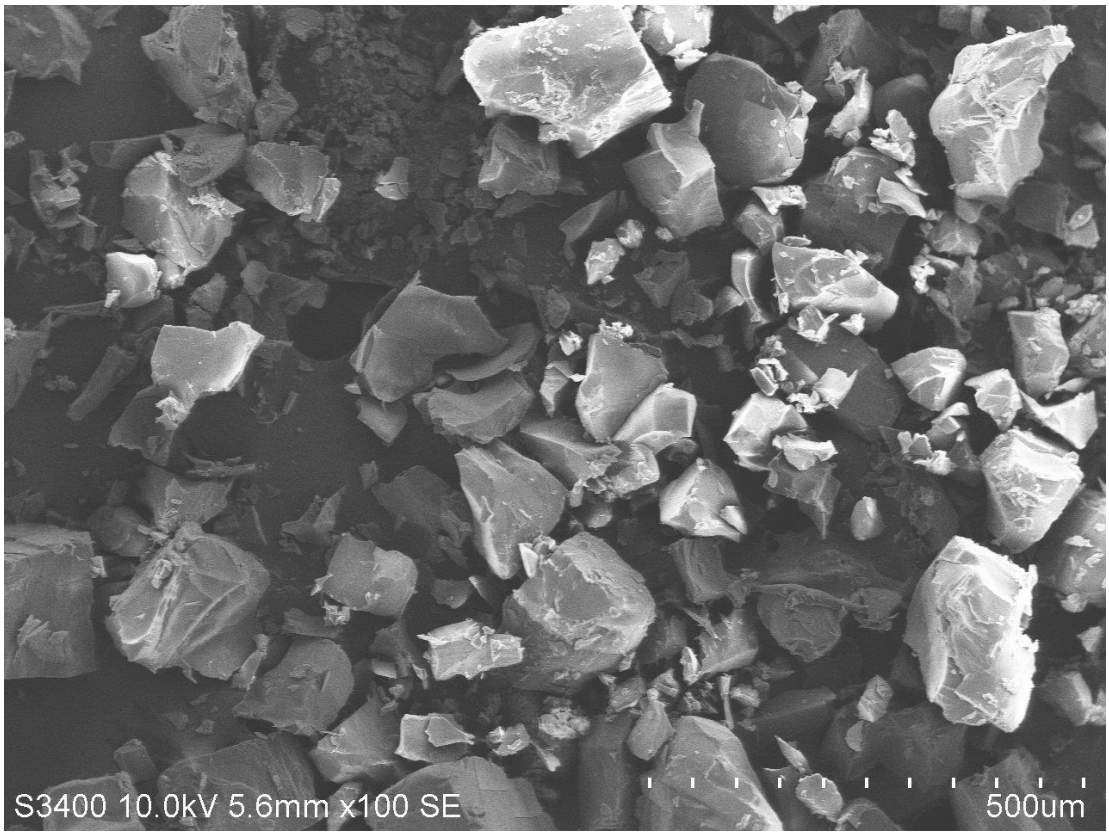

Figure S97: TEM of AgNp^COU@HDMOF(1:8)

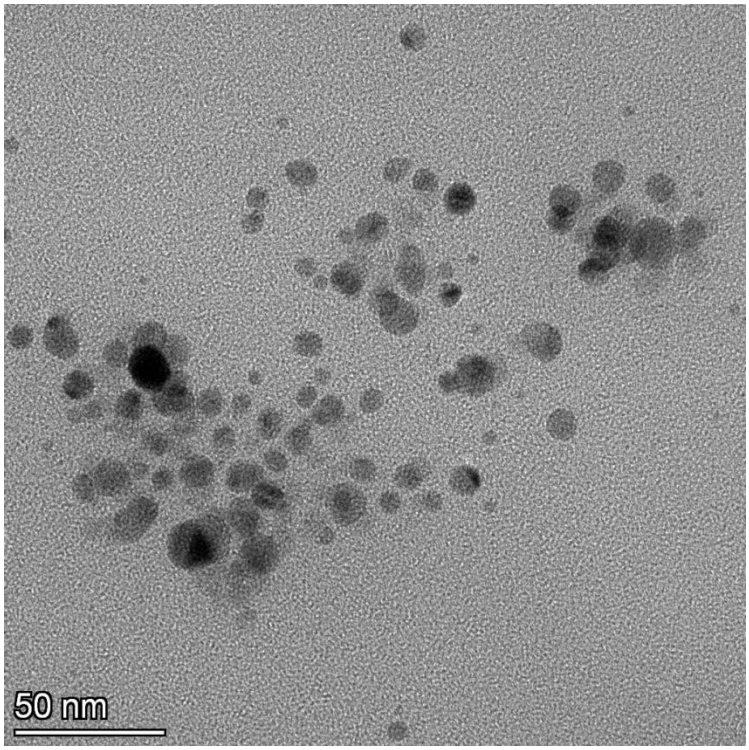


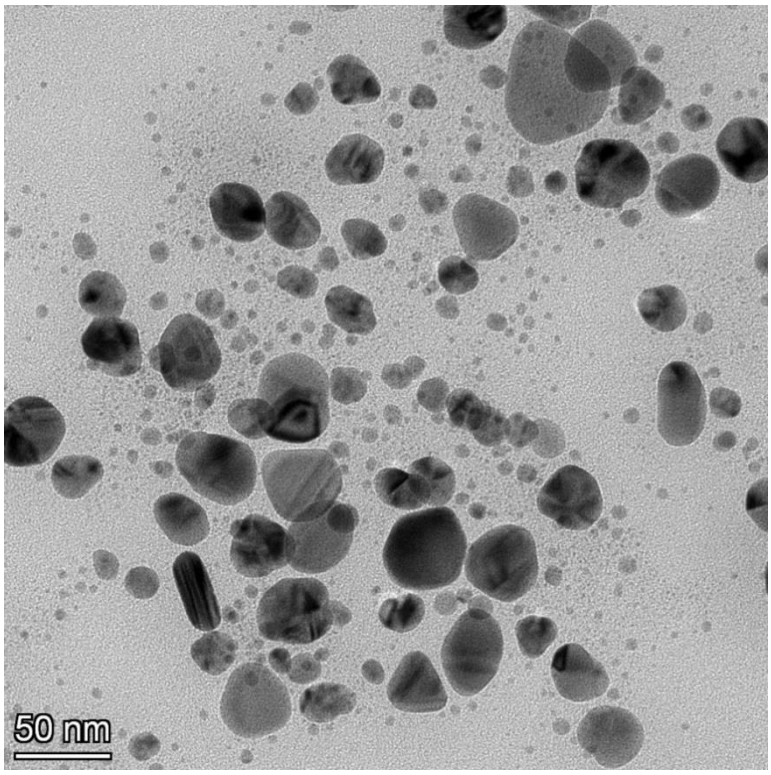

Figure S99\8: TEM of AgNp^FA@HDMOF(1:8)